ANNUAL RESEARCH REVIEW WORKSHOP 2024-2025

V (a) Farm Machinery and Postharvest Technology Division

BANGLADESH RICE RESEARCH INSTITUTE
GAZIPUR 1701

INDEX

INTRODUCTION

There are two research divisions under the **"Farm Mechanization and Postharvest Technology Programme Area"** that have been conducting research on the following projects.

Project Title	No. of Experiment
Project 1: Agricultural Machinery Development and Testing	07
Project 2: Milling and Processing Technology	02
Project 3: Renewable Energy	02
Project 5: Smart Agricultural Technology	02
Project 6: Industrial and Farm Level Extension of Agricultural Machinery	02
Total	**15**

PERSONNEL

Programme Performing Unit 1: Farm Machinery and Postharvest Technology Division

Name and Designation	Abbreviation	Working months
Md. Durrul Huda, *PhD* *Chief Scientific Officer and Head*	MDH	12
AKM Saiful Islam, *PhD* *Chief Scientific Officer*	AKMSI	12
Md. Golam Kibria Bhuiyan, *PhD* *Principal Scientific Officer*	MGKB	12
Md. Anwar Hossen, *PhD* *Principal Scientific Officer*	MAH	12
Bidhan Chandra Nath, *PhD* *Senior Scientific Officer*	BCN	12
Md. Kamruzzaman Milon, *PhD* *Senior Scientific officer*	MKM	12
Subrata Paul, *M Engg.* *Senior Scientific Officer*	SP	12
Md. Kamruzzaman Pintu*, *MS* *Senior Scientific officer*	MKP	00
Md. Monirul Islam*, *MS* *Senior Scientific Officer*	MMI	03
Sharmin Islam, *MS* *Senior Agriculture Engineer*	SI	12
Haimonti Paul, *MS* *Agriculture Engineer*	HP	12
Md. Mizanur Rahman, *MS* *Scientific Officer*	MMR	12
Md. Mahir Shahriyar*, *MS* *Scientific Officer*	MMS	01
Arafat Ullah Khan, *MS* *Scientific Officer*	AUK	12
Most. Sapna Khatun, *MS* *Scientific Officer*	MSK	12
Jannatoon Nime, *MS* *Scientific Officer*	JN	12
Md. Rasel Ahmed, B Sc. Engineering (Mechanical) *Foreman*		12
Md. Nurul Momin Mondal, *Dip-in-Engineering (Power)* *Research Assistant*		12
Md. Rakibul Islam+, *Dip-in-Agriculture* *Scientific Assistant*		09

*Deputation for higher study
+Joined FMPHT Division from Rangpur R/S

SUMMARY

Field trials were conducted in a mechanized village as well as on a farmer's field at Jashore during the Aman 2024 season with a view to compare the transplanting operational cost of the rice crop. BRRI developed a 4-row rice transplanter (Model: BRRI PRT2023) and imported waking type 4-row rice transplanter (Model: Janata 2ZS-4C) were used in this experiment. The hand transplanting method was also used for transplanting purposes. The performance of the BRRI-developed 4-row rice transplanter was found to be more satisfactory than the imported rice transplanter and the hand transplanting method. The field capacity, field efficiency, and fuel consumption of the BRRI-developed and imported 4-row rice transplanter were 40.12 decimal/h, 79.50%, 1.52 l/h, and 35.73 decimal/h, 78.03%, 1.32 l/h, respectively. The cost of transplanting for the BRRI-developed and imported 4-row self-propelled rice transplanter was found to be BDT 1200 Tk/decimal, 1500Tk/decimal as compared to BDT 3500 Tk/decimal as in the case of the traditional method of manual transplanting followed by farmers in the Jashore region.

The head feed combine harvester with a dimensions of 4250mm×2030mm×2580mm, 4-cylinder engine power of 77 hp and a cutting width of 1450 mm was designed, developed and fabricated considering ground pressure, foward speed, ease of operation, land condition, and business viability at the FMPHT divisional research workshop and Alim Industries Ltd, Sylhet with the help of other local agricultural machinery manufacturers. Laboratory and field tests of the combine harvester in load and no-load conditions were done in the workshop and rice field. Forward speed during harvesting ranged from 3.0 – 4.0 km/h. The effective field capacity of the harvester was obtained as 0.33 ha/h and fuel consumption 10-11 l/h. The developed combine harvester is suitable for operating in the fragmented farmland. The losses of paddy can be reduced by 4.47% using a combine harvester over manual harvesting. Also, all results revealed that a mechanical harvester, like a combine harvester, is a time, labor, and cost-saving system along with reducing harvesting losses, human drudgery, and increasing cropping intensity and crop productivity.

A study was conducted during the 2024-25 season in Sirajganj and Habiganj districts in Bangladesh, as part of the KGF-Funded and BRRI project "Validation and Up-Scaling of Rice Transplanting and Harvesting Technology in Selected Sites of Bangladesh (VRTHB)". Two trials focused on the impact of forward speed and crop density on the performance of whole-feed combine harvesters. The Zoomlion-FH-100 and Lovol-RG108+ models were tested under two crop densities (251–300 plants/m² and 301–350 plants/m²) and three forward speed levels (4 - 5 km/h, 5 - 6 km/h, and 6 - 7 km/h). The results indicated that actual field capacity increased with forward speed, with the highest values observed at 6 - 7 km/h. The Zoomlion-FH-100 consistently outperformed the Lovol-RG108+ model across all conditions. However, no significant interaction effects were found among the machine model, forward speed, and crop density ($p > 0.05$). Lower plant density resulted in higher field capacity, but grain losses increased with both forward speed and crop density. Lovol-RG108+ experienced higher grain losses (5.18%) at higher crop density and maximum speed, while Zoomlion-FH-100 had lower losses (3.74%).

The fast-moving spare parts research moved from identifying frequently failing components to piloting local fabrication. The last year's findings - which highlighted cutting blades, belts, bearings, fingers, threshing teeth, chains, and sprockets as high-failure items - the focus this year was on developing part-level specifications and engaging domestic manufacturers. A structured parts catalogue was compiled for the Daedong DXM73GF-SA model, listing seven key items including cutter blades, sprockets, shafts, and rotary blade tillers. Property comparisons showed promising results: fabricated cutter blades achieved 60.93 HRC against the original 48–60 HRC (Hardness Rockwell C), while rotary blade tillers met acceptable hardness ranges. These trials, led by Monno Agro & General Machinery Ltd., confirmed the feasibility of localized production. Quick metrics from the dataset: 7 items parsed, 1 with an explicit part number, and seven unique part names. The study recommends immediate stocking of high-rotation parts, strict quality control, preventive maintenance guidelines, vendor diversification, and supply chain targets of 7–10 days during peak harvest. The progress demonstrates Bangladesh's growing capacity to reduce reliance on imports, lower costs for farmers, and enhance the resilience of mechanized harvesting systems through sustainable local spare parts production.

The BRRI automatic rice seed sower machine was design, developed and fabricated jointly at the FMPHT divisional research workshop and Uttaron Engineering Workshop in Dinajpur using locally available materials. The laboratory test was done at BRRI's research workshop and fine-tuned for various soil textures and seed sizes. The machine, with capacity of hoppers 80 kg for bed soil, 10 kg for seed, and 40 kg for topsoil, was evaluated for seed distribution, performance, and economic aspects. Optimal settings for soil depth were determined, and seeds of BRRI Dhan103 were sown effectively with high efficiency (98.41%). The machine's forward speed was 0.1307 m/s, with a seeding capacity of 28 trays per minute and overall sowing efficiency of 78.57%. Post-sowing, a 6 mm layer of topsoil covers the seeds. Adjusting the seed rate for different rice varieties is

straightforward. Overall, the machine reduces time, increases accuracy, and enhances sowing efficiency.

The improvement of BRRI Prilled Urea Applicator was done by adopting an auger-based metering mechanism, combined with a full stainless steel and fiber-reinforced composite construction, results in a significant enhancement the field performance of the machine. The redesigned unit delivers improved precision, durability, and field adaptability, fully aligning with BRRI's objectives for practical, farmer-focused mechanization in rice fertilization.

A head feed thresher was manufactured using locally available materials at the Arafat Engineering workshop in Dinajpur, under a public-private partnership (PPP) financed by the "PARTNER" project, BRRI part. The study aimed to develop and fabricate a prototype of a high-capacity head feed thresher. The machine was powered by a 25 hp diesel engine and equipped with key components, including a wire-loop threshing drum, feeding chain, blower, auger-type grain conveyor, and a belt–pulley/gear-based power transmission system. The initial test of the machine was conducted in the 2024-25 Aman season at the FMPHT division of BRRI and the research field of the Bangladesh Agricultural Research Institute (BARI) to determine the mechanical errors of the machine, its capacity, and cleaning efficiency. The machine's average threshing capacity was 300kg/h for the Tulshimala variety at a 17.7% grain moisture content, and 469 kg/h for BRRI dhan87 at a 22.5% moisture content. The cleaning performance was found to be acceptable, with minimal grain loss and no mechanical issues reported. The study demonstrates that the developed thresher has the potential to improve threshing efficiency significantly. Further multi-season testing and refinements are recommended to ensure durability, optimize cleaning efficiency, and validate farmer acceptability at a larger scale.

The Farm Machinery and Postharvest Technology (FMPHT) Division fabricates a paddy de-husker to improve milling efficiency and head rice recovery. Husker is operated with a 5hp motor and two rubber rolls, each with a diameter of 240 mm and a length of 101mm, respectively. Average fixed and adjustable rubber roll rpm were found to be 1300 and 900, respectively. The adjustable rubber roll rotates 30 % less rpm than the fixed rubber roll. The average de-husking capacity of the husker ranged from 500-600 kg/h, and husking efficiency was about 80% which is found promising for paddy processing. The paddy husker may be suitable for rural areas for shifting the Engelberg huller to rubber roll rice processing.

The mechanical grain collector, built at the FMPHT Workshop, BRRI, features a mild steel chassis and grain-contact surfaces, a nylon brush reel for paddy pickup, and a stainless steel screw conveyor that transports grains to a 35 L hopper. It can be powered by a 6.5hp petrol engine, with power transmitted through a belt-pulley system. Field trials on concrete surfaces showed an average collection rate of 1212 kg/h, filling a standard gunny bag in 1.98 minutes, while cutting labor and operational costs by about 50% compared to manual collection. Soft nylon bristles, adjustable reel height, and an ergonomic handle minimized kernel breakage and operator fatigue. However, some minor breakage occurred at higher brush speeds, and the hopper capacity limited continuous operation. Overall, the collector provided efficient, uniform, and reliable grain collection, improving throughput and labor productivity. Recommendations include adding variable speed control, increasing hopper size, and improving traction for wet surfaces, with its modular petrol-compatible design offering flexibility for small- and medium-scale farms.

Bird-induced crop damage remains a constant threat to agricultural productivity, especially during the grain-filling and harvesting phases. This study introduces a solar-powered, AI-based smart bird repellent system utilizing the YOLOv8n deep learning model on a Raspberry Pi 4. The system combines a USB camera, stereo audio amplifier, motorized camera mount, and solar panel within a weather-resistant enclosure, ensuring autonomous operation in remote fields. A dataset containing native Bangladeshi bird species was used to train and validate the model, achieving a precision of 0.85, a recall of 0.80, an F1-score of 0.825, and a mean Average Precision (mAP) at 0.5 of 0.764. Field tests in real-world conditions confirmed its effectiveness, with detections triggering predator sounds and mechanical deterrents. A comparative analysis showed that YOLOv8n outperformed earlier YOLO variants, making it suitable for low-power, resource-limited environments. This research highlights the potential of edge AI and renewable energy integration for affordable and sustainable crop protection.

A solar-powered light trap developed by BRRI was evaluated for its potential use in managing stored-grain insect pests under indoor storage conditions. The trial was conducted at the BRRI grain storage facility, Gazipur, over four months (September–December 2024). The trap, powered by a 20 W solar panel and rechargeable battery, operated automatically from dusk until late evening and employed UV-blue LEDs to attract insects. Insect collections revealed that rice weevils (*Sitophilus oryzae*) and Angoumois grain moths (*Sitotroga cerealella*) were the dominant species, with peak activity during early evening (6–8 p.m.) under high light intensity (~250 lux). Lesser grain borers showed moderate presence, while red flour beetles and khapra beetles remained consistently scarce.

Captures declined both within nights and across successive days, indicating diel activity patterns, population depletion, and possible behavioral avoidance. The study demonstrated that the BRRI solar light trap is a practical, eco-friendly monitoring tool for major stored-product pests, reducing reliance on insecticides. However, broader adaptive trials at farmer and miller storage levels are needed to validate its broader applicability and adoption.

Bangladesh is highly vulnerable to climate extremes, with both flood and drought risks posing serious threats to agriculture. Using monthly rainfall data from 1981 to 2018, this study employed the Effective Drought Index (EDI) to evaluate drought severity, duration, and frequency. These findings were combined into a Drought Hazard Index (DHI) to assess spatial and seasonal drought risk nationwide. Annual rainfall showed substantial spatial variation, ranging from less than 1,500 mm in the northwest to over 4,000 mm in the northeast. The DHI identified the northwestern districts as the most drought-prone areas, with the Boro (December–April) season experiencing particularly severe hazards. Quantitatively, 30-40% of districts faced recurrent moderate to severe droughts. These results underscore the pressing need for drought-resistant cropping strategies and effective water management to ensure food security in Bangladesh.

The use of uncrewed aerial vehicles (UAVs) in agriculture is rapidly increasing worldwide, serving purposes such as the precise application of fertilizers and pesticides and crop monitoring. An effort was made to develop and use drones in agriculture for the Bangladesh context. An agricultural drone for spraying was assembled and developed using procured materials at S Agro Drone BD in Dinajpur, under a public-private partnership (PPP) financed by the “PARTNER” project, BRRI part. The initial test confirmed that both the flight and spraying systems were effective for operation. The drone demonstrated stable lift, good adjustability, and efficient liquid discharge in local field conditions. A comprehensive test will be organized in the upcoming season.

Training plays a crucial role in developing skilled personnel capable of efficiently operating, maintaining, and repairing agricultural machinery. Competent operators not only improve machine performance and extend service life but also minimize downtime, thereby enhancing productivity and creating greater income-generating opportunities for farming communities. Recognizing this need, the Farm Machinery and Postharvest Technology (FMPHT) Division of BRRI organized 2 batch 15-day residential training program at its headquarters in Gazipur under the PARTNER Project. The program placed strong emphasis on practical, hands-on learning alongside technical knowledge, aiming to strengthen mechanization practices and promote sustainability across Bangladesh’s agricultural sector.

Total 36 batch of two day long residential training programme was conducted under financial and technical support of SFMRA project of FMPHT division during the period of 2024-2025. Participants of the training programme were attended from all BRRI regional station adjacent area and from its jurisdiction districts. Total 740 numbers of participants were trained among them 500 were male and 240 were female. Participant were trained on operation, repair and maintenance of different agricultural machinery and technologies like; seed sower, transplanter, combine harvester, diesel engine, power weeder, prilled urea applicator, self-propelled reaper, power tiller etc theoretically and practically in the threshing floor and in the main field. At the end of the training, a post-evaluation and trainee’s reactions regarding the training were collected. Certificates, leaflets and a set of tools were distributed among the participants. Trainees opined that they are now more confident about the use of the agricultural machinery.

USEFUL SCIENTIFIC INFORMATION

PROJECT 1: AGRICULTURAL MACHINERY DEVELOPMENT AND TESTING

Experiment 1.1: Performance Assessment of BRRI Developed and Imported Self-Propelled 4-Row Walking-Type Rice Transplanters in Bangladesh

Principal Investigator: Arafat Ullah Khan
Co-Investigator: AKMSI, MSK, JN

Materials and Methods

The study was conducted at mechanized village of Jashore district and evaluated the performance of BRRI developed four-row self-propelled walking rice transplanter compared with imported rice transplanter (JANATA 2ZS-4C). Table 1 shows the detailed specifications of the BRRI developed and the imported rice transplanter machine.

Table 1: Specifications of the BRRI-developed rice transplanter and the imported rice transplanter

Particulars	Specifications	Specifications
Model	BRRI RT 2022	JANATA 2ZS-4C
Drive Method	2 Wheel 3-float type steering clutch	2 Wheel 3-float type steering clutch
Overall dimensions (L × W × H), mm	2140×1530×910	2140×1580×890
Weight, kg	172	165
Engine	Air-Cooled 4-stroke Petrol Engine	Air-Cooled 4-stroke Petrol Engine
Engine rated power, kW/hp	3.4	2.6
Fuel	Gasoline	Gasoline
Fuel tank capacity, l	4	4
Fuel consumption (l/hr)	1.5	1.4
No. of rows	4 Nos	4 Nos
Adaptable Seedlings	Mat Type	Mat Type
Transplanting space row to row, cm	30	30
Planting speed, m/s	0.44 and 0.54	0.6 and 0.7
Distance between hills, mm	130 (5 steps)	150 (5 steps)
Planting depth, mm	0-30	0-35
Travel Steering	Hydraulic power steering mode	Hydraulic power steering mode
Wheel Type	Rubber lug wheel	Rubber lug wheel
Gearshift	Forward: 2 levels, Reverse: 1 level	Forward: 2 levels, Reverse: 1 level
Transplanting Mechanism	Mechanical / Rotary	Mechanical / Rotary
Transplanting Distance, cm (plant to plant)	12, 14, 16	12, 14, 16
Seedling/ hills control	Adjustable (7 options)	Adjustable (5 options)
Transplanting Speed, m/sec	0.6 to 1.0	0.3 to 0.7

Table 2: Field and Nursery Condition

Particulars	Specifications
Date of sowing	15.07.25
Type of nursery	Mat Type
Variety of rice	BRRI dhan87
Seed rate, g/tray	135-150
Age of seedlings, days	17
Plant density, no/cm^2	2~5
Height of seedling, mm	121
Leaf stage	3-4
Root length, mm	20
Standing water level, mm	15-20

Table 2 shows the field and nursery conditions of transplanting process which were conducted in field (Plate 2). Figure 1 shows the Experimental design of the study. The soil type of the experimental site was sandy loam. BRRI developed four-row self-propelled rice transplanter (Model: BRRI PRT2023; Plate 1) and an imported rice transplanter (Model: JANATA 2ZS-4C) were used to

conduct this experiment. Mechanical transplanting requires a special type of seedlings raised in a mat-type nursery. 17 days old seedlings were used for mechanical transplanting. Transplanting was done lengthwise of the well puddled and leveled field maintaining 15-20 mm water to avoid floating hill. Observations on speed of operation, depth of placement of seedlings, number of seedlings per hill, number of missed hills, floating hill, buried hill, mechanically damaged hill, time taken for turning, time taken for loading of seedling mat onto the transplanter, total time taken for transplanting, total area covered, width of coverage, and fuel consumption for the transplanting operation were recorded. The following parameters were studied to evaluate the performance testing of the self-propelled four-row paddy transplanter.

1. Theoretical field capacity was calculated based on the speed of operation and the width of the transplanter machine.
2. Actual field capacity was calculated based on the area covered and the actual time taken for covering the region, including the time lost in turning.
3. Field efficiency was obtained by dividing actual field capacity by the theoretical field capacity.
4. Labor saving by using the machine compared to manual transplanting was also studied.

Plate 1. BRRI PRT 2022 rice transplanter

Plate 2. Data collection

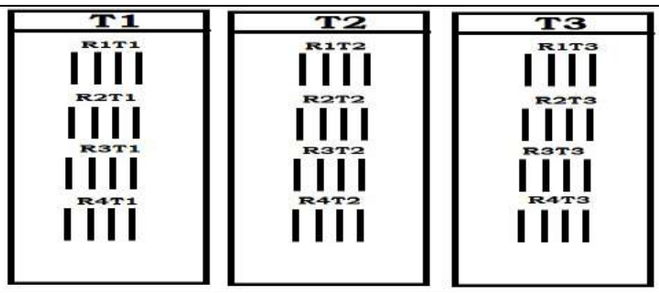

Figure 1. Experimental design

Hill spacing

Hill-to-hill spacing was measured by using a metric scale after transplanting. Ten randomly selected observations were taken, and the mean was calculated to represent hill spacing.

Number of seedlings per hill

The number of seedlings per hill was measured by directly counting the seedlings picked by the planting finger and transplanted in the field after transplanting. Ten randomly selected observations were taken, and the mean was determined to represent the number of seedlings per hill.

Depth of transplanting

The depth of transplanting was determined by uprooting the seedlings immediately after transplanting. The seedlings were held close to the puddle soil surface for uprooting. The distance from that point to the tip of the root was measured by scale to find the depth of transplanting. Ten randomly selected observations were taken for the depth of transplanting.

Missing hills

The number of missing hills was counted along with the total number of hills in m^2. Five observations were taken randomly, and the mean was represented as a percentage of missing hills. The percentage of missing hills was calculated using the following relationship.

$$Missing\ hills, \% = \frac{\text{Number of missing hills per } m^2}{\text{Total number of hills per } m^2} \times 100 \quad ---------- (1)$$

Floating hills

Floating hills are characterized by seedlings that are either floating on the surface or just placed on the mud's surface. Floating hills were counted in m2 area after transplanting. Five observations were taken, and the mean was calculated as a percentage of floating hills. The following formula calculates the percentage of floating hills.

$$Floating\ hills, \% = \frac{\text{Number of floating hills per } m^2}{\text{Total number of hills per } m^2} \times 100 \quad ---------- (2)$$

Burried hills

Hills that are completely buried under soil after transplanting are called buried hills. Buried hills were counted in a square meter area after transplanting. Five observations were taken, and the mean was represented as a percentage of missing hills. The following formula calculated the percentage of buried hills:

$$Burried\ hills, \% = \frac{\text{Number of burried hills per } m^2}{\text{Total number of hills per } m^2} \times 100 \quad ---------- (3)$$

Damaged hills

These can be divided into two categories. Damage is caused by cutting or bending of the seedlings, or internal damage to the growing point of the seedling due to crushing by the planting fork. Damaged hills were counted in a square meter area after transplanting. Five observations were taken, and the mean was represented as a percentage of buried hills. The following formula calculated the percentage of damaged hills:

$$Damaged\ hills, \% = \frac{\text{Number of damaged hills per } m^2}{\text{Total number of hills per } m^2} \times 100 \quad ---------- (4)$$

Theoretical field capacity

Theoretical field capacity of an implement is the rate of coverage that would be obtained if the machine were performing its function 100% of the time at the rated forward speed and always covered 100% of its rated width.

$$TFC = \frac{\mathrm{W \times S}}{C} \quad \text{.....(5)}$$

Where,

TFC= Theoretical field capacity, ha/h

W = Operating width of the machine, m

S =Speed of travel, in km/h

C = Constant, 10

Actual field capacity

The actual field capacity was determined as a function of transplanted area (A) and operation time (T) using the formula.

$$AFC = \frac{\mathrm{A}}{T} \quad \text{..... (6)}$$

Where,

AFC = Actual field capacity, ha/hr

A = Total area transplanted, ha

T = Total operating time required for transplanting, h

Field efficiency

The field efficiency is the ratio of actual field capacity and theoretical field capacity, expressed as a percentage and calculated by the following formula.

$Ef = \frac{\text{AFC}}{TFC} \times 100$ …….. (7)

Where,

Ef = Field efficiency, %

Fuel consumption

At the start of the transplanting operation, the fuel tank of the transplanter was filled with fuel, and the required fuel was measured at the end of the transplanting. Fuel consumption was calculated as a function of required fuel volume and transplanting time.

$F_{cu} = \frac{\text{V}}{T}$.....(8)

Where,

F_{cu} = Fuel consumption rate, l /h

V = Fuel used during operation, l

T = Time needed for operation, h

Effective field capacity

It is the actual area covered by the implement, based on its total time consumed and its width. For calculating effective field capacity, the time consumed for actual work and the loss for other activities, such as turning and cleaning clogged crop residues and fueling, are considered. Additionally, the effective field capacity is dependent on field patterns. The following formula calculates the effective field capacity.

$$EFC = \frac{A}{TP - T_n}$$

Where,

EFC= Effective field capacity, ha/h

A= Total transplanted area, ha

TP= Total operating time required for transplanting, h

T_n= Non-productive time, h (Time loss for turning)

Seedling and Tray Preparation

Standard-sized plastic seedling trays, measuring 58×28×2.5 cm, were used to prepare seedlings in the farmer's field. For this experiment, BRRI dhan87 variety seeds were used and sown at the specified seed rate in trays before 17 days of transplanting.

Data Collection

The following parameters were collected or measured during the experiment for each plot: seedling height, leaf number, seedling density in tray, field size and shape, machinery adjustment, seedling spacing, seedling density per hill, missing hill, floating hill, damaged hill, fuel consumption, depth of seedling, number of tray required in each decimal, number of turn, total time of operation, actual time of operation.

Field Operations

Transplanting speed: The transplanting speed was obtained by recording the time required for the mechanical rice transplanter to travel a 20 m distance in the field. The speed of transplanting can be computed using the following equation.

S = D× t /3.6 (i)

where S is the transplanting speed in Km/hr; D is the distance in m; t is the time required to cover the distance D in second

Result and Discussions

i. *Transplanting Depth:* The transplanting depth across the three treatments showed noticeable variation. The BRRI developed rice transplanter (T1) achieved an average transplanting depth of 3.10 cm, while the imported RT model (T2) showed a slightly lower depth of 3.05 cm**.** In contrast, manual hand transplanting (T3) exhibited a higher average transplanting depth of 3.36 cm **(Figure 2).** This indicates that hand transplanting ensures deeper placement of seedlings compared to both mechanical options. Both mechanical transplanting models displayed relatively uniform but shallower transplanting depths, which may affect initial plant anchorage and establishment in certain soil conditions. The slight variance between the BRRI-developed and imported models suggests minimal mechanical advantage or disadvantage in depth control precision between local and imported units.

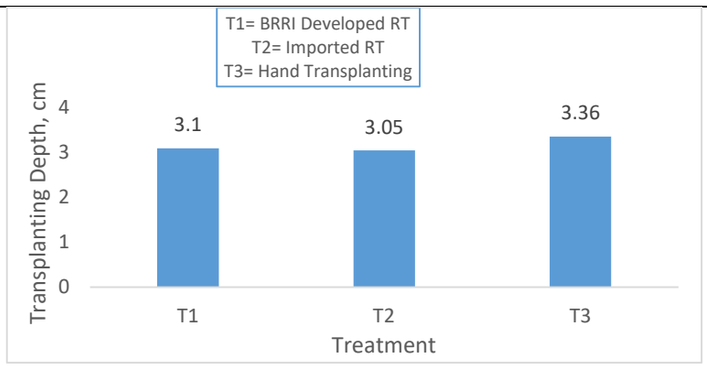

Figure 2. Transplanting depth is adjusted at different treatment depths using the depth controller

ii. ***Seedling per hill at off-field condition****:* During off-field testing on a concrete surface, the number of seedlings per hill was found almost similiar but in some cases little bit higher in the imported rice transplanter compared to the BRRI-developed model across all planting positions. At the high position, the imported RT and BRRI model delivered an average of 4 seedlings per hill, however low and medium position BRRI model delivered less seedling compared to imported model (**Figure 3)**. In the medium setting, the imported model achieved 4 seedlings per hill versus 3 in the BRRI model, marking a 14.28% rise. At the low position, the imported RT planted 3 seedlings per hill, compared to 2 from the BRRI-developed model, a 15.38% increase. This pattern suggests that the planting fingers or pickup mechanism in the imported model grips and releases more seedlings in operation. While this could enhance plant population density, especially in low-tillering or hybrid varieties, it may also risk overcrowding if not appropriately adjusted for spacing and variety type. The results indicate a need for calibration or design adjustment based on planting objectives and crop management strategies.

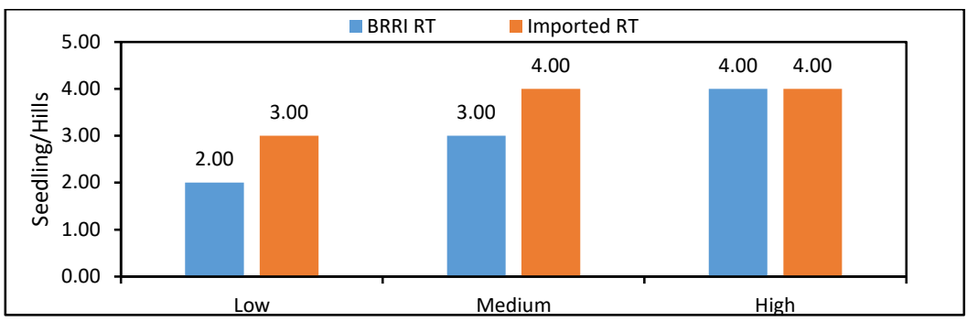

Figure 3. Seedling per hill at different positions for off-field conditions

iii. ***Seedling per hill in field condition:*** During field testing, the number of seedlings per hill showed slight variation between the BRRI-developed and imported rice transplanters, depending on tray position. At the high tray position, the imported RT placed 5 seedlings per hill, while the BRRI model placed 4, indicating a 9.09% increase**.** For the medium position, the imported RT placed 4 seedlings per hill, while the BRRI model placed 3, indicating a 9.09% increase**.** (**Figure 4)**. However, at the low tray position, both models delivered an equal number of seedlings, 3 per hill**,** showing no difference These results suggest that while performance between the two models was mainly comparable at medium depth, the imported RT tends to deliver more seedlings at both low and high positions. This implies a potentially more sensitive or responsive seedling pickup mechanism in the imported unit under field conditions. Such variations, although minor, can influence plant population density and may require machine calibration depending on the crop variety and field requirements.

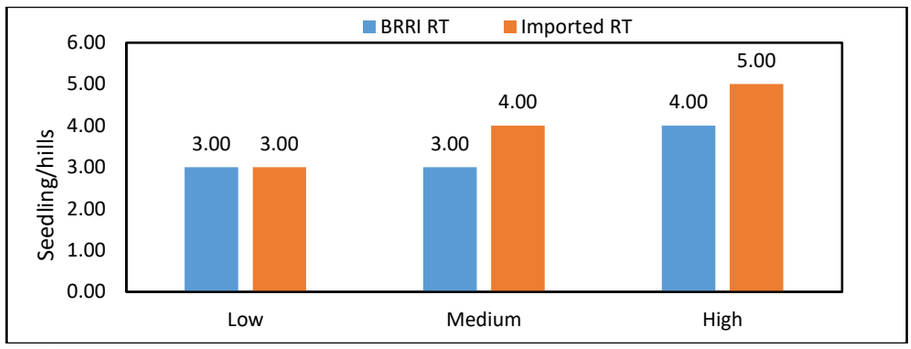

Figure 4. Seedling per hill at different positions for in-field conditions

iv. ***No. of seedlings:*** The seedling count was monitored from day 0 to 60 after transplanting to evaluate early establishment and survival. During the initial stages (0 to 30 days), the BRRI-developed rice transplanter (T1) consistently showed a higher number of seedlings per hill compared to the imported RT (T2) and hand transplanting (T3). Specifically, T1 maintained a lead at day 0, 15, and 30, indicating better early seedling placement and establishment. However, by day 45 and 60, the seedling counts for both T1 and T2 became nearly identical, suggesting that the initial advantage of the BRRI-developed RT equalized over time due to plant mortality or thinning (**Figure 5)**. Hand transplanting (T3) consistently showed a slightly lower seedling count throughout, possibly due to non-uniform planting and manual error. These results highlight the BRRI-developed RT's strength in early establishment, which may be beneficial in ensuring crop uniformity and vigor during the early growth stages.

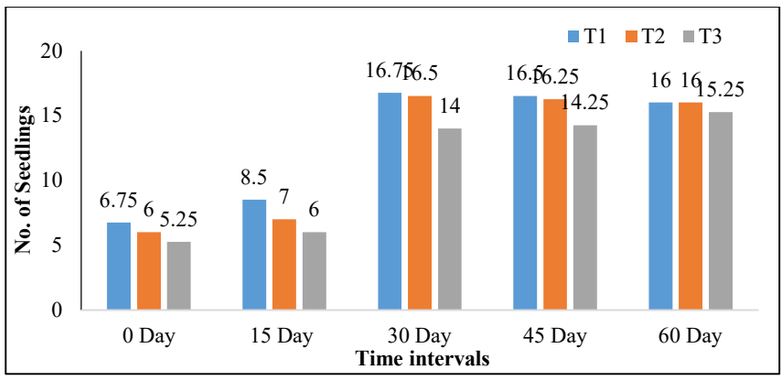

Figure 5. No. of Seedling count at different intervals of time in field conditions.

v. ***No. of Panicles:*** After transplanting, the number of panicles observed was highest in the BRRI-developed rice transplanter (T1), with an average count of 151.75, compared to 146.75 in the imported RT (T2) and 149 in hand transplanting (T3). This corresponds to a 3.29% increase over T2 and a 1.81% increase over T3**,** suggesting that the BRRI model may offer slightly better conditions for tillering and panicle development (**Figure 6)**. The higher panicle count reflects improved seedling establishment and possibly better spacing or root anchoring, especially in the early growth phase. Although the difference is modest, it indicates a performance edge of the BRRI-developed RT in supporting productive tillers, which could translate into marginally higher yield potential under similar agronomic conditions.

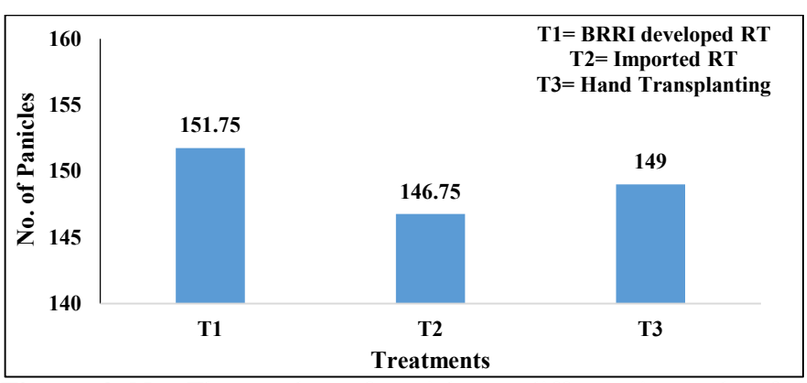

Figure 6. No. The number of panicles at different intervals of time in field conditions.

vi. ***Percent of missing hills:*** The percentage of missing hills—comprising floating, buried, and damaged hills was highest in the imported RT model (T2)**,** recording 5%**,** followed by the BRRI-

developed RT (T1) at 3.5%**,** and the lowest in hand transplanting (T3) at 2.75% (**Figure 7).** This result suggests that the imported RT may have relatively less control or stability during seedling placement, leading to a higher rate of planting errors. The BRRI-developed RT performed better in minimizing planting gaps, though it still lagged behind manual transplanting, which naturally benefits from human judgment and placement accuracy. These findings highlight the need for further optimization in mechanical transplanters to reduce missed planting spots, particularly in imported models where floating or improper placement may be more frequent.

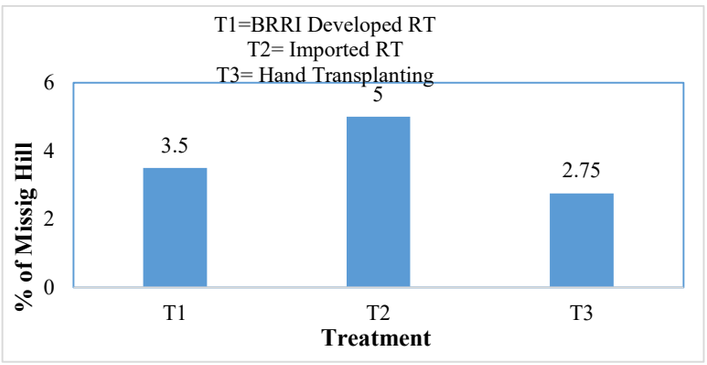

Figure 7. Percent of missing hills during field operation

vii. ***Actual field capacity:*** The actual field capacity was evaluated based on the total time taken to transplant a fixed area of 10.84 decimal. The BRRI-developed PRT2022 model completed the operation in 16.21 minutes**,** achieving a field capacity of 40.12 decimal/hr**,** while the imported RT took 18.20 minutes for the same area, resulting in a lower field capacity of 35.73 decimal/hr (Table 3). This indicates that the BRRI model performed 10.94% more efficiently in terms of area coverage per hour. The improved performance of the BRRI PRT2022 may be attributed to better maneuverability, faster transplanting speed, or reduced non-productive time. The findings suggest that the BRRI-developed transplanter offers a time-saving advantage in field operations, making it a more efficient option under similar conditions.

Table 3: Comparison of Field Operation Time and Actual Field Capacity between BRRI PRT2022 and Imported RT Models.

Model name	Starting time	End time	Total operation (min)	Area covered (Decimal)	Field capacity (decimal/hr)
BRRI PRT2022	9:41:23	9:57:45	16.21	10.84	40.12
Imported RT	10:05:32	10:23:53	18.20	10.84	35.73

viii. ***Fuel consumption:*** The fuel consumption rate was found to be slightly higher in the BRRI-developed PRT2023 model**,** which recorded a usage of 1.52 liters per hour, compared to 1.32 liters per hour in the imported RT (Table 4)**.** Despite this difference, the fuel consumption between the two models is nearly similar**,** especially when factoring in the faster operation time and higher field capacity of the BRRI model. Specifically, the BRRI PRT2023 completed the operation in 16.21 minutes, while the imported RT took 18.20 minutes for the same area. This indicates that the BRRI model consumes slightly more fuel per hour, but its higher efficiency and faster performance offset this. In practical terms, the marginal increase in fuel use is justifiable given the time savings and improved field output.

Table 4: Comparison of Fuel Consumption between BRRI PRT2023 and Imported RT Models during Field Operation

Model name	Starting time	End time	Total operation (min)	Area covered (Decimal)	Total fuel consumption (ml)	fuel consumption (l/h)
BRRI PRT2023	9:41:23	9:57:45	16.21	10.84	420	1.52
Imported RT	10:05:32	10:23:53	18.20	10.84	400	1.32

ix. ***Field efficiency:*** The field efficiency of the two rice transplanter models revealed that the BRRI-developed RT (T1) achieved a field efficiency of 79.50%**,** slightly higher than the 78.03% recorded for the imported RT (T2)**.** This represents a 1.84% improvement in efficiency for the BRRI model (**Figure 8)**. The higher efficiency indicates that the BRRI transplanter utilized productive time more effectively, likely due to reduced turning time,

quicker adjustment mechanisms, or better maneuverability. Although the margin is modest, it reinforces the advantage of the BRRI-developed RT in real-world field conditions where efficiency directly influences operational cost, fuel use, and overall timeliness of transplanting.

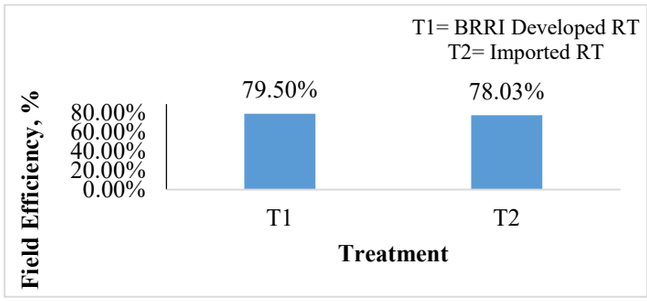

Figure 8. Field efficiency of BRRI-developed RT and Imported RT

Conclusions

Field performance of both rice transplanter and hand transplanting was found to be generally satisfactory. No breakdowns occurred during operation. The fingers and fork worked well without clogging. However, the depth control mechanism was more comfortable in the BRRI-developed PRT model compared to the imported RT model. The field capacity of the BRRI-developed model was higher than that of the imported RT model. The field efficiency of the BRRI-developed was 79.5%, which is 1.84% higher than the imported RT. The working time includes both productive time (transplanting) and non-productive time (losses in the field). Proper transplanting depth and speed help reduce missing, floating, damaged, and buried hills. Based on these observations and experiments, it can be concluded that the BRRI-developed rice transplanter is more efficient and suitable than the imported one.

Experiment 1.2: Design, development, and performance evaluation of a BRRI head feed combine harvester (funded by SFMRA project)

Principal Investigator: Arafat Ullah Khan
Co-Investigator: AKMSI, JN
Objectives

- To design and develop a BRRI head feed combine harvester
- To evaluate the field performance of the developed head feed combine harvester
- To compare the performance with an imported combine harvester

Materials and Methods

There are several types of combine harvesters available at the field level, which are imported from China, Japan, Korea, and other countries of the world. The adoption of the combine harvester depends on factors such as the size of the land, the types of crops, and the purchasing power of the user. Consideration of engine power, ground pressure, cutting width, harvesting capacity, harvesting loss, plot area, land condition, ease of operation, plot size, land condition, and business viability of the imported combine harvester, a prototype of a head feed combine harvester was fabricated at Alim Industries Ltd, Sylhet with the help of other local agricultural machinery manufacturers. The prototype was fabricated using locally available raw materials except the crawler, gearbox, and engine. Rubber track/crawler and engine were imported with the help of a local agricultural machinery importer. The gearbox is also imported and used with some modifications.

Design Consideration

The research idea for the head feed combine harvester emerged in response to the existing demand for Bangladeshi farmers to meet the targets outlined in the mechanization roadmap and policy. The head feed combine harvester consists of a basement, main body, engine unit, header, conveying hopper, threshing, and storage units. The machine will, in addition to providing better operating conditions for the operator, also be designed to provide good visibility lighting when required. The design of the BRRI head feed combine harvester was done with the help of AutoCAD engineering tools (software). The prototype of the machine was fabricated in Alim Industries Ltd, Sylhet, according to the design. Laboratory tests and field tests of the developed head feed combine harvester were conducted in both workshop and field conditions. The design considerations of a combine harvester are as follows:

- Locally available raw materials should be used to minimize the fabrication cost
- Easy to repair and maintain using local spare parts
- It should have a single delivery chute to avoid grain cracks or regular troubles
- The overall dimension of the machine should be less than 2000mm to transport from one place to another
- Delivery unit without cutting blade
- Grain tank with a minimum half-ton capacity
- Ground clearance greater than 270mm
- Four-cylinder engine to avoid excessive vibration and noise
- Weight of the harvester is about 3000 kg
- Power transmission should be mechanical with HST
- Harvesting capacity minimum 1 acre with minimum loss (1%).

Conceptual framework

The research is conducted according to a conceptual framework that encompasses an in-depth performance analysis of available combine harvesters used at the field level, design considerations tailored to Bangladesh's conditions, fabrication utilizing locally sourced quality materials, testing under both load and unloading conditions, fine-tuning, evaluation, and finalization of the machine (Figure 9).

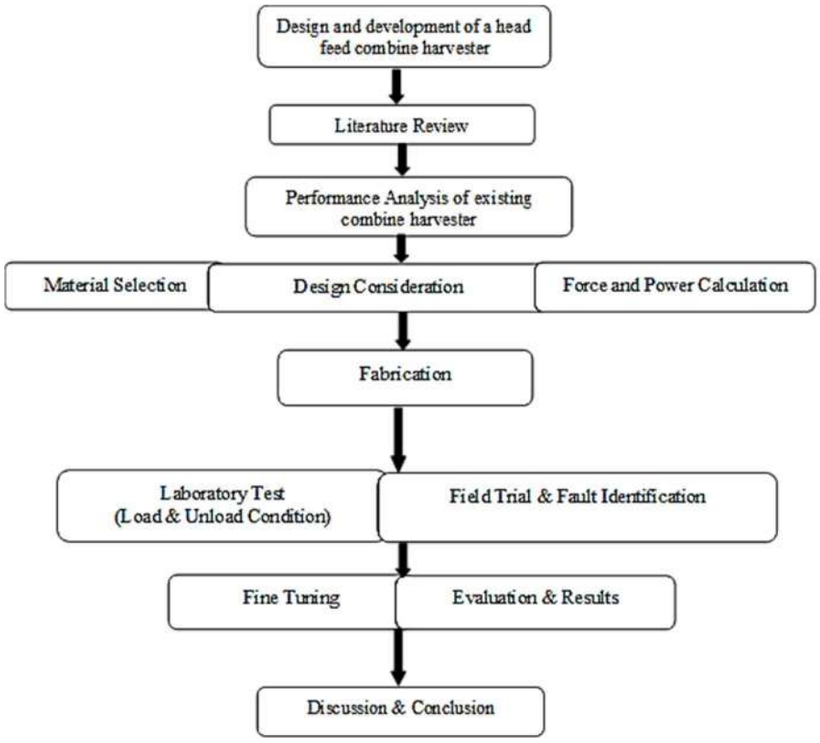

Figure 9. Conceptual framework

Table 5 describes the Design steps of the proposed BRRI head feed combine harvester

Table 5: Design steps of the proposed BRRI head feed combine harvester

First step	**Second step**
➢ **Walking Section** 1. Original Base Assembly 2. Walking Wheels Assembly 3. Double Brace Bar Assembly 4. Guide Wheel Assembly 5. Supporting Wheel Assembly 6. Thrust Wheel Assembly 7. Crawler Assembly	➢ **Main Power Section** 1. Main Gear Box Assembly 2. Engine Assembly
Third step	**Fourth step**
➢ **Operating Section** 1. Panel Board Side Assembly 2. Ready water Box and Cover Assembly 3. Manipulation Turning Assembly 4. Main Gearshift Operating Assembly 5. Auxiliary Gearshift Operating Assembly 6. Working Clutch Operating Assembly 7. Walking Clutch and Tension Wheel Assembly 8. Reel Lifting up/down Operating Assembly 9. Parking Brake Assembly	➢ **Hydraulic Section** 1. No. 1 Slide Valve Hydraulic System Assembly 2. No. 2 Slide Valve Hydraulic System Assembly 3. HST Type Oil Supply System Assembly 4. Hydraulic Oil Tank Assembly 5. Hydraulic Transmission Input Assembly

10. Tension Pulley Assembly	
Fifth step ➢ **Cleaning Section** 1. Left and Right Rack Plate Assembly 2. Front Fan Assembly 3. Vibrating Screen Assembly 4. Screen Plates Assembly 5. Straw-Expelling Plate Assembly 6. Screen Body Assembly 7. Separating Plate Assembly 8. Vibration Screen Rear Axle Assembly 9. Cylinder Assembly 10. Suction Fan Gear Box (internal) Assembly 11. Suction Fan Gear Box (external) Assembly 12. Suction Fan Guide Assembly	**Sixth step** ➢ **Grain Conveying Section** 1. No. 1 Conveying Auger Assembly 2. No. 1 Horizontal Auger Assembly 3. No. 2 Conveying Auger Assembly 4. No. 2 Horizontal Auger Assembly 5. No. 1 Bottom Gearbox Assembly 6. No. 1 Lifting / Conveying Auger Assembly 7. No. 2 Lifting / Conveying Auger Assembly 8. No. 2 Bottom Gearbox Assembly
Seventh step ➢ **Threshing Section** 1. Left and Right Rack Plate Assembly 2. Concave Screen Assembly 3. Separation Drum Assembly 4. Dusting Fan Assembly 5. Upper Frame Assembly 6. Rack Assembly 7. Rotary Axis Assembly 8. Tension Assembly 9. Roller Cover and Roller Cover Handle Assembly 10. Resale and Open Handle Assembly 11. Roller Shaft Assembly 12. Threshing drum Barrel and Threshing Drum Tooth Assembly 13. Feeding Chain Frame Assembly 14. Feeding Chain Assembly 15. Row of Grass Ear End Chine Assembly 16. Grass Guide Assembly	**Eighth step** ➢ **Large Grain Tank Section** 1. Big Grain Tank 2. Portfolio Cover Assembly 3. No. 3 Vertical Auger Assembly 4. Welded No. 3 Horizontal Auger Assembly 5. No. 3 Bottom of the gearbox combination Assembly 6. Gearbox Assembly 7. Transmission Input Assembly
Ninth step ➢ **Header Section** 1. Harvest Gear Box and Harvest Shaft Box Assembly 2. Harvester Drive Case and pick-up Driving Shaft Assembly 3. Pick-up Speed Change Case and Pick-up Gear Case Assembly 4. Pick-up Drive Case Assembly 5. Right Crop-Root Conveying Case 1 and 2 Assembly 6. Left Crop-Root Conveying Case and Feed Case Assembly 7. Harvest Frame and divider Assembly 8. Pick-up Frame and Pick-up Chain Assembly 9. Side Cover and Pic-up Support Assembly 10. Dustproof Cover and Blade Reaping Assembly 11. Blade Reaping Crank 1(LH) and 2(LH) Assembly 12. Blade Reaping Crank 1(RH) and 2(RH) Assembly 13. Packer Left, Center, Right Assembly 14. Conveying Left, Center, Right Assembly 15. Conveying guide Bar and Crop-Root Frame LH/RH Assembly 16. Crop-Root Rail, Crop-Root Tension and Crop-Root Retainer Assembly 17. Crop-Head Frame 1 and 2 Assembly 18. Crop-Head Tension 1 and 2 Assembly 19. Feeding Frame and Crop- Root Feed Cover Assembly 20. Rail Base and Crop-Head Guide Plate Assembly 21. Depth Frame and Depth Chain Assembly Depth Swing Case and Depth Motor Assembly	

Design and drawing of fabricated parts

Based on the design consideration, the conceptual design of the head feed combine harvester was modeled using AutoCAD engineering tools (software).

Modeling and assembly

The research idea for the head feed combine harvester emerged in response to the existing demand from Bangladeshi farmers to meet the targets outlined in the mechanization roadmap and policy. The harvester consisted of a basement, main body, and engine unit, as well as cutting, conveying hopper, threshing, and storage units. The machine will provide better operating conditions for the operator by offering a seat and cover, and will also be designed to provide good visibility lighting when required. The power transmissions were achieved through the use of B & C type belts, V-groove

pulleys, and chain sprockets to transmit power from the engine to the gearbox, then to the crawler and conveyor belt, cutting section, threshing and winnowing unit. Another transmission line was designed with a blower pulley, grain discharge, and a recycle auger. Existing design types, operations, efficiency, materials, weight, and cost were examined during the design of the machine. Several common factors, such as weather, topography, and farming system, about the region of operations were also considered to meet the demand of the local farmers of Bangladesh.

Basement

The machine's basement, made of an MS box, houses the crawler, engine, and main body, and is connected to the harvester's cutting section.

Engine

Engine power is measured based on the sum of the required power of the cutting unit, conveyor unit, threshing unit, winnowing unit, discharge unit, and travelling unit, considering sixty percent engine efficiency. A 77 hp diesel engine is used to transmit power through a belt-pulley, chain sprocket, and shaft to different parts of the harvester. A self-starter is also used to run the machine.

Threshing section

The threshing part consists of the top cover, the concave screen, the driving middle axle, and the front and rear threshing rollers.

Winnowing section

The winnowing part consists of a vibrating screen, a screen plate, a screen body, a separating plate, and a blower.

Field performance

The field performance of BRRI head feed combine harvester was done during Aman 2024 season at the BADC farm and farmers field in Sylhet district and West Byed research plot at Bangladesh Agricultural Research Institute in the presence of Honorable Secretary of MoA, Director General of Research Institutes, Director (Research), Director (Admin & standard service), Project Director, Divisional Scientists, Bangladesh Agricultural University teacher, local agricultural machinery manufacturer, operator of imported combine harvester and farmers. All the members present at the field test expressed satisfaction over the effectiveness of the head feed combine harvester. The specifications and results of the field test are summarized in Table 6. The development and detailed study will be conducted during the next Boro and Aman season of 2024.

Plate 3. Field performance of the developed BRRI head feed combine harvester

Table 6: The specification of the BRRI head Feed Combined Harvester

Particulars	Unit
Model	BRRI HCH2023
Dimension, mm (L×W×H)	4250×2030×2580
Cutting width, mm	1450
Rubber track (Crawler)	400×90×51
Engine power, hp	77, 4 cylinder
Engine type	Diesel Engine
Grain tank, kg	500-550
Hydraulic cylinder, kg	2000
Fuel tank capacity, L	60
Total weight, kg	2900
Ground clearance, mm	250
Forward speed, km/h	4-7

Sensor indicator	Grain tank, fuel tank, straw delivery
Harvesting capacity, acre	1-1.2
Fuel consumption, Lh^{-1}	12~13
Total harvesting loss, %	Less than 1.25~1.5%

Performance indicating parameters

To evaluate technical and economic performances of the combine harvester during paddy harvesting and performance indicators were identified i.e. (i) operational time, (ii) labor requirement for harvesting, (iii) fuel consumption, (iv) field capacity, (v) working speed, (vi) effective harvesting time, (vii) grain yield and (viii) grain losses.

Field capacity

For evaluation of field capacity, the following data were taken during paddy harvesting operation: (i) area of the plot; (ii) forward speed of the machine; (iii) cutting width of the machine; (iv) time required to harvest the specified area.

Forward speed

Forward speed was measured by dividing the distance by the time required to travel that distance. The following equation was used to determine the forward speed of a combine harvester (Hunt, 1995).

Forward speed (km/h), S = 3.6D/t ……(i)

where, D = distance (m) and t = time (s).

Effective field capacity

The effective field capacity is the actual average rate of coverage by the harvester, based upon the total field time. The area covered divided by the total time is the effective field capacity. The effective field capacity was determined by measuring all the time elements involved while harvesting (Hunt, 1995).

Effective field capacity (ha/h), Ceff = A / T.....(ii)

where, T = total time for reaping operation (h) and A = area of land reaping at specified time.

Fuel consumption

For economic analysis, fuel consumption was determined after harvesting of each plot. Before starting the harvesting operation, the fuel tank of the combine harvester was filled up. At the end of the harvesting operation of each plot, the required fuel to fill the tank was determined by using a measuring flask. For determining fuel consumption per unit area, the following equation was used (Hunt, 1995).

Fuel consumption (L/ha), F = Fa/A ....……...…(iii)

where, Fa = fuel used during operation (l) and A= area of operation, (ha).

Determination of harvesting losses

In general, four types of losses are considered when using a combine harvester. These are i) shatter loss, ii) cutter bar loss, iii) cylinder loss, and iv) separating loss. In the experiment, the following procedures were considered for mechanical harvesting losses measurement.

i) Shatter loss

Shatter losses in direct combining include heads, pods, or ears, and free grain, lost during cutting and conveying operations. The following equation was used to determine the shatter loss (Hunt, 1995).

Shatter loss, kg/ha= D/A ……(iv)

Where, D = average weight of dropped grain on the ground during cutting and conveying (kg), and A =area (ha)

ii) Cutter bar loss

Cutter bar loss refers to grains that are lost due to rough handling by the cutter bar. The following equation was used to determine cutter bar loss (Hunt, 1995).

Cutter bar loss (kg/ha) = Average weight of grain lost due to cutter bar, kg /Area Covered, ha.....……(v)

iii) Cylinder loss

Grains lost at the rear of the combine, in the form of threshed heads, indicate cylinder loss. The following equation was used to determine cylinder loss (Hunt, 1995).

Cylinder loss, kg/ha = Average weight of unthreshed heads lost out the rear of combine, kg /Area Covered, ha.....…….(vi)

iv) Separating loss

Separating loss refers to the grains lost from the rear of the combine, in the form of threshed grain. The following equations were used to determine separating loss (Hunt, 1995).

Separating loss, kg/ha = Average weight of threshed grains lost out the rear of the combine, kg /Area Covered, ha.....…….(vii)

Total loss and percent of loss

The summation of all losses is the estimated total manual harvesting loss. The following equations were used to determine the total manual harvesting loss and the percentage of loss.

Total loss (g) = Shutter loss (g) + Cutting loss (g) + Gathering loss (g) + Carrying loss (g) + Threshing loss (g) + Cleaning loss (g) .....(viii)

Loss (%) = Total loss/ Total yield × 100 …….....(ix)

Grain weight measurement

After mechanical harvesting of paddy, all losses were collected in a polythene bag, weighed using a digital balance, and recorded for analysis.

Financial analysis

For the financial performance evaluation of a combine harvester during mechanical harvesting of paddy, the cost of operation of the harvesting machine was determined by calculating fixed and variable costs. Harvesting cost, time, and labor involvement in mechanical harvesting were also measured.

Results and Discussion

Technical performance of a combine harvester. After mechanical harvesting using a combine harvester during Aman/2024 at Sylhet district and West Byed research plot at Bangladesh Agricultural Research Institute of Bangladesh, average values of forward speed, fuel consumption, and effective field capacity were determined as presented in Table 7. The average values of forward speed, fuel consumption, and effective field capacity were found to be 6.71 km/h, 10.76 L/h, and 0.33 ha/h, respectively. The total area was 0.28 ha for experimenting with a mechanical harvester. Slight variations of these parameters in three plots are mainly due to the variation of the operator's skill, soil condition, and plot size.

Table 7: Technical performance of the combine harvester

Plot	Forward speed (km/h)	Fuel Consumption		Effective Field Capacity (ha/h)
		(L/ha)	(L/h)	
Plot 1	6.48	29.63	10.37	0.35
Plot 2	6.98	34.09	11.25	0.33
Plot 3	6.66	34.39	10.66	0.31
Average	6.71	32.70	10.76	0.33

Economic analysis of a combine harvester

Economic analysis was carried out and supported that investment in a combine harvester is highly profitable. Khadr et al. (2009) obtained similar results, with costs saved 58.3% for using a Yanmar combine and 56.7% for using a Kubota combine harvester over the manual harvesting system. Cost savings depend on machine conditions, including increased fuel consumption, higher repair and maintenance costs, and a gradual decrease in field capacity.

Paddy harvesting losses from the harvesting to the cleaning operation

Mechanical paddy harvesting losses (harvesting to cleaning operation) were measured, and to calculate mechanical harvesting losses, 3 (three) plots were harvested using the combine harvester, and harvesting losses were found to be 1.26%, 1.36% and 1.38%, respectively, in plot-1, plot-2, and plot-3 (**Table 8)**. These results represent the total harvesting loss of each plot during mechanical harvesting. Finally, average total paddy harvesting losses were found to be 1.33% using a combine harvester. The average mechanical harvesting loss using the combine harvester is comparatively less than that of the manual harvesting system.

Table 8: Grain losses during harvesting by a combine harvester

Plot	Total loss, %	Average loss, %
Plot 1	1.26	

Plot 2	1.36	1.33
Plot 3	1.38	

Loss of paddy saved using mechanical harvesting

A comparison of paddy loss between the combine harvester and manual harvesting systems revealed that the combine harvester saved 4.47% of paddy. Amponsah et al. (2017) mentioned grain loss using a combine ranging from 1.43% to 4.43% and 1.85% to 5.6% for two different rice varieties, respectively. Kannan et al. (2013) reported similar post-harvest loss of paddy. They found a 6.87 percent manual harvesting loss. Hossain et al. (2015) estimated that the average grain saving from loss reduction by a combine harvester over manual methods was 2.75%. Paddy loss might vary with the operator's skill, soil condition, harvesting time, and agronomic characteristics of the paddy. Generally, early harvesting reduced pre-harvest and shattering loss in operation; on the other hand, delayed harvesting caused more loss due to low moisture content and faced natural calamities.

Labor is saved over manual harvesting.

Labor requirements during paddy harvesting using a combine harvester and a manual system were measured. Total labor required was found to be 18 man-day/ha and 61 man-day/ha for using a combine harvester and a manual system, respectively. Labor requirement during paddy harvesting by a combine harvester was less than that of the manual harvesting system. Labor could be saved 70% by using the combine harvester over manual harvesting of paddy.

Conclusion

This research shows it's feasible to design and produce a combine harvester to address farmers' harvesting issues in Bangladesh. The machine's technical and financial parameters were carefully evaluated and compared with manual harvesting. Results indicate that using a combine harvester is highly profitable, with cost savings of 57.61% and labor savings of 70%. Paddy loss decreases by 4.47% compared to manual methods. Overall, mechanical harvesters save time, labor, and costs, reduce losses and human effort, and increase crop productivity and rural livelihoods. Efforts ensured production costs are minimized, making the harvester accessible to small-scale farmers. It is more efficient for fragmented farms than imported models. The BRRI-developed head feed combine can meet domestic needs, reduce imports, and be exported with government support.

Experiment 1.3: Harvesting Performance and grain losses: Impact of paddy harvester type, speed, and crop density

Principal Investigator: Md. Anwar Hossen
Co-Investigator: BCN, SP, AUK, JN

Methodologies

Holistic research approaches were applied to validate and upscale the imported combine harvester (whole feed) in Sadar upazila of Habiganj district (24.351263 N, 91.424143 E) and Raiganj upazila of Sirajganj district (24.5295° N, 89.5452° E) of Bangladesh. In the Boro/2023-24 season (Irrigated dry season), two models, Zoomlion (FH-100) and Lovol (RG108PLUS), of whole feed combine harvesters were studied to identify the field performance and grain losses of whole feed combine harvesters under different forward speeds and crop densities in the Boro season.

Physical parameters of the studied combine harvester

Before the field study, each model's dimensions, load-bearing capacity, and cutting width were measured; nevertheless, general data about the combine harvester's engine and machine were also recorded from stickers (Table 9-10).

Table 9: Whole feed Combine Harvester: ZOOMLION (FH100)

Items	Name/specification
1. Physical Information	
1.1: Brand	ZOOMLION
1.2: Model	FH100
1.3: Country of origin	China
1.4: Country of Manufacturer	China
1.5 Types (Head feed/whole feed)	Full feed type
1.6: Wheel type (Tyre/crawler)	crawler
2. Dimensions	
2.1: Overall length × width × height (mm)	5270×2600×2960
2.2: Overall weight (kg)	3300
2.3: Displacement (CC)	3470
2.4 Engine power (kW)	
2.5: Fuel	
▪ Tank capacity (L)	160
▪ Provision for draining of sediments/water	Second stage
2.6: Oil	
▪ Capacity (L)	20（Hydraulic Oil）
▪ Oil changing period	50 hours for the first time, then every 300 hours afterwards
2.7: Grain tank	
▪ Capacity (kg)	1500 liter
▪ Grain discharge system	Hydraulic high-level unloading
3. Prime mover (Discourage)	
3.1: Brand (Make)	Quanchai
3.2: Model	4C6-100M22
3.3: Type and number of cylinders	4-cylinder, in-line, water-cooled
3.4: Engine speed (rpm)	2400
4. Travelling	Given
4.1: Steering	Unilateral braking steering
4.2: Gearshift	
▪ Forward speeds (m/s) km/hr	2.1m/s
▪ Reverse speeds (m/s) km/hr	1.4m/s
4.3: Driving wheel/crawler	
▪ Type	crawler
▪ Number and size (Pitch x Number x width)	2（500mm×90mm×53 sections）
▪ Track width (mm)	500
▪ Load per unit area (Kg/mm^2)	0.00402439
5. Reaping	Given
5.1: Reaping mechanism	Reel + cutter + feed screw
5.2: Cutter bar	
▪ Working width (mm)	2200
▪ Effective width (mm)	2000
6. Threshing Drum	Given
6.1: Type	Pin-tooth structure
6.2: Width (mm)	2000mm
6.3: Outside dia (mm)	620mm

Table 10: Whole feed Combine Harvester: LOVOL (RG108 PLUS V2.0)

Items	Name/specification
1. General Information	
1.1: Brand	LOVOL
1.2: Model	RG108 PLUS V2.0
1.3: Country of origin	CHINA
1.4: Country of Manufacturer	CHINA
1.5 Types (Head feed/whole feed)	Water Cool
1.6: Wheel type (Tyre/crawler)	Crawler
2. Dimensions	
2.1: Overall length × width × height (mm)	5200×254×2800
2.2: Overall weight (kg)	2970
2.3: Displacement (CC)	1470
2.4: Engine power (kW)	72.08
2.5: Fuel	
▪ Tank capacity (L)	165
▪ Provision for draining of sediments/water	

Items	Name/specification
2.6: Oil	
▪ Capacity (L)	9
▪ Oil changing period	200 h
2.7: Grain tank	
▪ Capacity (kg)	1200
▪ Grain discharge system	Auger
3. Prime mover (Discourage)	
3.1: Brand (Make)	QUANCHAI
3.2: Model	4C6-100M22
3.3: Type and number of cylinders	4-stock in line-vertical water cool-supercharge
3.4: Engine speed (rpm)	2500
4. Travelling	
4.1: Steering	Lever/Yes
4.2: Gearshift	Lever/Yes
▪ Forward speeds (m/s)	0-1.65
▪ Reverse speeds (m/s)	0-1.35
4.3: Driving wheel/crawler	
▪ Type	Crawler
▪ Number and size	2/ 56
▪ Track width (mm)	500
▪ Traction area (mm2)	2170000
▪ Load per unit area (kg/mm2)	0.001368
5. Reaping	
5.1: Reaping mechanism	
5.2: Cutter bar	
▪ Working width (mm)	2380
▪ Effective width (mm)	2000
6. Threshing Drum	
6.1: Type	
6.2: Width (mm)	2058
6.3: Outside dia (mm)	2050

Table 11: Basic Information on the trials

Items	Sirajganj	Habiganj
1.1: Season	Boro/2023-24	Boro/2023-24
1.2: Crop (Rice/wheat) and variety	Rice and BRRI dhan92	Rice and BRRI dhan92
1.3: Soil/field condition		
▪ Type	Sandy loam type and wet condition	Sandy loam type and wet condition
▪ Standing water (if any, mm)	No	No
1.4: Crop condition		
▪ Height of crop (mm)	1092	1075
▪ Lodging condition	No loading	No loading
▪ Grain maturity (%)	84	87
▪ Grain moisture content (%)	22.95	23.02
1.5: Date of harvesting	08/06/24	31/05/24
1.6: Cutting height (mm)	300-350	300-350
1.7: Crop yield at 14% m.c (t/ha)	7.70	7.68
1.8: Field size		
▪ Length (L) and width (W) in meters	75.0 and 50.0	60.0 and 50.0
▪ Area (A) in ha	0.375	0.300

Field condition and Crop attributes

In the Boro/2023-24 season, the study has been conducted in two different locations of the country (Table 11). Only the whole feed type combine harvesters were used to determine the effect of forward speed and plant Density (tiller/m^2) on the field performance and grain losses of the machine. BRRI dhan92 was harvested in both locations of Sirajgaj and Habiganj. Prior to operation, plant height, average grain moisture content, average grain yield, and average grain maturity during harvesting (%) of the crops were measured (Table 11). The hard soil layer in the respective field locations was almost the same. The hard soil layer was measured manually during machine operation (Table 12). The soil type of the field and field conditions during machine operation are also presented in Table 12.

Table 12: Field size and condition

Trials	Depth of hard soil layer (mm)	Soil type	Field condition (dry/wet/standing water in mm)
1	22.5	Sandy	Wet
2	29.0	Sandy	wet
3	32.5	Sandy loam	wet

Experimental design

A three-factor design was used, where the two whole-feed combine harvester models were tested in three locations with three replications. Within each area, the same field length (m), the same cutting height, and the same operator's skill were used. Factor 1 (2 levels): Combine harvester model/type (e.g., Model A: Zoomlion-FH100 and Model B: Lovol-RG108+), Factor 2 (3 levels): Forward speed (e.g., low: 4-5, Medium: 5-6 and high: 6-7 km/h) and Factor 3 (2 levels): Plant density (e.g., low: 250-300 and high: 301-350 plant/m^2) were considered to conduct the study. Each combination is replicated three times, resulting in 36 experimental plots**.**

Data collection and calculation procedure

Three different speed levels were identified and marked on the machine to maintain the respective speeds during the field operation of the combine harvester. The lengthwise time per pass, without accounting for turning or any other losses, was measured to determine the theoretical field capacity of the machine as well as its forward speed. Total operational time and total area were measured to calculate the effective field capacity for different field lengths. The machine's field efficiency in the specified type of field was computed using both the actual and theoretical field capacity. Forward speed was determined by dividing the distance by the time needed to run the machine over that distance. The actual average rate of harvester coverage, depending on the total time of operation, is known as the actual field capacity. The actual field capacity is calculated by dividing the area covered by the entire time. Theoretical field capacity is the rate of field coverage of an implement that would be obtained if the machine were performing its function 100% of the time at the rated forward speed and always covered 100% of its width. Field efficiency is the ratio of effective field capacity and theoretical field capacity, expressed in percentages.

Grain losses analysis

Pre-Harvest Losses

Grains lie on the ground in the standing crop ahead of the combine before the harvesting operation. These losses include shattered grains, broken grains in panicles or broken stems used by insects, weeds, rusts, and wind.

Header loss

Grains on the ground due to the processes that take place at the head, including guiding, gathering, cutting, and conveying, which is the process of feeding the crop into the machine header prior to hushing. Header loss results from several factors, including cutter bar strokes, the height of the reel, reel peripheral speed, travel speed, the width of harvest, the height of cutting, crop moisture, height and density of crop, and feed rate of the crop. These losses include-

- **Shatter Loss:** Rice Grains shattered on the ground during the head operation.
- **Stubble Loss:** Grains in panicles attached to the plant stem below the height of the cutter bar remain there after the passage of the machine.
- **Loose Stem Loss:** Grains in panicles attached to stems that are cut but are not recovered by the header.
- **Lodging loss:** Grains in panicles in stems that are uncut but lie on the ground. > Grains in panicles on uncut stems lying on the ground.

Cylinder Loss

Unthreshed grains that are left behind by the combine head are transported to the machine's rear via a straw rack. This loss is dependent on feed rate, cylinder/rotor speeds, concave clearance, and crop moisture.

Separation loss

Threshed loose grains are discharged at the back of the combine along with the straw, following a separation and cleaning process by sieves and walkers, or a chain conveying process for straw. The

separating and cylinder losses of the combine harvester were measured by collecting grains and straw in a net placed behind the harvester. The measurements were taken over a 15-meter length, covering the full cutting width of the combine harvester after completing all processing.

Calculation of the Harvest losses (%)

$$Harvesting\ Loss = Head\ Loss\ (\%) + Cylinder\ Loss\ (\%) + Separation\ Loss\ (\%)$$

Where,

$$\textbf{\textit{Header Loss}}\ (\%) = \frac{Weight\ of\ head\ loss\ grains}{Total\ weight\ of\ grains\ from\ the\ measurement\ section}\ x\ 100$$

$$\textbf{\textit{Cylinder Loss}}\ (\%) = \frac{Weight\ of\ cylinder\ loss\ grains}{Total\ weight\ of\ grains\ from\ the\ measurement\ section}\ x\ 100$$

$$\textbf{\textit{Separation Loss}}\ (\%) = \frac{Weight\ of\ separation\ loss\ grains}{Total\ weight\ of\ grains\ from\ the\ measurement\ section}\ x\ 100$$

Analysis

Data were analyzed using a one-way factorial design (field length) according to Gomez and Gomez (1984) with the Statistix 10 program. Means were compared using the least significant difference (LSD) at the specified level of significance, also using the Statistix 10 program (Statistix 10 Software, 2013).

Results and discussions

A total of two trials were conducted in the Boro/2023-24 season using a three-factor design, where the two different models of whole feet combine harvesters (Zoomlion-FH-100 and Lovol-RG108+) were tested in two different crop densities under three varying speeds. Within each location, the same field length (m), same cutting height, and same operator's skill were evaluated, with three replications. The analysis data are presented below.

Operational performance

Actual Field Capacity

The interaction effects among machine model (M), forward speed (S), and crop density (CD) on actual field capacity (ha/h) were not statistically significant ($p > 0.05$), indicating that their combined influence did not introduce any distinct variation beyond the effects observed in individual and two-factor interactions. Although actual field capacity varied across different machine models, forward speeds, and crop densities, no significant three-way interaction was detected (Table 13). The highest actual field capacity was observed at the highest forward speed (6–7 km/h) for both combine harvester models, Zoomlion-FH-100 and Lovol-RG108+, across both crop densities. Conversely, the lowest actual field capacity was recorded at the lowest forward speed (4–5 km/h) for both harvester models and crop densities. Among the two models, Zoomlion-FH-100 consistently exhibited a higher actual field capacity compared to Lovol-RG108+ at all speeds and crop density levels. The interaction between machine model and forward speed was not significant ($p > 0.05$), indicating that forward speed affected actual field capacity similarly across both machine models. However, actual field capacity increased as forward speed increased in both Zoomlion-FH-100 and Lovol-RG108+, following a similar rate of increase. Similarly, the interaction between machine model and crop density was not significant ($p > 0.05$), suggesting that crop density influenced actual field capacity in both harvester models similarly. Both models exhibited higher actual field capacity at lower crop density (251–300 plants/m²) compared to higher crop density (301–350 plants/m²), with Zoomlion-FH-100 outperforming Lovol-RG108+ in both cases. However, no statistical evidence indicated a machine-specific advantage in handling different crop densities. The interaction between forward speed and crop density was also not significant ($p > 0.05$), demonstrating that the increase in actual field capacity with increasing forward speed occurred independently of crop density. Across all density levels, actual field capacity was highest at the highest forward speed (6–7 km/h) and lowest at the lowest speed (4–5 km/h). Lower crop density (251–300 plants/m²) resulted in slightly higher actual field capacity compared to higher crop density (301–350 plants/m²), but the rate of increase due to speed remained consistent. Conversely, the single effects of machine model, forward speed, and crop density were all statistically significant ($p < 0.05$). Zoomlion-FH-100 exhibited a significantly higher mean actual field capacity (0.77 ha/h) compared to Lovol-RG108+ (0.68 ha/h),

confirming its superior operational performance. Forward speed significantly influenced actual field capacity, with the highest capacity (0.81 ha/h) recorded at 6–7 km/h and the lowest (0.68 ha/h) at 4–5 km/h. Crop density also had a significant effect, where a density of 251–300 plants/m² resulted in a higher actual field capacity (0.77 ha/h) compared to 301–350 plants/m² (0.71 ha/h). These findings highlight the individual influence of each factor on actual field capacity, despite the absence of significant interaction effects.

Table 13: Effect of forward speed, crop density (plants/m^2), and brand/model of combine harvester on Actual field capacity (ha/h)

Machine Brand	Crop Density	Forward speed of operation (km/h)			Mean
		S1	S2	S3	
M1	CD1	0.71	0.76	0.84	0.77
	CD2	0.66	0.71	0.78	0.71
M2	CD1	0.62	0.67	0.74	0.68
	CD2	0.57	0.62	0.68	0.62
Mean		0.64	0.69	0.76	
LoS		M=*, S=*, CD=*, M×S=ns, M×CD=ns, S×CD=ns, M×S×CD=ns			
$LSD_{0.05}$		M=0.026, S=0.019, CD=0.016			
% of CV		3.29			

Note: * means $P \leq 0 \cdot 05$, ** means $P \leq 0 \cdot 01$, *** means $P \leq 0 \cdot 001$, NS means Non-significant, LoS means level of significance, M=Machine Brand/Model (M1=Zoomlion-FH-100 and M2=Lovol-RG108+), S=Forward speed (S_1=4-5, S_2=5-6 and S_3=6-7 km/h), CD=Crop density (CD_1=251-300 and CD_2=301-350 plants/m^2).

Figures 10 and 11 analyze the influence of forward speed, crop density, and machine model on actual field capacity (ha/h) in combine harvester operations. The results indicate that forward speed significantly impacts field capacity, with the highest recorded capacity of 0.81 ha/h at 6–7 km/h (S3). Among the two tested models, Zoomlion-FH-100 demonstrated superior field capacity (0.77 ha/h) compared to Lovol-RG108+ (0.68 ha/h), emphasizing the role of machine design in harvesting efficiency. Crop density also exhibited a substantial impact, where lower plant density (251–300 plants/m², CD1) resulted in a higher field capacity (0.77 ha/h), whereas higher plant density (301–350 plants/m², CD2) reduced capacity to 0.71 ha/h. The interaction of forward speed and crop density revealed that the highest actual field capacity is achieved at 6–7 km/h (S3) with lower crop density (CD1). Conversely, the lowest field capacity was recorded at 4–5 km/h (S1) under higher crop density (CD2), where the harvester experienced greater resistance in cutting and threshing operations. These findings suggest that optimizing both speed and crop density is crucial for enhancing the operational performance of combine harvesters.

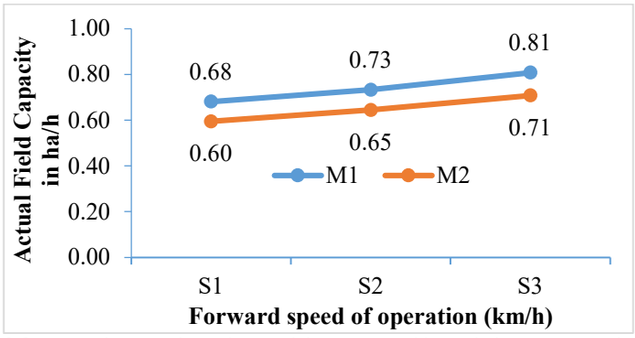

Figure 10. Effect of forward speed and machine Brand/model on Actual field capacity (ha/h)

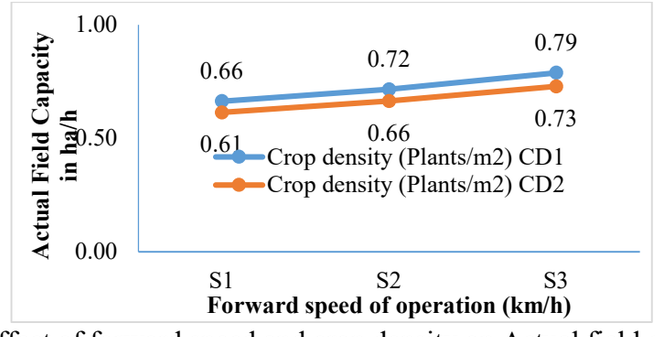

Figure 11. Effect of forward speed and crop density on Actual field capacity (ha/h)

Field efficiency

The interaction effects among machine model (M), forward speed (S), and crop density (CD) on field efficiency (%) were not statistically significant ($p > 0.05$), indicating that their combined influence did not introduce any distinct variation beyond the effects observed in individual and two-factor interactions. Although field efficiency varied across different machine models, forward speeds, and crop densities, no significant three-way interaction was detected. The highest field efficiency (84.40%) was recorded for Zoomlion-FH-100 at a lower forward speed (4–5 km/h) under a crop density of 251–300 plants/m², while the lowest efficiency (51.16%) was observed for Lovol-RG108+ at a higher forward speed (6–7 km/h) under a crop density of 301–350 plants/m² (Table 14). The interaction between machine model and forward speed was not significant ($p > 0.05$), indicating that the effect of forward speed on field efficiency was consistent across both machine models. Field efficiency declined with increasing forward speed in both Zoomlion-FH-100 and Lovol-RG108+, but the rate of decline remained similar. On average, Zoomlion-FH-100 maintained a higher efficiency than Lovol-RG108+ across all speed levels. Similarly, the interaction between machine model and crop density was not significant ($p > 0.05$), suggesting that crop density affected both harvester models similarly. Both models exhibited higher field efficiency at lower crop density (251–300 plants/m²) compared to higher crop density (301–350 plants/m²), with Zoomlion-FH-100 outperforming Lovol-RG108+ at both density levels. However, no statistical evidence indicated a machine-specific advantage in handling different crop densities. The interaction between forward speed and crop density was also not significant ($p > 0.05$), demonstrating that the decline in field efficiency with increasing speed occurred independently of crop density. Across all density levels, efficiency was highest at lower speeds (4–5 km/h) and lowest at higher speeds (6–7 km/h). Lower crop density (251–300 plants/m²) resulted in slightly higher efficiency than higher crop density (301–350 plants/m²), but the rate of decline due to speed remained consistent. Conversely, the single effects of machine model, forward speed, and crop density were all statistically significant ($p < 0.05$). The Zoomlion-FH-100 exhibited a significantly higher mean field efficiency (71.15%) compared to Lovol-RG108+ (62.67%), confirming its superior operational performance. Forward speed significantly influenced field efficiency, with the highest efficiency (75.84%) observed at 4–5 km/h and the lowest (56.52%) at 6–7 km/h. Crop density also had a significant effect, where a density of 251–300 plants/m² resulted in higher efficiency (70.84%) compared to 301–350 plants/m² (63.16%).

Table 14: Effect of forward speed, crop density (plants/m^2), and brand/model of combine harvester on field efficiency (%)

Machine Brand	Crop Density	Forward speed of operation (km/h)			Mean
		S1	S2	S3	
M1	CD1	84.40	72.49	62.43	73.11
	CD2	76.80	65.97	56.81	66.53
M2	CD1	74.09	63.67	55.67	64.48
	CD2	68.07	58.51	51.16	59.25
Mean		75.84	65.16	56.52	
LoS		M=*,S=*, CD=*, M×S=ns, M×CD=ns, S×CD=ns, M×S×CD=ns			
$LSD_{0.05}$		M=1.44,S=1.76, CD=1.45			
% of CV		3.17			

Note: $*$ means $P \leq 0 \cdot 05$, $**$ means $P \leq 0 \cdot 01$, $***$ means $P \leq 0 \cdot 001$, NS means Non-significant, LoS means level of significance, M=Machine Brand/Model (M1=Zoomlion-FH-100 and M2=Lovol-RG108+), S=Forward speed (S_1=4-5, S_2=5-6 and S_3=6-7 km/h), CD=Crop density (CD_1=251-300 and CD_2=301-350 plants/m^2).

Figures 12 and 13 analyze the influence of forward speed, crop density, and machine model on field efficiency (%) in combine harvester operations. The results indicate that forward speed significantly affects field efficiency, with the highest recorded efficiency of 80.60% at 4–5 km/h (S1). As speed increases, efficiency gradually declines, reaching 69.23% at 5–6 km/h (S2) and further decreasing to 59.62% at 6–7 km/h (S3) for Zoomlion-FH-100. This suggests that excessive speed negatively impacts machine performance by increasing grain losses and reducing operational control.

Among the two tested models, Zoomlion-FH-100 demonstrated superior efficiency (73.11%) compared to Lovol-RG108+ (64.48%), highlighting the role of machine design in performance.

Crop density also exhibited a substantial impact, where lower plant density (251–300 plants/m², CD1) resulted in higher efficiency, whereas higher plant density (301–350 plants/m², CD2) reduced efficiency.

The interaction of forward speed and crop density revealed that optimal efficiency is achieved at 4–5 km/h (S1) with lower crop density (CD1). In contrast, the lowest efficiency was observed at 6–7 km/h (S3) with higher crop density (CD2), where the harvester faced increased biomass resistance and energy demand.

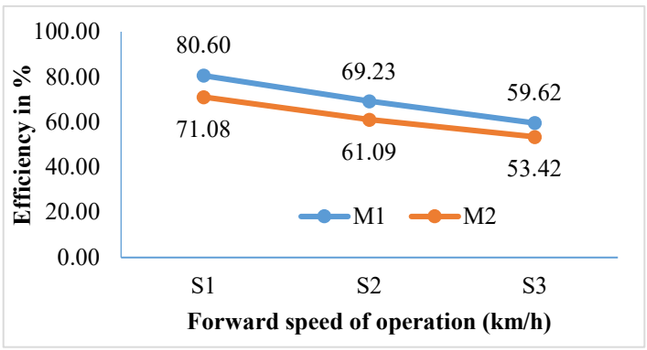

Figure 12. Effect of forward speed and machine Brand/model on field efficiency (%)

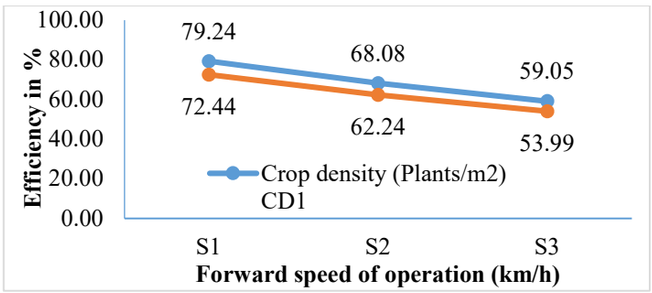

Figure 13. Effect of forward speed and crop density on field efficiency (%)

Grain losses

Pre-harvest losses

Pre-harvest losses are not associated with machine performance or operational speed; instead, they are influenced by biological and environmental factors. These losses primarily depend on crop characteristics such as plant maturity, pest and disease infestation, lodging, and weather conditions (e.g., wind, rain, and temperature fluctuations) before harvesting. Although crop density may have some indirect influence on pre-harvest losses by affecting plant structure and microclimate, these losses are fundamentally unrelated to mechanical or operational parameters. The status of pre-harvest losses observed in the experimental fields is presented in Table 15.

Table 15: Pre-harvest losses of the experimental field in kg/ha

Machine Brand	Crop Density	Forward speed of operation (km/h)			Mean
		S1	S2	S3	
M1	CD1	8.67	10.18	9.23	9.36
	CD2	9.37	9.71	9.96	9.68
M2	CD1	8.30	9.50	9.56	9.12
	CD2	10.33	9.97	9.90	10.07
Mean		9.17	9.84	9.66	
LoS		M=ns, S=ns, CD=ns, M×S=ns, M×CD=ns, S×CD=ns, M×S×CD=ns			
% of CV		9.88			

Header losses

The interaction effects among machine model (M), forward speed (S), and crop density (CD) on header loss (kg/ha) were not statistically significant ($p > 0.05$), indicating that their combined influence did not introduce any distinct variation beyond the effects observed in individual and two-factor interactions. Although header loss varied across different machine models, forward speeds, and crop densities, no significant three-way interaction was detected. The highest header loss was recorded for Lovol-RG108+ at a higher forward speed (6–7 km/h) under a crop density of 301–350 plants/m², while the lowest header loss was observed for Zoomlion-FH-100 at a lower forward speed (4–5 km/h) under a crop density of 251–300 plants/m² (Table 16).

The interaction between machine model and forward speed was not significant ($p > 0.05$), indicating that the effect of forward speed on header loss was consistent across both machine models, consistent with findings by Shafiekhani et al. (2019). Header loss increased with higher forward speed in both

Zoomlion-FH-100 and Lovol-RG108+, but the rate of increase remained similar. On average, Lovol-RG108+ exhibited higher header losses than Zoomlion-FH-100 across all speed levels. Similarly, the interaction between machine model and crop density was not significant ($p > 0.05$), suggesting that changes in crop density affected header loss similarly in both harvester models, as also reported by Adisa et al. (2022). Higher crop densities resulted in greater header losses for both machines, with Lovol-RG108+ consistently showing higher losses than Zoomlion-FH-100. However, no statistical evidence indicated a machine-specific advantage in reducing header loss under varying crop densities.

The interaction between forward speed and crop density was also not significant ($p > 0.05$), indicating that the increase in header loss with higher speed occurred independently of crop density. Regardless of crop density, header loss was lowest at lower speeds (4–5 km/h) and highest at higher speeds (6–7 km/h). Lower crop density (251–300 plants/m²) resulted in slightly lower header loss compared to higher crop density (301–350 plants/m²), but the overall rate of loss increased due to speed remaining consistent across both densities. Conversely, the single effects of machine model, forward speed, and crop density were all statistically significant ($p < 0.05$). The Lovol-RG108+ exhibited significantly higher mean header loss compared to Zoomlion-FH-100, confirming its inferior performance in minimizing losses. Forward speed had a significant impact on header loss, with the lowest losses recorded at 4–5 km/h and the highest at 6–7 km/h. Crop density also played a crucial role, as higher crop densities (301–350 plants/m²) resulted in significantly greater header losses than lower densities (251–300 plants/m²). These findings highlight the individual influence of each factor on header loss, despite the absence of significant interaction effects.

Table 16: Effect of forward speed, crop density (plants/m^2), and brand/model of combine harvester on header loss in kg/ha

Machine Brand	Crop Density	Forward speed of operation (km/h)			Mean
		S1	S2	S3	
M1	CD1	51.30	75.75	121.32	82.79
	CD2	66.17	97.72	156.50	106.80
M2	CD1	85.42	107.40	9.56	67.46
	CD2	114.47	143.91	132.25	130.21
Mean		79.34	106.20	177.22	
LoS		M=*,S=*, CD=*, M×S=ns, M×CD=ns, S×CD=ns, M×S×CD=ns			
$LSD_{0.05}$		M=12.41,S=15.19, CD=12.41			
% of CV		16.2			

Figures 14 and 15 analyze the influence of forward speed, crop density, and machine model on header loss (kg/ha) in combine harvester operations. The interaction of forward speed and machine model revealed that the lowest header loss (99.95 kg/ha) was recorded at 4–5 km/h (S1) for the Lovol-RG108+ combine harvester. Conversely, the highest header loss (154.74 kg/ha) occurred at 6–7 km/h (S3) for the same model, consistent with findings reported by Shafiekhani et al. (2019), where increased speed significantly elevated header losses. Among the two tested models, Zoomlion-FH-100 demonstrated lower header loss (82.79–106.80 kg/ha) compared to Lovol-RG108+ (108.36–145.20 kg/ha), emphasizing the role of machine design in minimizing grain loss, as similarly observed by Yadav et al. (2018) in comparative combine evaluations. Crop density also exhibited a strong impact, where lower plant density (251–300 plants/m², CD1) resulted in lower header loss, whereas higher plant density (301–350 plants/m², CD2) increased losses. This aligns with findings by Adisa et al. (2022), who reported that denser crops increase resistance at the header, leading to inefficiencies and greater grain shattering. The interaction of forward speed and crop density revealed that the lowest header loss was recorded at 4–5 km/h (S1) with lower crop density (CD1), while the highest header loss occurred at 6–7 km/h (S3) under higher crop density (CD2). Similar results were noted by Verma et al. (2017), where higher speeds and denser stands compounded losses due to mechanical inefficiencies during cutting.

These findings suggest that optimizing both speed and crop density is crucial for reducing header loss and enhancing the operational performance of combine harvesters, reinforcing the conclusions made by Godwin et al. (2003) regarding the significant influence of operational parameters on grain loss during harvesting.

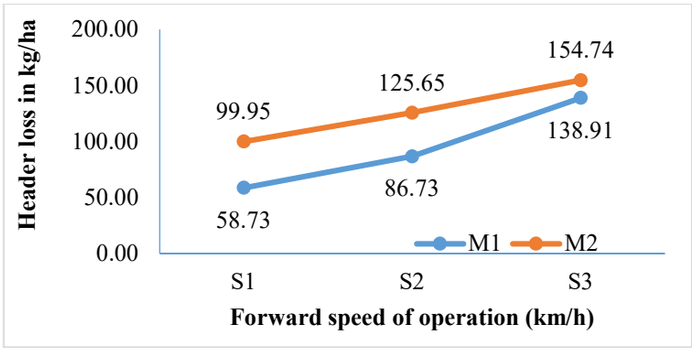

Figure 14. Effect of forward speed and machine Brand/model on header loss in kg/ha

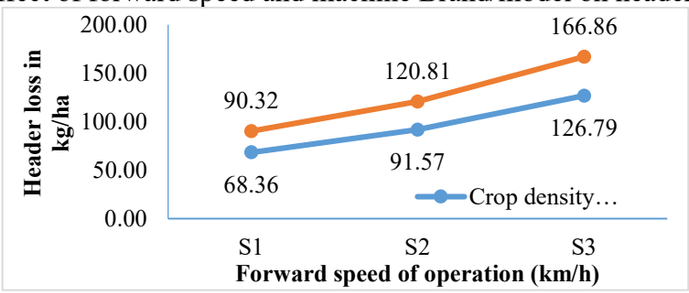

Figure 15. Effect of forward speed and crop density on header loss in kg/ha

Cylinder and separating losses

The interaction effects among machine model (M), forward speed (S), and crop density (CD) on cylinder and separating losses (kg/ha) were statistically significant ($p < 0.05$), indicating that their combined influence introduced distinct variations beyond the effects observed in individual and two-factor interactions. The highest cylinder and separating loss was recorded for Lovol-RG108+ at a higher forward speed (5–6 km/h) under a crop density of 301–350 plants/m² (CD2), reaching 284.82 kg/ha, while the lowest loss was observed for Zoomlion-FH-100 at a lower forward speed (4–5 km/h) under a crop density of 251–300 plants/m² (CD1), with 86.01 kg/ha (Table 17). The interaction between machine model and forward speed was significant ($p < 0.05$), indicating that the effect of forward speed on cylinder and separating loss varied across machine models. Similarly, the interaction between forward speed and crop density was significant ($p < 0.05$), indicating that the increase in cylinder and separating loss due to speed was more pronounced under higher crop density conditions. Regardless of machine model, the lowest loss (86.01 kg/ha) occurred at 4–5 km/h (S1) with a lower crop density (CD1), whereas the highest loss (284.82 kg/ha) was recorded at 5–6 km/h (S2) with a higher crop density (CD2). Conversely, the single effects of machine model, forward speed, and crop density were all statistically significant ($p < 0.05$). The Lovol-RG108+ exhibited significantly higher mean cylinder and separating loss compared to Zoomlion-FH-100, confirming its inferior performance in minimizing losses. Forward speed had a significant impact on losses, with the lowest losses recorded at 4–5 km/h and the highest at 6–7 km/h. Crop density also played a crucial role, as higher crop densities (301–350 plants/m²) resulted in significantly greater losses than lower densities (251–300 plants/m²). These findings highlight the complex interplay between machine model, speed, and crop density on cylinder and separating losses, emphasizing the need for optimized speed and machine selection to minimize grain losses during combine harvester operations.

Table 17: Effect of forward speed, crop density (plants/m^2), and brand/model of combine harvester on Cylinder and separating losses in kg/ha

Machine Brand	Crop Density	Forward speed of operation (km/h)			Mean
		S1	S2	S3	
M1	CD1	90.77	124.35	177.17	130.76
	CD2	118.91	162.90	232.09	171.30
M2	CD1	86.01	131.98	202.00	140.00
	CD2	186.10	284.82	262.39	244.44
Mean		120.45	176.01	177.22	
LoS		M=*,S=*, CD=*, M×S=*, M×CD=**, S×CD=*, M×S×CD=*			
$LSD_{0.05}$		M=12.18, S=14.92, CD=12.18, M×S=21.09, M×CD=17.23, S×CD=21.09, M×S×CD=29.84			
% of CV		10.27			

Figures 16 and 17 analyze the influence of forward speed, crop density, and machine model on cylinder and separating losses (kg/ha) in combine harvester operations. The results indicate that forward speed significantly impacts cylinder and separating losses, with the lowest recorded loss of 104.84 kg/ha at 4–5 km/h (S1) for Zoomlion-FH-100 (M1). Losses gradually increase with speed, reaching 232.20 kg/ha at 6–7 km/h (S3) for Lovol-RG108+ (M2). Among the two tested models, Zoomlion-FH-100 demonstrated lower cylinder and separating loss (104.84–204.63 kg/ha) compared to Lovol-RG108+ (136.05–232.20 kg/ha), emphasizing the role of machine design in minimizing grain loss. Crop density also exhibited a strong impact, where lower plant density (251–300 plants/m², CD1) resulted in lower losses (130.76–139.99 kg/ha), whereas higher plant density (301–350 plants/m², CD2) increased losses (171.30–244.44 kg/ha). This indicates that increased crop density imposes resistance, leading to inefficiencies in grain separation and threshing.

The interaction of forward speed and crop density revealed that the lowest cylinder and separating loss (88.93 kg/ha) was recorded at 4–5 km/h (S1) with lower crop density (CD1). Conversely, the highest loss (247.24 kg/ha) occurred at 6–7 km/h (S3) under higher crop density (CD2), where the harvester experienced greater resistance in threshing and separation. These findings suggest that optimizing both speed and crop density is crucial for reducing cylinder and separating losses and enhancing the operational performance of combine harvesters.

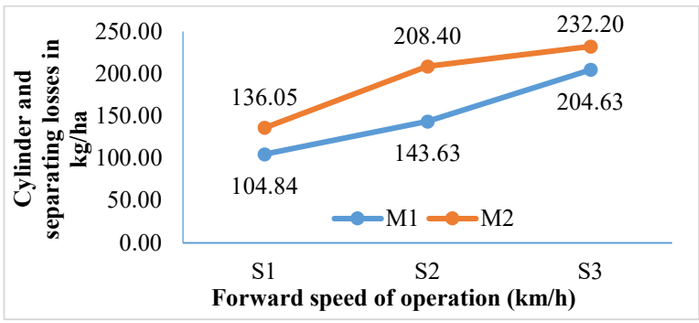

Figure 16. Effect of forward speed and machine Brand/model on Cylinder and separating losses in kg/ha

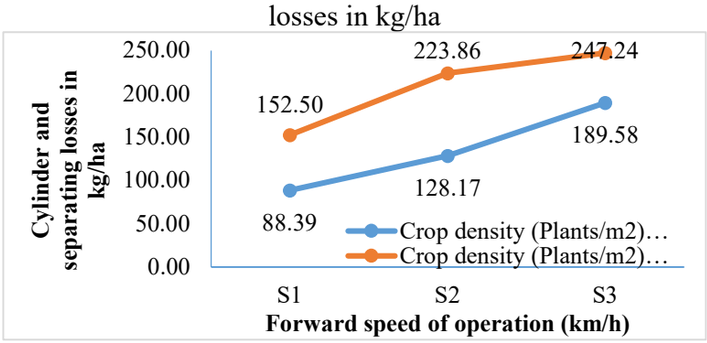

Figure 17. Effect of forward speed and crop density on Cylinder and separating losses in kg/ha

Total losses

The interaction effects among machine model (M), forward speed (S), and crop density (CD) on total grain losses (kg/ha) were statistically significant ($p < 0.05$), indicating that their combined influence contributed to variation in grain losses beyond the effects observed in individual and two-factor interactions.

The highest grain loss was recorded for Lovol-RG108+ at a higher forward speed (6–7 km/h) under a crop density of 301–350 plants/m², while the lowest grain loss was observed for Zoomlion-FH-100 at a lower forward speed (4–5 km/h) under a crop density of 251–300 plants/m² (Table 18).

The interaction between machine model and forward speed was statistically significant ($p < 0.05$), indicating that the effect of forward speed on grain loss varied between the two machine models. Grain loss increased with higher forward speed in both Zoomlion-FH-100 and Lovol-RG108+, but the rate of increase differed slightly between the models, with Lovol-RG108+ exhibiting higher losses across all speed levels. Similarly, the interaction between machine model and crop density was statistically significant ($p < 0.05$), suggesting that the effect of crop density on grain loss was different for each machine model. Higher crop densities resulted in greater grain losses for both machines, with Lovol-RG108+ consistently showing higher losses than Zoomlion-FH-100 at all density levels.

Furthermore, the single effects of machine model, forward speed, and crop density were all statistically significant ($p < 0.05$). The Lovol-RG108+ exhibited significantly higher mean grain loss compared to Zoomlion-FH-100, confirming its inferior performance in minimizing losses. Forward

speed had a significant impact on grain loss, with the lowest losses recorded at 4–5 km/h and the highest at 6–7 km/h. Crop density also played a crucial role, as higher crop densities (301–350 plants/m²) resulted in significantly greater grain losses than lower densities (251–300 plants/m²). These findings highlight the significant influence of each factor on grain loss, as well as the significant interaction effects among them.

Table 18: Effect of forward speed, crop density (plants no/m^2), and brand/model of combine harvester on total grain losses in kg/ha

Machine Brand	Crop Density	Forward speed of operation (km/h)			Mean
		S1	S2	S3	
M1	CD1	150.73	210.28	307.72	222.91
	CD2	194.45	270.33	398.55	287.78
M2	CD1	179.73	248.88	343.81	257.47
	CD2	310.89	438.69	449.52	399.70
Mean		208.95	292.05	177.22	
LoS		M=*,S=*, CD=*, M×S=*, M×CD=*, S×CD=ns, M×S×CD=*			
$LSD_{0.05}$		M=18.59, S=22.76, CD=18.58, M×S=32.19, M×CD=26.29, S×CD=ns, M×S×CD=45.53			
% of CV		9.21			

Figures 18 and 19 analyze the effect of forward speed, crop density, and machine brand/model on total grain losses (kg/ha) in combine harvester operations. The results indicate that forward speed significantly impacts total grain losses, with the highest losses recorded at 6–7 km/h (S3). Losses gradually decrease at lower speeds, reaching the lowest values at 4–5 km/h (S1), suggesting that higher speeds may increase grain loss due to inefficiencies in threshing and separation. Among the two tested models, Lovol-RG108+ exhibited greater grain losses at CD2, compared to Zoomlion-FH-100 at CD1, emphasizing the role of machine design in minimizing losses. Crop density also had a significant impact, where higher plant density (301–350 plants/m², CD2) resulted in greater grain losses, whereas lower plant density (251–300 plants/m², CD1) resulted in reduced losses. This suggests that increased crop density introduces more resistance, leading to inefficient threshing and higher losses. The interaction of forward speed and crop density revealed that the highest total grain losses occurred at 6–7 km/h (S3) under higher crop density (CD2). Conversely, the lowest losses were observed at 4–5 km/h (S1) under lower crop density (CD1), where threshing and separation processes were more effective. These findings highlight the importance of optimizing forward speed and crop density to minimize grain losses and enhance combine harvester efficiency.

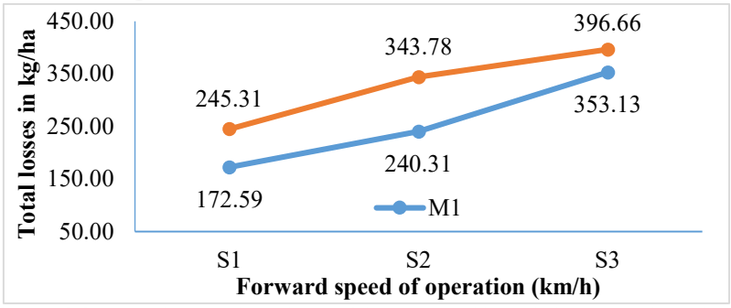

Figure 18. Effect of forward speed and machine Brand/model on total grain losses in kg/ha

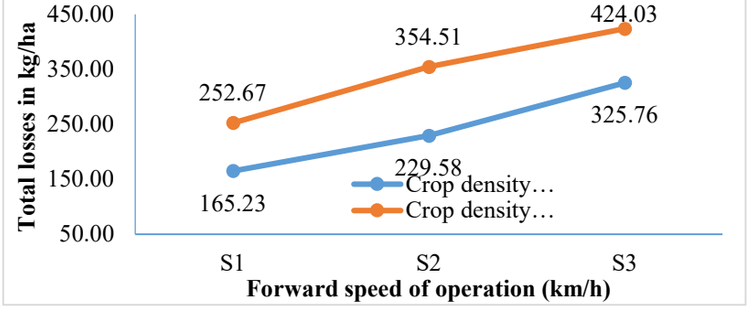

Figure 19. Effect of forward speed and crop density on total grain losses in kg/ha

Percentage of losses

The interaction effects among machine model (M), forward speed (S), and crop density (CD) on grain losses (%) were statistically significant ($p < 0.05$), indicating that their combined influence contributed to variation in grain losses beyond the effects observed in individual and two-factor interactions. The highest grain loss was recorded for Lovol-RG108+ at a higher forward speed (6–7 km/h) under a crop density of 301–350 plants/m², while the lowest grain loss was observed for

Zoomlion-FH-100 at a lower forward speed (4–5 km/h) under a crop density of 251–300 plants/m² (Table 19). The interaction between machine model and forward speed was statistically significant ($p < 0.05$), indicating that the effect of forward speed on grain loss varied between the two machine models. Grain loss increased with higher forward speed in both Zoomlion-FH-100 and Lovol-RG108+, but the rate of increase differed slightly between the models, with Lovol-RG108+ exhibiting higher losses across all speed levels. Similarly, the interaction between machine model and crop density was statistically significant ($p < 0.05$), suggesting that the effect of crop density on grain loss was different for each machine model. Higher crop densities resulted in greater grain losses for both machines, with Lovol-RG108+ consistently showing higher losses than Zoomlion-FH-100 at all density levels.

The interaction between forward speed (S) and crop density (CD) was not statistically significant ($p > 0.05$), indicating that the increase in grain loss with higher forward speed occurred independently of crop density. Regardless of crop density, grain loss was lowest at lower speeds (4–5 km/h) and highest at higher speeds (6–7 km/h). Although higher crop density (301–350 plants/m²) resulted in slightly greater grain loss compared to lower crop density (251–300 plants/m²), the overall rate of increase in grain loss due to speed remained consistent across both densities.

Furthermore, the single effects of machine model, forward speed, and crop density were all statistically significant ($p < 0.05$). The Lovol-RG108+ exhibited significantly higher mean grain loss compared to Zoomlion-FH-100, confirming its inferior performance in minimizing losses. Forward speed had a significant impact on grain loss, with the lowest losses recorded at 4–5 km/h and the highest at 6–7 km/h. Crop density also played a crucial role, as higher crop densities (301–350 plants/m²) resulted in significantly greater grain losses than lower densities (251–300 plants/m²). These findings highlight the significant influence of each factor on grain loss, as well as the significant interaction effects among them.

Table 19: Effect of forward speed, crop density (plants/m^2), and brand/model of combine harvester on grain losses in %

Machine Brand	Crop Density	Forward speed of operation (km/h)			Mean
		S1	S2	S3	
M1	CD1	1.96	2.74	4.01	2.90
	CD2	2.52	3.51	5.17	3.74
M2	CD1	2.34	3.24	4.47	3.35
	CD2	4.03	5.68	5.82	5.18
Mean		2.71	3.79	4.87	
LoS		M=*,S=*, CD=*, M×S=*, M×CD=*, S×CD=ns, M×S×CD=*			
$LSD_{0.05}$		M=0.24, S=0.30, CD=0.24, M×S=0.42, M×CD=0.34, S×CD=ns, M×S×CD=0.59			
% of CV		9.21			

Figures 20 and 21 analyze the influence of forward speed, crop density, and machine model on grain losses (%) in combine harvester operations. The results indicate that forward speed significantly impacts grain losses, with the highest recorded losses of 5.15% for Lovol-RG108+ and 4.59% for Zoomlion-FH-100 at 6–7 km/h (S3).

Losses gradually decrease with lower speeds, reaching 3.19% for Lovol-RG108+ and 2.24% for Zoomlion-FH-100 at 4–5 km/h (S1), suggesting that higher forward speed increases grain loss due to reduced threshing efficiency. Among the two tested models, Lovol-RG108+ exhibited higher grain losses across all conditions, with the highest loss (5.18%) observed under higher crop density (301–350 plants/m², CD2). In contrast, Zoomlion-FH-100 recorded lower losses (3.74%) under the same crop density, emphasizing the role of machine design in minimizing grain losses.

Crop density had a significant impact, where higher plant density (CD2) resulted in greater grain losses compared to lower plant density (251–300 plants/m², CD1), with recorded values of 5.18% and 3.35% for Lovol-RG108+ and 3.74% and 2.90% for Zoomlion-FH-100, respectively. The interaction of forward speed and crop density revealed that the highest grain losses (5.50% for Lovol-RG108+ and 4.24% for Zoomlion-FH-100) occurred at 6–7 km/h (S3) under higher crop density (CD2). Conversely, the lowest losses (3.28% for Lovol-RG108+ and 2.15% for Zoomlion-FH-100) were observed at 4–5 km/h (S1) under lower crop density (CD1), where threshing and separation were more effective. These findings suggest that optimizing forward speed and crop density is crucial for minimizing grain losses and improving harvesting efficiency.

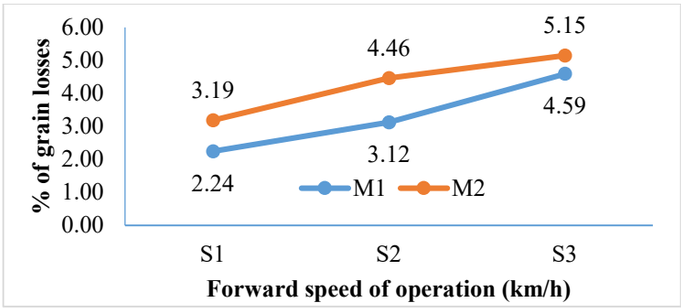

Figure 20. Effect of forward speed and machine Brand/model on grain losses in %

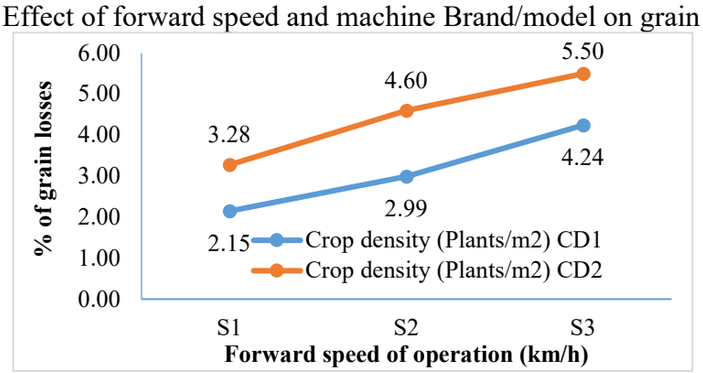

Figure 21. Effect of forward speed and crop density on grain losses in %

Conclusion

The field evaluation conducted during the Boro 2023–24 season in Sirajganj and Habiganj districts revealed significant insights into how harvester model, forward speed, and crop stand condition influence the performance of combine harvesters in mechanized rice harvesting. Between the two tested models, the Zoomlion combine generally exhibited higher field capacity and better fuel efficiency, especially at medium speeds, while maintaining comparatively lower grain losses**.** The Lovol harvester, though capable, tended to show higher grain losses at increased forward speeds and slightly lower field efficiency. The study also found that medium forward speeds consistently delivered the most balanced outcomes—achieving good field capacity without compromising grain quality or causing excessive losses. In contrast, high forward speeds increased grain losses for both harvester models, particularly under weak or lodged crop conditions. Moreover, crop stand quality had a substantial impact on harvester performance. Fields with good crop stands resulted in more efficient harvesting with reduced grain losses, while poor crop stands—characterized by lodging or uneven maturity—led to increased losses and reduced harvesting performance.

Overall, the findings emphasize that:

- **Zoomlion outperformed Lovol** in terms of efficiency and loss minimization under the tested conditions.
- **Medium forward speeds** are optimal for maintaining a balance between field performance and grain retention.
- **Good crop stands** are essential to maximize the benefits of mechanized harvesting, indicating the need for integrated crop management alongside mechanization.

Experiment 1.4: Identification and Fabrication of Fast-Moving Spare Parts of Combine Harvester Enhancing Sustainable Mechanization in Bangladesh

Principal Investigator: Md. Anwar Hossen
Co-Investigator: SI, HP, SP

Summary of Last Year's Findings

In 2024, a comprehensive survey of Sirajganj and Habiganj districts identified the spare parts most prone to failure in whole-feed and head-feed combine harvesters. Failure frequency increased with operational hours, becoming critical after 250 hours. The most failure-prone items included:

• Cutting blades (highest frequency of failure)
• Various belts (power transmission, threshing, gear, engine)
• Bearings (roller, auger, fan, shaft)
• Fingers and finger belts
• Threshing teeth
• Chains and finger chains
• Sprockets

It was concluded that the availability of these parts at lower prices through local manufacturing is essential for sustainable mechanization.

Objectives

- Consolidate part-level specifications for high-rotation components across multiple brands.
- Pilot local fabrication of critical spare parts with Monno Agro & General Machinery Ltd.
- Validate fabricated parts' quality against original specifications (e.g., hardness values, carbon composition).
- Reduce dependency on imported spare parts and enhance timely availability during harvesting seasons.
- Expand knowledge base by creating a structured parts catalogue that includes drawings, properties, and fabrication readiness.

Methodology

The 2025 methodology combined desk-based synthesis of last year's multi-season failure logs with hands-on work to structure the parts catalogue and engage with local fabricators:

Parts Cataloguing: Each item was parsed to separate name, application, and part number (where available).

Material Properties Verification: Original specifications (e.g., 48–60 HRC hardness for blades) were compared with values achieved in locally fabricated samples (e.g., 60.93 HRC in fabricated cutter blades).

Vendor Engagement: Monno Agro & General Machinery Ltd. produced initial fabricated samples, which were visually inspected and chemically tested for compliance.

Cross-validation: Frequent-failure parts (cutting blades, sprockets, bearings) were aligned with locally fabricable items.

Results and Discussion

This year's dataset contained a structured list of spare parts specifically for the Daedong DXM73GF-SA. A total of 7 primary items were identified and documented, including the cutter blade, sprocket, drive sprocket, drive shaft, blade drive shaft (C7620-45573), and cutter set. Among these, the cutter blade had detailed property data for both original and fabricated parts, showing promising results for localized production (Table 20).

The transition from identification to fabrication is distinct. Unlike last year's field-survey heavy dataset, this year's work produced actual specification-level comparisons between original and fabricated parts. This demonstrates feasibility for local production.

Conclusion

In 2025, the study achieved significant progress by moving from spare parts identification to pilot localization. The Daedong DXM73GF-SA served as a test case for developing fabrication-ready specifications and validating the quality of locally produced parts. With further scaling, Bangladesh can reduce reliance on imported fast-moving spare parts, lower costs for entrepreneurs and farmers, and strengthen the sustainability of mechanized paddy harvesting.

Table 20: Design and photographic views of the different fast-moving parts of the Daedong DXM73GF-SA combine harvester

Sl. No.	Name of the Parts	Original View and properties	View or Photo of the Fabricated Parts	Drawing Views		
				Top	Side	Isometric
1	Cutter Blade			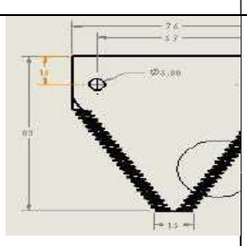		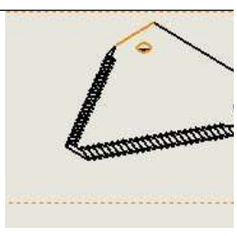
		Hardness Value:48-60HRC, Carbon:0.80-0.95, Si:0.15-0.30, Mn:0.30-0.50	Hardness Value:48-60HRC, Carbon:0.80-0.95, Si:0.15-0.30, Mn:0.30-0.50			

Sl. No.	Name of the Parts	Original View and properties	View or Photo of the Fabricated Parts	Drawing Views		
				Top	Side	Isometric
2	Sprocket			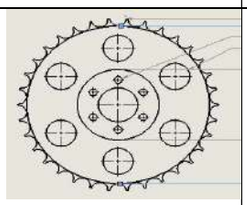		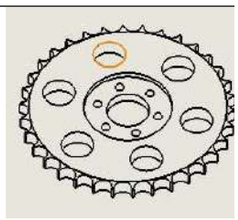
3	Drive Sprocket			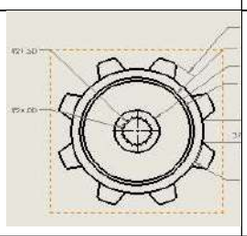		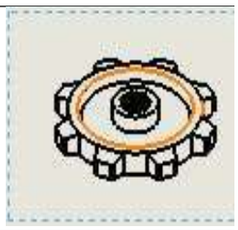
4	Drive Shaft					
5	Shaft 2, Blade drive (Part no. C7620-45573)			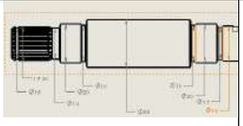	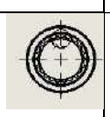	
6	Cutter Set				`	
7		1. Knife Guide		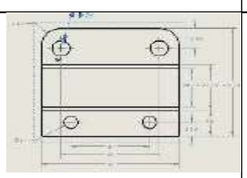	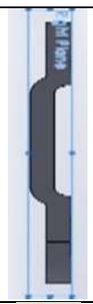	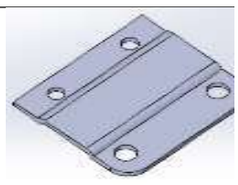
		2. Knife Guide		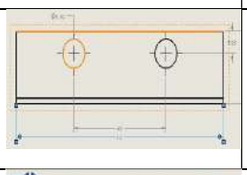		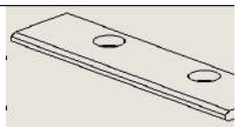
		3. Spacer 1		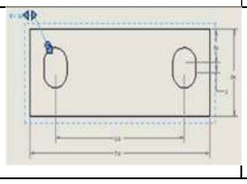	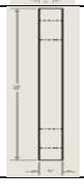	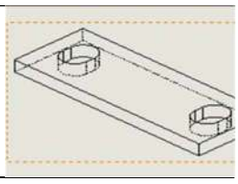

Sl. No.	Name of the Parts	Original View and properties	View or Photo of the Fabricated Parts	Drawing Views		
				Top	Side	Isometric
		4. Spacer 2		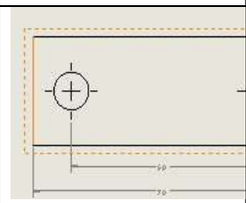	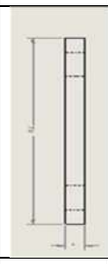	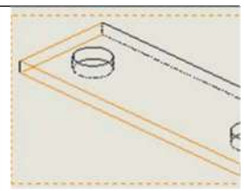
		5. Spacer 3		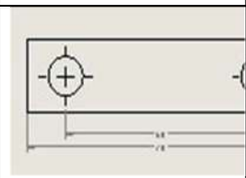	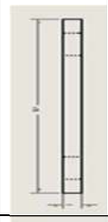	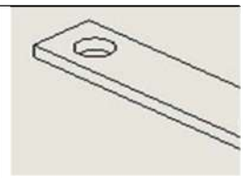
		6. Spacer 4		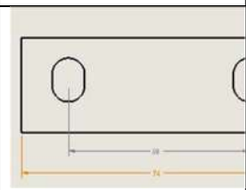		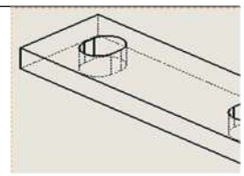
		7. Spacer 5		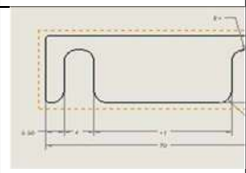		
		8. Slider Top		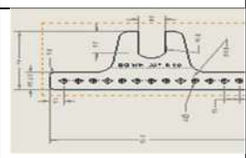		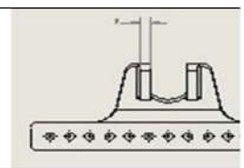
		10. Slider Bottom		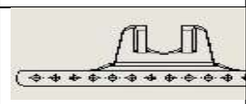		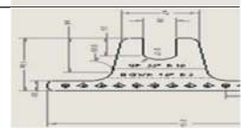
		11. Guide 1		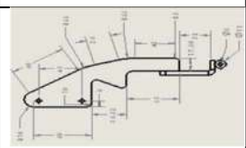		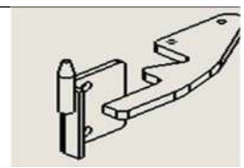
		12. Guide 2		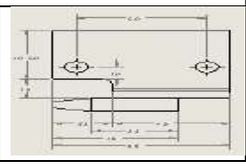	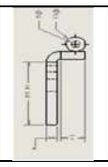	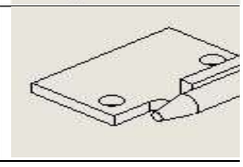

Recommendations

- Immediate Stocking: Ensure cutting blades, belts, bearings, finger belts, threshing teeth, chains, and sprockets are prioritized for local production and stocking.
- Specification Control: Standardize drawings and hardness values for each part before scaling production.
- Preventive Maintenance: Disseminate guidelines for operators to replace blades and belts after ~200–250 operational hours to minimize downtime.
- Price & Supply Chain: Target locally fabricated parts to be 20–30% cheaper than imports, with a restocking cycle not exceeding 7–10 days during peak harvest.
- Expansion: Replicate the parts catalogue and fabrication trials for Yanmar and Kubota models, given their higher adoption in the field under a priority project.

Experiment 1.5: Design, Development, and Performance of a BRRI Automatic Seed Sower Machine for raising mat-type seedling (funded by SFMRA project)
Principal Investigator: Arafat Ullah Khan
Co-Investigator: AKMSI
Objective

- To design, develop, and performance evaluation of a BRRI automatic seed sower machine for raising seedlings in tray

Materials and Methods

A BRRI automatic seed sower machine was designed and fabricated at the FMPHT divisional research workshop using locally available materials. This machine was developed under the SFMRA project of BRRI. Careful analysis of material selection and metallurgy was undertaken to ensure the quality of the product. The machine's components include the main basement, bed soil hopper, seed hopper, water tank base, topsoil hopper, reduction gear, electric housing, and driver and driven shaft. The machine was fabricated using the AutoCAD Engineering drawing tools, and a prototype was fabricated according to the design. Jigs, fixtures, and molds for the main basement, soil hopper base, seed hopper base, water tank base, and motor basement were developed for quick replication. Calibration for different soil types and various sizes of paddy seeds was achieved by adjusting the lever. The prototype's performance was tested in the FMPHT divisional research workshop, Uttaron Engineering at Dinajpur, and in farmers' fields. The automatic seed sower machine is a device that helps in the sowing of seeds in the desired position, hence assisting the farmers in saving time. The results of the performance tests were satisfactory.

Design Consideration

The following design considerations were taken into account for developing the machine: ease of use, simplicity, economy, and efficiency in operation.

- The width of the machine should be kept at 61 cm, as the width of the seedling tray is 58 cm.
- Locally available materials should be used to minimize the fabrication cost.
- The machine should be suitable for sowing all varieties uniformly.
- There should be soil rate and seed rate control by lever and knob mechanisms.
- Efficiency of the machine should be higher compared to manual sowing.
- The operation, repair, and maintenance of the machine should be easy.
- The power transmission system should be smooth and straightforward.
- Two men can operate this machine.

Design Steps

The following design steps were followed to develop the automatic seed sower machine.

- Seeding preparation on the tray for the mat-type seedling was complicated, which was identified.
- Information about mat-type seedling raising, the seed sower machine, and farmers' demand was taken into consideration.
- Drawing and fabrication were completed according to the following guidelines.
- A chain-sprocket arrangement was used to distribute power from the equipped roller to the metering device of the seeding hopper and the rubber belt of the soil hoppers. Different types of sprockets (12 teeth, 12/9 teeth,16 teeth, 18 teeth, 20 teeth, and 24 teeth) were used to transmit power on both sides in this machine.
- The seed metering device has two knob which are used to maintain the seed rate properly in the seeding hopper
- A tray conveyor was designed to hold the entire machine structure while maintaining clearance for tray movement.
- The holding capacities of the bed soil hopper, seeding hopper, and cover-up hopper were designed to be approximately 80kg of soil, 10kg of seed, and 40kg of soil, respectively.
- The knob and adjusting lever were designed with each hopper for controlling the soil rate, seed rate, and changing as per requirement.

The following section/steps for making the BRRI automatic seed sower machine:

a. Main Basement Section

• Frame: Bears all the load of the machine. The frame measures 3657.5 mm in length, with the channel created by cutting a 60 mm section in the middle.

• Legs: The lower part of the foot is made of floor-supporting clamps. A 6.5 mm drill is drilled above the legs to bear the weight of the frame. The total number of legs is 5. The distance from the foot to the foot is 730 mm.
• Hole in frame: A Hole is cut with hole cutters of different sizes (42, 34, 22, 10 mm) to place the bearing cover on the frame. Of these, 12 holes for 42 mm, eight holes for 34 mm, two holes for 22 mm, and 16 holes for 10 mm have to be made.
• Shaft: Two 25 mm shafts (length 780 mm, dia 25 mm) are ground and pulled in the lathe machine to make bearing size and pulley size. An 8.5mm drill was run. The 3" V pulley is drilled 7mm, and the 8mm tap drill is done.
• Supporting V pulleys: A total of 8 nos. 10 mm bore and 12 nos. 15 mm bore V pulleys are made of plastic.
• Idle roller pulley: A total of 16 idle roller pulleys of plastic 10mm bore are made to move the seedling tray forward. A circlip on both sides of the shaft holds the idle roller pulley.
• Idle shaft and roller pulley shaft: A total of 12 (plastic V pulley, a total of four idle shafts of 10 mm bore, and eight roller pulley shafts of 10 mm bore) were manufactured.
• Bearings and bearing covers: Total 68 bearings, including covers (UC 204=2, 6304=2, 6202=14, 6000=8, 6001=8) bearings

b. Main Power Section:

• Power shaft: 6 of 20 mm shafts and 2 of 25 mm shafts will get power to the machine with the help of 8 shafts. Table 21 describes the specification of the BRRI Auto Seed Sower Machine.
• Pulley, V-pulley & V-belt: The seedling tray of the machine will run with 4 3-inch pulleys made of iron and 12 V pulleys of 15 mm bore and 235 E. 2 V belts

c. **Motor Basement Section:**

• Square Box and Motor: The square box size will be 1"*1", and two-phase motors with ½ hp of 1400 rpm will be used.
• Gearbox: The power transmission gearbox of the machine will be used at 1:20.
• Sprocket & Chain: The machine will get main power through the sprocket and chain by connecting the gear bush of the gearbox to the motor.

d. Tray conveyor with the equipped rollers

The tray conveyor of the automatic seed sower machine was used to convey the tray easily during machine operation and to provide support for the whole body of the machine. The tray conveyor roller, 64 cm long, held the bed soil hopper, seeding hopper, top soil hopper, and water container. The width of the tray conveyor was 60 cm, whereas the seedling tray width is 58 cm, and the trays move easily from the beginning to the completion side during machine operation. Five supporting stands were attached below the tray conveyor at a 900-degree angle and a height of 45.5 cm from ground level for the standing position.

e. Bed soil hopper and Top soil hopper:

The bed soil hopper and the top soil hopper were attached to the tray conveyor at a certain distance. These hoppers were used to contain the sieved soil. During operation, this soil was dropped onto the tray. A total of 2 (two) conveyor rollers with 16 teeth (length 640mm, dia 60mm) help to rotate the belt. One conveyor belt, measuring 640 mm in length, diameter, and thickness, helps to distribute soil on the seedling tray quickly. The tension-bearing house is fitted by welding the clamp to the main base, and the tension-bearing shaft is used to tension the conveyor belt through a 6 mm screw shaft. Supporting bearing & bearing cover helps the conveyor roller to rotate easily. The bed soil hopper and cover-up soil hopper were designed to contain about 80 kg and 40 kg of soil, respectively. The bed soil hopper has two parts: the base portion and the hopper portion.

f. Seeding hopper:

The seeding hopper was located on the tray conveyor between the bed soil hopper and the top soil hopper at a specific distance. This hopper was used to contain the sprouted seeds. During machine operation, the sprouted seeds were dropped to maintain a specific seed rate on the tray. A 4mm plastic sheet was used to make this hopper. The seeding hopper was designed to contain about 10 kg of seed.

g. Water Tank Basement Section:

The capacity of the tank is 44 liters. The pipe used with a 20mm pipe connector tank for water flow in a seedling tray. The tank base is made with a 20*4 mm flat bar to hold the tank. The base is made with 25 * 25 * 4 mm angle to hold the tank base.

h. Tray Cleaner Brush Section:

Two brushes are used to clean and level the soil at the top of the seedling tray. The brush measures 380 mm in length and 50 mm in width, and is placed at an angle of 55 degrees with the main base. A brush base 700 mm long and 25 mm wide is used to hold the tray cleaner brush.

Plate 4. Laboratory trial of the BRRI Auto Seed Sower Machine

Table 21: The specification of the BRRI Auto Seed Sower Machine

Particulars	Unit
Model	BRRI ASSM 2023
Dimension, mm (L×W×H)	3048×730×1135
Motor power, hp & rpm	0.5 & 1400
Gear ratio	1:20
Bed soil hopper capacity, kg	80
Top soil hopper capacity, kg	40
Seed hopper capacity, kg	10
Power transmission System	V-belt
Total weight, kg	100
Speed of Sower(km/h)	Adjustable
No of Tray/min	28

Field performance of the BRRI Auto Seed Sower Machine

The machine is easy to fabricate using materials found locally in a workshop, and it can be operated by both men and women with minimal training. The distribution of bed soil is precisely adjusted using a lever. The seed distribution rate can be finely tuned with a brush adjustment meter, allowing for 120 to 160 grams of sprouted seeds to be placed in each tray. With the auto seed sower machine, a worker can sow seeds in 1680 trays per hour, a significant improvement compared to the 50-60 trays done manually. After sowing the sprouted seeds, the topsoil layer (6 mm) of each tray can be covered with loose soil. Controlling the seed sowing rate for different rice varieties is simple. The machine has a bed soil hopper, seed hopper, and topsoil hopper with capacities of 80 kg, 10 kg, and 40 kg, respectively. This experiment was conducted using the BRRI auto seed sower machine at an adjusting lever position of 3. There were five trays taken to do this experiment, and three boxes were used for each tray to determine the uniform distribution of seeds (Table 22).

Table 22: Seed distribution of BRRI dhan103 by the BRRI auto seed sower

No of tray	Box 1		Box 2		Box 3		Total weight of the seed (gm)
	No. of seed	Weight of seed (gm)	No. of seed	Weight of seed (gm)	No. of seed	Weight of seed (gm)	
1	115	2.2	120	2.3	114	2.2	148
2	118	2.3	115	2.1	114	2.2	152
3	122	2.4	132	2.7	120	2.4	149
4	125	2.4	125	2.4	120	2.4	150
5	120	2.3	122	2.3	119	2.3	156

Figure 22 presents a comparison of the number of seeds and their weight across five trays for three different boxes (Box 1, Box 2, and Box 3).

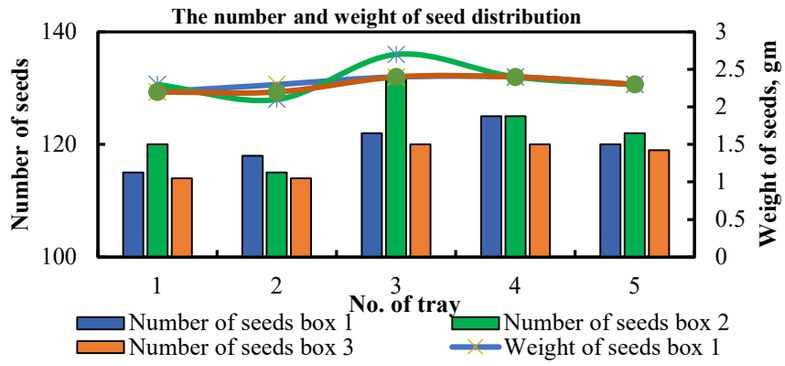

Figure 22. Comparison of seed count and weight across different boxes and trays

The comparative evaluation of the number and weight of seeds across trays shows distinct patterns. Box 2 exhibits the highest variability in seed count, peaking in Tray 3 and consistently maintaining high counts in other trays. In contrast, Box 1 and Box 3 have moderate seed counts overall, with Box 3 showing a slightly lower count in Tray 1. Despite these variations, the seed count across all trays remains relatively balanced, generally falling between 115 and 130 seeds. Regarding the weight of seeds, Box 2 stands out with a notable peak in Tray 3, reaching around 2.7 grams, while the weights for Box 1 and Box 3 stay closer to 2.3–2.5 grams. Overall, the weight of seeds across the boxes remains similar across trays, except for this peak in Tray 3. In summary, Box 2 distinguishes itself in both seed count and weight in Tray 3, suggesting a possible difference in seed characteristics for that tray. The seed weights generally exhibit limited fluctuation, maintaining a range of 2.3 to 2.5 grams, which implies consistency in seed mass across trays. This graph indicates that while minor fluctuations are present in both seed count and weight, especially in Tray 3, the overall values across trays and boxes are stable. This analysis suggests that Tray 3 may have specific conditions or factors influencing both the seed count and weight in Box 2.

The bar graph (Figure 23) illustrates the variation in seed weight distribution across five trays. Trays 1, 3, and 4 each have similar seed weights, recorded at 148g, 149g, and 150g, respectively, indicating minimal variation among them. These three trays form a consistent baseline in seed distribution, showing that the weight of seeds spread across these trays is nearly identical. However, Tray 2, with 152g, and Tray 5, with 156g, display slightly higher seed weights. This difference suggests a minor variation in distribution for these trays compared to the others. Despite this increase, the overall range of weights remains relatively close, reflecting a controlled but slightly varied seed distribution pattern across the trays.

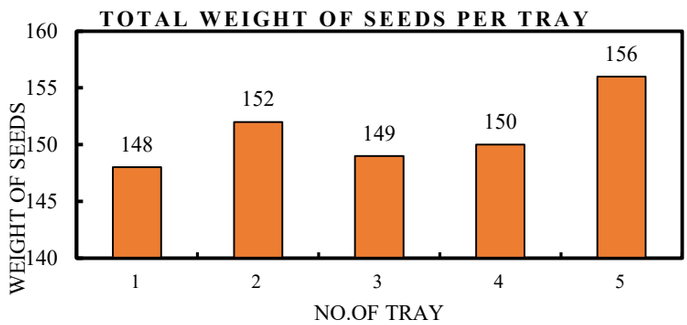

Figure 23. Total weight of seeds per tray

Several trials were conducted at the FMPHT division of BRRI, involving official personnel, local agricultural machinery manufacturers, and farmers (Plate 4). All participants in the field trial expressed satisfaction with the machine's effectiveness. As part of the SFMRA project, some machines have been given to the 'Mechanized Village' and regional stations of BRRI for field-level extension and preparing seedling trays for mechanical transplanting. Introducing a community-based seedling production system using the machine could potentially create rural entrepreneurship. However, the machine should not be used if the germinated seeds are more than one day old or if the radical length is more than 2mm. In this model, the seed-sowing process is automated to reduce human effort and increase yield. The AC motor takes care of the automatic distribution of soil, water, and seeds. The BRRI auto seed sowing machine is more efficient and less time-consuming. In the present era, all sectors, including agriculture, are progressing rapidly. To meet future food demands,

farmers need to adopt new techniques that do not compromise soil texture but enhance overall crop production.

Conclusion

The BRRI auto seed sower was fabricated and tested at the FMPHT workshop, fine-tuned for various soil textures and paddy seed sizes. It performed well both in research and farmers' fields, offering a time-saving solution for preparing seedling trays for mechanical transplanting with minimal manpower and simple installation. The design was successful, suitable for large-scale use, with accurate seed metering and no seed damage during operation. While automated, it ranks lower in distribution uniformity and efficiency, so selection depends on operational needs, balancing cost, efficiency, uniformity, and seed loss. Optimal soil depth for seedling growth is 15-20mm, with the sower achieving depths from 5.44mm to above 25mm, especially at positions 3 and 4. The machine's lower uniformity suggests room for improvement.

Recommendation

Some recommendations should be developed to enhance the performance of these seed sowers.

- An automatic seed regulator could be implemented to control the speed of the seed metering device, allowing for easier and more accurate calibration with the BRRI auto seed sower.
- Improving the adjusting lever for seed control could enhance the uniformity of seed distribution.

Experiment 1.6: Modification of the BRRI Prilled Urea Applicator (PUA)

Principal Investigator: M Kamruzzaman Milon
Co-Investigator: MMR

Overall Objective

To develop and promote a farmer-friendly, durable, and precise prilled urea applicator that improves nitrogen-use efficiency, reduces input losses, and enhances the sustainability of rice production in Bangladesh.

Objectives

- Improve metering precision by replacing the fluted roller with an auger-based mechanism capable of fine flow adjustments.
- Enhance durability and field life through the use of stainless steel and fiber-reinforced composites, suitable for muddy and high-silt soils.
- Reduce clogging incidents by integrating an agitator within the auger housing to ensure smooth fertilizer flow.
- Facilitate farmer usability with ergonomic design, adjustable flow lever, and balanced handling.
- Validate performance of the modified applicator through laboratory calibration and multi-location field evaluations.
- Promote adoption by demonstrating efficiency gains, reduced maintenance needs, and improved fertilizer management outcomes

Methodology

The initial design of the BRRI Prilled Urea Applicator (PUA) faced challenges in maintaining consistent metering accuracy and long-term durability under field conditions (Plate 5). Farmers frequently reported difficulties in achieving uniform application rates, particularly in muddy and high-silt environments. To address these issues, BRRI initiated a comprehensive redesign aimed at enhancing precision, reliability, and user-friendliness.

The fundamental modification replaced the conventional fluted roller system with an auger (helical screw) mechanism. This innovation allows fine-tuned control of fertilizer flow through adjustable pitch and rotation, ensuring more accurate and efficient nutrient delivery. In parallel, the applicator's structural components, including the body and skids, were upgraded from lightweight aluminum and plastic materials to stainless steel and fiber-reinforced composites. These enhancements significantly improved durability, reduced maintenance frequency, and extended field life, even under demanding operating conditions. Together, these modifications represent a strategic step toward developing a farmer-centric mechanization solution that minimizes input losses, increases efficiency, and strengthens the long-term sustainability of rice cultivation in Bangladesh.

Plate 5. Original BRRI Prilled Urea Applicator (9 kg model).

Design Modifications

To enhance the performance of the Prilled Urea Applicator, BRRI implemented targeted improvements to the metering mechanism, construction materials, and flow adjustment system. The conventional fluted roller was replaced with an adjustable auger, providing continuous and precise control of fertilizer flow (Table 23 and Figure 24). Structural components, including the body and skids, were upgraded to stainless steel and fiber-reinforced composites, improving durability under wet and muddy conditions. Additionally, an integrated agitator was installed within the auger housing to prevent clogging and ensure smooth, reliable operation.

Table 23: Key Modifications and Improvements in the BRRI Prilled Urea Applicator.

Component	Previous Design	Enhanced Design
Metering Mechanism	Fluted roller / star-wheel	Adjustable auger (helical screw) with manual control lever
Materials	Aluminium & HDPE	Full stainless steel and fiber-reinforced composites
Anti-Clogging Feature	Internal agitator (spring fingers)	Integrated agitator within auger housing
Flow Adjustment	Fixed geometry + gate	Direct auger pitch/rotation tuning and variable gate

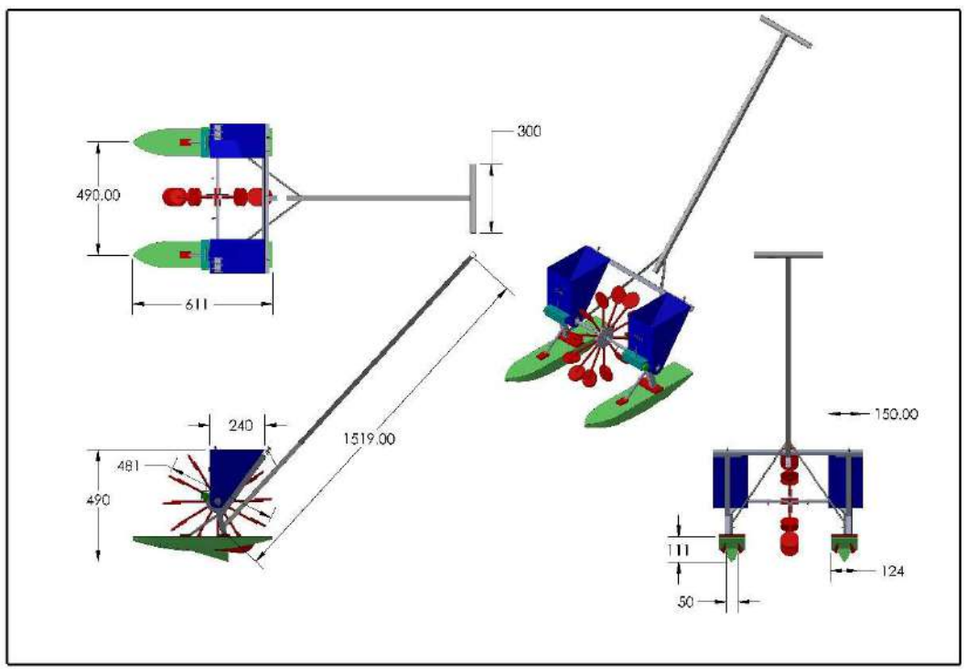

Figure 24. Modified BRRI Prilled Urea Applicator with auger metering.

Result and discussion

Performance Outcomes

Field and laboratory evaluations of the modified applicator demonstrated substantial improvements in efficiency, accuracy, and durability compared to the original design (Table 24). The auger-based metering system achieved a more uniform fertilizer flow, while the upgraded stainless steel and fiber-reinforced body enhanced field life and reduced maintenance requirements. Farmers also reported easier handling due to improved balance and smoother operation, despite the slightly reduced weight.

Table 24: Comparative performance of the BRRI prilled urea applicator before and after modifications.

Performance Metric	Original Prototype	Auger & Material Upgrade
Weight	~9 kg	~ 6.5 kg
Metering Accuracy (CV)	<10%	~ 3–4%
Flow Adjustability	Limited	Infinitely variable via auger control
Durability (field life)	Moderate	High (due to SS & fiber body)
Clogging Incidents	Minimal	Negligible

Fabrication of the modified version

Following the design changes, BRRI fabricates prototype units of the improved Prilled Urea Applicator to test its field performance. The manufacturing focused on the precise engineering of the auger-based metering system and the integration of an upgraded stainless steel and fiber-reinforced composite body, ensuring ergonomic balance, ease of use, and durability in puddled rice fields. The adjustable auger lever allows farmers to control fertilizer flow as needed, while the reinforced body and skids resist corrosion, abrasion, and long-term water exposure. Final assembly at BRRI's workshop included quality checks for metering accuracy, flow consistency, and mechanical strength. These prototypes represent a significant improvement over earlier versions, offering enhanced precision, longer service life, and reduced maintenance, thereby supporting cost-efficient and effective fertilizer management in rice farming.

Plate 6. Field evaluation of the modified applicator in puddled rice plots.

Field observation

Operators reported significantly improved control over fertilizer application due to the manual adjustment lever for the auger (Plate 6). Clogging was virtually eliminated, even under heavy silt conditions. Although the unit's weight increased slightly, enhanced material durability and ergonomic design facilitated easier handling and reduced maintenance requirements.

Experiment 1.7: Design and Development of High-Capacity Head Feed Thresher

Principal Investigator: S Paul
Co-Investigator: MDH, BCN, MGKB, MMR, MMA

Objective

- To develop and fabricate a high-capacity head feed paddy thresher
- To evaluate the performance of the developed thresher

Materials and methods

Fabrication of the Prototype

A head feed power thresher prototype was designed and fabricated at the Arafat Engineering Workshop, Dinajpur, under a public–private partnership (PPP) with financial support from the PARTNER project, BRRI part. Locally available materials were primarily used to minimize fabrication cost and ensure ease of maintenance. The main materials included mild steel (MS) sheet, flat bar, angle bar, shaft bar, galvanized iron (GI) pipe, nuts and bolts, gears, belts, and pulleys. Key mechanical elements incorporated into the design were a wire-loop threshing drum, a feeding mechanism, and a belt–pulley/gear arrangement for power transmission from the engine.

Design consideration

The thresher was designed as per the following considerations:

- The machine should thresh traditional bundled paddy easily.
- The operation should be possible with two laborers.
- The threshing capacity should be higher than that of the existing threshers commonly used in Bangladesh.
- The structure and mechanism should be simple, easy to operate, and maintain.

- The machine should incorporate a self-starting system.
- The use of locally available materials was prioritized to reduce costs.
- The capacity should be acceptable to farmers.
- The machine should ensure trouble-free operation in field conditions.

Functional components of the developed thresher

The developed high-capacity head feed paddy thresher is a comprehensive machine designed to modernize the rice harvesting process (Table 25). Its operation involves feeding the crop tops into the machine for threshing, either by hand or with the gripper chain, while separating the straw. It is also designed for easy separation of rice and straw through the half-feed mode. The developed thresher comprised several integrated units:

Feeding Unit

The feeding unit is designed to introduce paddy bundles into the machine in a controlled and continuous manner. It can be operated either manually or with the assistance of a gripper chain mechanism. The feeding chain ensures uniform delivery of crop material to the threshing cylinder, minimizing clogging and maintaining steady throughput. The feeding tray is inclined at an ergonomic height (127 cm), allowing operators to work comfortably while reducing fatigue.

Threshing Unit

The threshing unit is the core of the machine, responsible for separating grains from the panicles. It consists of a high-speed rotating wire-loop type threshing drum with nine teeth per foot, mounted on a shaft. The main threshing drum is 160 cm long with a diameter of 82 cm, while secondary drums (148 cm length) provide additional separation. During operation, the rotating drum applies stripping and impact forces to detach grains efficiently from straw. The loop-type teeth were selected to reduce grain breakage and improve threshing performance, even for small-grain varieties such as Tulshimala.

Cleaning Unit

The cleaning unit ensures the removal of chaff, husk, and light impurities from the threshed grain. It consists of a blower with a 126 cm length and 38 cm diameter, positioned to direct a stream of air through the grain flow. Adjustable airflow allows regulation of cleaning intensity, ensuring minimal loss of good grains while maintaining a high level of purity. This mechanism produces market-ready clean grain directly after threshing.

Grain Conveying Unit

After threshing and cleaning, the cleaned grains are transported to the collector by a combination of a screw auger and a cup-type belt conveyor. The auger, with a length of 213 cm and a diameter of 15.7 cm, carries the grains horizontally, while the conveyor belt delivers them to the output point (180 cm long, 14 cm wide). This system ensures smooth transfer of grains without spillage or damage and facilitates easy bagging or storage.

Power Transmission System

A 25 hp diesel engine powers the machine. Power is transmitted through a combination of belt–pulley, chain–sprocket, and gearbox mechanisms. This arrangement allows efficient distribution of engine power to the threshing drum, feeding chain, blower, and conveyors. The system is designed to operate with minimal energy loss while enabling speed adjustment to match crop variety and moisture conditions.

Main Frame and Transport Unit

The structural integrity of the thresher is maintained by a robust mild steel frame fabricated from angle bars, flat bars, and MS sheets (Plates 7 and 8). The frame provides stable support for all functional units during operation. For field mobility, the machine is equipped with three durable rubber wheels, enabling easy transportation between fields and threshing yards. The design ensures both operational stability and portability.

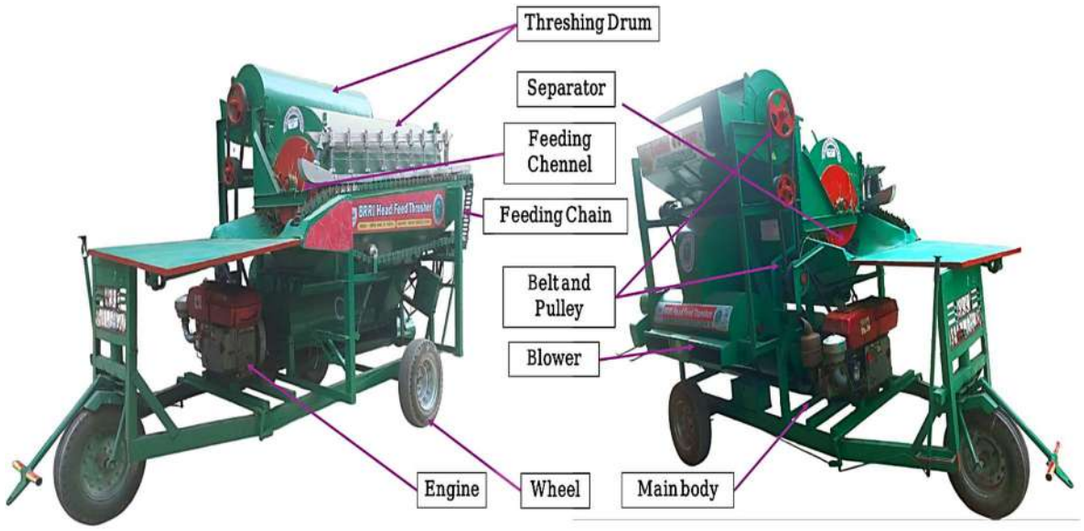

Plate 7. Functional components/units of the developed thresher

Essential parts of the head feed thresher


Main body with 2nd threshing drum


Feeding chain


Blower


Grain Conveyor


Feeding tray


Main threshing drum

Plate 8. Significant parts of the newly developed head feed thresher

Table 25: The general features of the head feed thresher

Item	Features	Item	Features
Engine type	25 hp Diesel engine	Horizontal auger length	213.0 cm
Operator requirement (labor)	Two nos.	Horizontal auger diameter	15.7 cm
Operation	Head feed and whole feed	Clean grain delivery output length	180.0 cm
Cleaning facility	Blower	Clean grain delivery output width	14.0 cm
Movement of the thresher	Three rubber wheels	Extra straw outlet length and width	34.0 cm and 23.0 cm
Grain collector	Auger/screw, cup-type belt conveyor	Grain delivery belt conveyor length	185.0 cm
Power transmission system	Belt pulley, chain-sprocket, and gearbox	Feeding chain length	540.0 cm
Threshing teeth	loop type	Feeding chain width	6.0 cm
Main threshing drum length	160.0 cm	Teeth per feet	Nine nos
Main threshing drum dia.	82.0 cm	Feeding height	127.0 cm
2nd and 3rd threshing drum length	148.0 cm	Machine height	235.0 cm
Blower length	126.0 cm	Machine width	175.0 cm
Blower diameter	38.0 cm	Machine length	370.0 cm

Experimental Procedure

The initial performance test of the prototype was conducted during the 2024–25 Aman season at two locations: the threshing yard of the Farm Machinery and Postharvest Technology (FMPHT) Division

of BRRI and the research field of the Bangladesh Agricultural Research Institute (BARI). The machine was evaluated for threshing capacity, cleaning efficiency, and operational reliability. Two rice varieties were tested: Tulshimala (small grain size) and BRRI dhan87 (medium grain size). For each test, bundled paddy was fed into the thresher, and the following parameters were recorded:

- Grain moisture content (%) before threshing
- Threshed grain weight (kg)
- Threshing time (minutes)

Threshing capacity (kg/h) was calculated using the formula:

❖ Threshing Capacity $\left(\frac{\text{kg}}{\text{h}}\right) = \frac{Threshed\ Grain\ Weigh\ \ (kg)}{Threshing\ Time\ (h)}$

The average capacity and cleaning performance were determined for both varieties.

Results and Discussion

Performance test of the newly developed thresher

The prototype high-capacity head feed thresher underwent initial field evaluation during the 2024–25 Aman season at two sites: the threshing yard of the FMPHT Division, BRRI, and the research field of BARI (Table 26 and Plate 9). The objectives were to assess its threshing capacity, cleaning efficiency, and operational performance. During the trials, the machine demonstrated smooth functioning without significant mechanical faults. Minor modifications were incorporated after the preliminary test to enhance reliability further.

BARI research field

BRRI threshing yard

Plate 9. Initial performance test of the high-capacity head feed thresher

Table 26: Capacity of the machine with moisture content

Parameter	Variety (Tulshimala)				Average	Variety (BRRI dhan87)				Average
Moisture Content (%)	18.2	17.6	17.2	17.9	**17.7**	22.7	22.1	22.9	22.4	**22.5**
Threshed Grain weight (kg)	88.2	102.3	110.4	108.3	**102.3**	165.6	153.4	160.8	159.1	**159.7**
Time, (Min.)	17	20.5	23.2	21.2	**20.48**	20.9	20.2	20.1	20.5	**20.4**
Threshing Capacity (kg/h)	311.2	299.4	285.5	306.5	**300.65**	475.4	455.6	480.0	465.7	**469.2**

Effect of Drum Speed on Performance

It was observed that increasing drum speed enhanced both threshing and cleaning efficiency. The higher speed resulted in greater stripping and impact pressure applied to the grains, which improved the separation of paddy from straw. This confirmed the importance of optimizing drum speed for efficient threshing operations.

Threshing Performance by Variety

For the Tulshimala variety (small grain size), the average moisture content was 17.7%, the average threshed grain weight obtained was 102.3 kg, with an average threshing time of 20.48 minutes. This resulted in a threshing capacity of 300.65 kg/h. For the BRRI dhan87 variety, the average moisture content was 22.5%. The variety produced a significantly higher threshed grain weight of 159.7 kg,

with a slightly lower average threshing time of 20.40 minutes. This resulted in a considerably higher threshing capacity of 469.2 kg/h, demonstrating strong potential for high-yield and time-efficient operations. The significant gap in threshing capacity between the two varieties can be attributed to differences in their moisture content and its impact on threshing efficiency.

Cleaning Efficiency and Grain Quality

The blower mechanism of the thresher effectively removed chaff and impurities. The cleaning performance was judged as acceptable for both varieties, with minimal admixture in the cleaned grain. Grain breakage was within acceptable limits, and no significant clogging or operational issues were observed.

Operational Feasibility

The machine required only two operators and demonstrated good mobility with its three-wheel system. Farmers involved in the demonstration reported that the machine's simplicity, combined with its higher throughput compared to existing threshers, makes it a promising option for large-scale adoption.

Conclusion

A prototype high-capacity head feed paddy thresher was successfully designed and fabricated using locally available materials under a public–private partnership arrangement. The machine demonstrated promising performance during initial field trials conducted at BRRI and BARI. The average threshing capacity was found to be 300.6 kg/h for Tulshimala (with a moisture content of 17.7%) and 469.2 kg/h for BRRI dhan87 (with a moisture content of 22.5%), achieving acceptable levels of grain cleanliness and minimal mechanical issues. The results indicate that the newly developed thresher can significantly improve threshing efficiency compared to existing small-scale machines, while requiring only two operators and ensuring farmer-friendly operation. Its use of locally available materials, simple design, and mobility enhances the potential for large-scale adoption in rural areas. However, the study also highlights the need for further testing across multiple seasons and varieties to validate the consistency of performance, durability, and long-term operational reliability. Future improvements may focus on optimizing drum speed, reducing grain loss, and enhancing cleaning mechanisms. Overall, the machine shows strong potential to modernize paddy threshing in Bangladesh by reducing labor dependency, increasing capacity, and lowering postharvest losses.

Recommendations

- More extensive testing should be conducted across multiple locations and crop varieties to confirm the machine's reliability and adaptability under different field conditions.
- Long-duration performance trials are required to detect potential wear-and-tear issues in the threshing drum, feeding chain, and power transmission system.
- Comparative studies with conventional threshers will be helpful to quantify improvements in capacity, grain quality, and operational cost.

PROJECT 2: MILLING AND PROCESSING TECHNOLOGY

Experiment 2.1: Design and development a paddy de-husker for two-stage rice mill

Principal Investigator: Md. Golam Kibria Bhuiyan
Co-investigator(s): MDH, BCN, SP, MMR

Objectives

- To design and fabricate a two-stage rice mill
- To evaluate the performance of the fabricated rice mill
- Compare the performance with the engelberg huller

Materials and Methods

The Farm Machinery and Postharvest Technology (FMPHT) Division has successfully designed and developed a paddy de-husker for a two-stage rice milling system at the Salam Engineering Workshop, Kushtia, to improve milling efficiency and head rice recovery. The FMPHT division provides technical (drawing and design) and financial support to the workshop. The paddy de-husker was designed using SolidWorks CAD software to optimize dimensions and component alignment (Figure 25). The overall dimension (H x W x B) of the husker is 2134 x 1410 x 457mm, and the base dimension is 1410 x 528 x 457mm. The base of the machine is fabricated with a 76 x 38mm angle

bar. De-husker dimension is 1590 x 528 x 457mm. The pictorial view of the husker is shown in Plates 10 and 11.

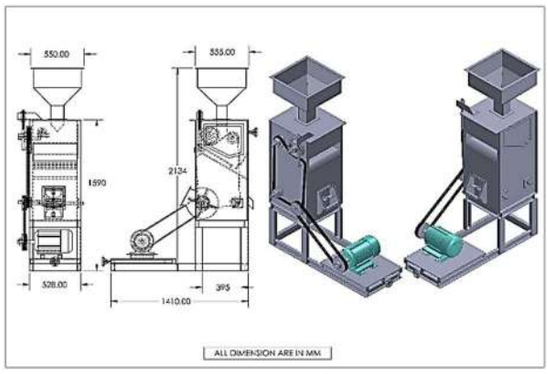

Figure 25. SolidWorks CAD drawing of the developed Paddy de-husker

Developed rubber roll de-husker operates with a 5hp (3-phase 4-wire 1450 rpm) electric motor. Fixed rubber roll diameter and length are 240 mm and 101 mm, respectively. The RPM of the fixed rubber roll is about 1300 rpm. The adjustable rubber roll diameter and length are also the same as the fixed rubber roll. The RPM of the adjustable rubber roll is about 900 rpm. The elevator will be used to carry the paddy in the hopper. The blower diameter is 300mm, and it runs at 2000 rpm. The bottom end of the de-husker is connected with a pipe (dia. 152 mm). A cyclone separator is attached to the de-husker for collecting husk, which keeps the working area free from dust and husk. In the first stage, paddy grains are fed into the hopper and directed to the de-husker, where rubber rollers apply pressure and friction to remove the husk, producing a mixture of brown rice, husk, and unhulled paddy. The husk is separated using a cyclone separator, while the unhulled grains are recirculated for reprocessing. The rubber roll de-husker does not damage the aleuronic layer of paddy. An airstream is blown over the grains, and immature grains drop into the separate hopper for discharge. The operating condition of the machine is shown in Plates 10 and 11. BRRI dhan28 (un-parboiled) was used in this experiment. The moisture content was 12.2% (wb.), and each sample size was 20 kg.

Husking efficiency

The percentage of total mass of milled rice (head and broken rice) recovered from the mass of the corresponding input paddy to the rice mill (husker or huller and whitener). It is also called total milling recovery.

$$Husking\ \ efficiency(\%) = \frac{Weight\ of\ milled\ rice}{Weight\ of\ rough\ rice} \times 100$$

Plate 10. Pictorial view of the de-husker

Plate 11. Operating condition of the de-husker

The major components of the Husker, including their functions and technical specifications, are shown in Tables 27 and 28.

Table 27: Major components of the de-husker and their functions

Component	Function
Hopper	Holds and feeds paddy into the rubber rolls for processing.
Bucket Elevator	Lifts and transfers paddy from the hopper to the husker.
Husker	Removes the outer husk from paddy using rubber rollers.
Blower	Creates airflow to carry away husk.
Cyclone Separator	Separates husk from brown rice using centrifugal action.
Motor (5 hp)	Provides power to operate all units through a belt and pulley system.
Bucket	Collects and discharges processed rice and by-products separately.

Table 28: Technical Specifications of the de-husker for the two-stage rice mill

Particulars	Specifications
Type of Mill	De-husker
Frame Material	Mild Steel sheet, angle bar
Overall Dimensions (H x W x B)	2134 x 1410 x 457mm
Motor Power	5 hp (1450 rpm) electric motor
Power Transmission	Belt and pulley drive system
Feeding System	Hopper (capacity: 25 kg) with bucket elevator
Husker	Rubber roller type, two rollers (240 mm diameter and 101 mm length)
Processing Capacity	500 – 600 kg paddy/hour
Operating Voltage	440 V, 3-phase AC

Performance evaluation

The average de-husking capacity of the husker ranged from 500-600 kg/h, and husking efficiency was about 80%. Husking efficiency can be increased by closing the adjustable roller, which reduces the amount of broken rice (brown rice). The brown rice and paddy were collected from the discharge chute, and the husk was collected from the cyclone separator. The average fixed and adjustable rubber roll rpm was found to be 1300 and 900, respectively. The adjustable rubber roll rotates 30 % less rpm than the fixed rubber roll. The difference in peripheral speed subjects the paddy grain falling between the rolls to a shearing action that strips off the husk. The clearance between the rolls is adjustable, and it should be less than the thickness of the grain.

Experiment 2.2: Design and Development of Paddy Collector

Principal Investigator: Md. Golam Kibria Bhuiyan
Co-investigator(s): MDH, BCN, SP, HR, MMA

Objectives

- To design and develop a Paddy collector
- To evaluate the performance of the fabricated collector
- Compare the collector with the manual method
- Disseminate the Paddy collector

Materials and Methods

The mechanical grain collector was designed using SolidWorks CAD software to optimize dimensions and component alignment (Figure 26). Field trials were conducted on the concrete floor of the BRRI drying yard to evaluate collection efficiency, throughput, uniformity of bag weights, and ease of operation

Working Principle

The grain collector operates by sweeping scattered paddy using a rotating nylon brush reel. As the brush rotates close to the ground, it gently lifts and directs the grains toward the intake section, where they fall into a screw conveyor. The conveyor transports the grains and discharges them by moving the collecting elevator into the hopper for collection. The motor/engine powers the reel and conveyor through a pulley-belt system, while the operator pushes the unit forward. Reel height and rotation speed can be adjusted depending on the surface, minimizing kernel loss and breakage.

Design Considerations

The mechanical grain collector features soft nylon bristles to minimize grain breakage, along with an adjustable reel height and skid to accommodate various surfaces. All parts that contact the grain are made from durable mild steel, and removable panels facilitate easy cleaning and maintenance. Safety is improved by guarding the moving parts, while an ergonomic handlebar height of 1100 mm helps reduce operator fatigue. The modular design supports both electric and petrol drive options,

and using locally available pulley, belt, and bearing parts makes repairs easier and keeps costs down. Figure 26 shows the Layout of the grain collector

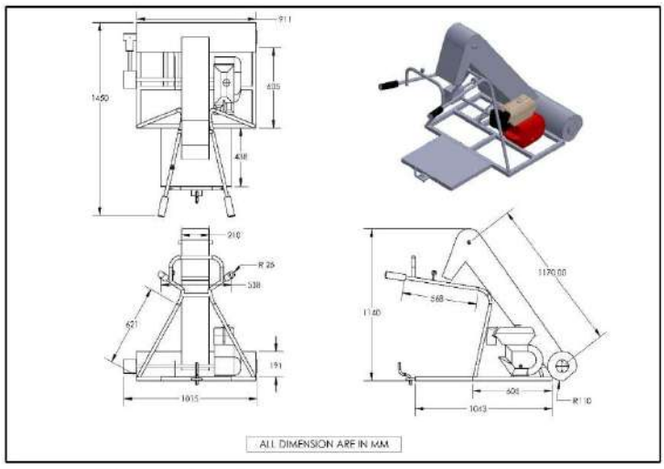

Figure 26. Layout of the grain collector

Table 29: Function of main components

Component	Material	Function
Chassis	Mild steel (MS)	Provides structural support and stability for all components
Brush reel	Nylon bristles	Sweeps and lifts scattered paddy toward the intake
Screw conveyor	Stainless steel (SS-304)	Transports collected grains from the ground to the moving elevator, which then feeds into the hopper.
Hopper	Stainless steel (SS-304)	Stores grains temporarily during collection
Engine	Petrol 6.5 hp	Powers brush reel, screw conveyor, and collecting elevator
Transmission	belt–pulley	Transfers power from the engine to the moving parts
Handle	MS tubular	Allows the operator to push and maneuver the machine ergonomically
Wheels	Rubber	Maintains ground clearance and enables smooth movement on different surfaces

Performance Evaluation

The mechanical grain collector was evaluated at the BRRI drying floor under actual working conditions (Figures 27 and 28). Necessary data, including bag filling time, collected grain weight, and throughput, were recorded. The machine demonstrated an average collection capacity of 20.2 kg/min (approximately 1212 kg/h) with uniform bag weights of 39.6 kg. Compared to manual collection, it reduced labor requirements and operational costs while improving efficiency.

Figure 27. Developed a grain collector

Figure 28. Operation of the grain collector

Table 30 presents the performance data of the mechanical grain collector across eight trials. The time required to fill a standard gunny bag ranged from 1.8 to 2.1 minutes, with an average of 1.98 minutes per bag. The average capacity of the machine was 20.2 kg/min, equivalent to approximately 1212 kg/h, demonstrating consistent performance under field conditions. The collected bag weights were relatively uniform, averaging 39.6 kg, which indicates reliable collection efficiency across multiple operations.

Table 30: Performance of Mechanical Grain Collector

Obs. No.	Grain to fill a gunny bag (kg)	Time to fill a gunny bag (min)	Capacity (kg/min)
1	40.0	2.0	20.0
	38.5	1.8	21.4
	39.0	1.9	20.5
2	41.0	2.1	19.5
	39.5	2.0	19.8
	40.5	2.0	20.3
3	38.0	1.85	20.5
	39.0	1.95	20.0
	38.5	1.92	19.6
Average	39.6	1.98	20.2

Table 31: Comparison with the Manual paddy collector

Items	Mechanical Grain Collector	Manual grain collector
Labor required to fill a gunny bag (no.)	1	2
Time required to fill a gunny bag (min)	1.98	5.0
Bags per hour (bags/h)	30.3	12.0
Throughput (kg/h)	1212	472
Operational cost (Taka/bag)	4.0	8.0
Cost per tonne (Taka/t)	101	203
Labor productivity (kg per labor-hour)	1212	236
Time saving per bag vs manual	60% faster	—
Cost saving per ton vs manual	50% lower	—

Table 31 compares the mechanical grain collector with the traditional manual collection system. The mechanical collector required only one laborer per bag, whereas the manual system required two. It reduced the time to fill a gunny bag by approximately 60% and nearly doubled throughput, achieving 1212 kg/h compared to 472 kg/h for manual collection. The operational cost per bag and per ton was about 50% lower for the mechanical collector. Overall, the table highlights the advantages of mechanization in terms of labor efficiency, time saving, throughput, and cost-effectiveness. Table 32 describes the features of the grain collector.

Table 32: Features of the grain collector

Parameter	Specification
Overall dimensions (L×W×H)	1300 × 700 × 950 mm //1450 x 1015 x 1140 mm
Pick-up width	600 mm (effective 560 mm)/1000 mm
Brush reel	Ø300 mm, nylon bristles, 180–220 rpm
Screw conveyor	Ø100 mm SS, pitch 80 mm, 120–160 rpm
Hopper capacity	35 kg paddy
Power source	6.5 hp petrol engine
Transmission	belt–pulley system
Forward speed	3.0 km/h
Field capacity	0.06 ha/h
Collection capacity	400 kg/h
Noise at the handle	≤78 dB(A) at 2.5 m
Ground clearance	40 mm (adjustable ±10 mm)

Limitations and recommendations

The mechanical grain collector performs less effectively on wet or uneven surfaces due to brush reel slippage, and minor kernel breakage may happen at high brush speeds. Its limited hopper capacity requires frequent emptying during large-scale operations, while the fixed forward speed can limit its adaptability in large or sloped fields. Additionally, the machine's relatively high weight demands a skilled operator for safe and efficient handling. Suggested improvements include increasing hopper capacity or adding a continuous collection bin, installing rubberized or adjustable wheels to improve traction, conducting long-term durability tests on the nylon bristles and stainless steel conveyor, and exploring solar-assisted electric drives for more sustainable operation.

PROJECT 3: RENEWABLE ENERGY

Experiment 3.1: Design and develop a solar-powered smart bird repellent
Principal Investigator: Md. Mizanur Rahman
Co-investigator(s): MMH, HR, SP, MDH
Objectives

The study intends to design a solar-powered smart bird repellent for sustainable crop protection. The specific objectives are:

i. Develop a real-time bird detection and repellent system for crop protection.
ii. To identify the scary melodies for carnivorous birds
iii. Train and validate the model using native bird datasets and cross-dataset evaluation.
iv. Assess performance through metrics and comparison with earlier YOLO models.
v. Enable autonomous field operation with solar-powered audio and mechanical deterrents.

Bird infestation is a major threat to agricultural productivity in Bangladesh, causing 10–50% yield loss depending on species and crop stage (Hassani & Dackermann, 2023; Hidayatulloh et al., 2022). Common birds such as sparrows, mynas, crows, and pigeons damage rice during the milky and ripening stages (Gojiya et al., 2023), with some species causing up to 40% yield loss (Upendra et al., 2025). These damages severely impact smallholder farmers and threaten food security, highlighting the need for sustainable bird deterrent systems. Traditional deterrents—scarecrows, firecrackers, cloth flags, and traps—are labor-intensive and short-lived (Riya et al., 2020). Modern devices like lasers, ultrasonic tools, and sound emitters provide temporary relief but lose effectiveness as birds adapt (Li et al., 2019). A survey found that 73% of farmers consider bird damage serious, and 85% support eco-friendly automated repellents (Riya et al., 2020). Thus, a smart, real-time, and low-cost system is essential for sustainable agriculture.

Recent advances in computer vision and deep learning have improved precision farming. Object detection models such as YOLO, SSD, and Faster R-CNN have been used for pest and crop monitoring (Kamilaris & Prenafeta-Boldú, 2018). Among them, YOLOv8n, a lightweight nano version, offers high speed and low power consumption, making it ideal for edge devices like Raspberry Pi (Bochkovskiy et al., 2020). At the same time, integrating solar power with IoT systems ensures continuous operation in rural areas. Solar-based systems have been applied in various agricultural technologies (Meral & Diner, 2011; Ramesh et al., 2022). Previous solar bird repellents used batteries, sensors, and audio emitters (Muminov et al., 2017; Koyuncu & Lüle, 2009), but lacked AI-based detection and adaptive control. A clear research gap exists in combining real-time vision, solar energy, and autonomous control within a single platform. Most AI-based systems are energy-intensive, while solar systems lack intelligence. This study develops a solar-powered, AI-enabled bird detection and repellent system using YOLOv8n on a Raspberry Pi 4 Model B. The system autonomously detects birds and triggers sound deterrents, offering real-time performance, low power use, and field adaptability. It provides a sustainable, low-cost solution for smallholder farmers, supporting eco-friendly precision agriculture in Bangladesh.

3. Materials and Methods

3.1 System Overview

The proposed bird repellent system is a low-cost, solar-powered, and autonomous solution for protecting crops during grain-filling and harvesting. It integrates a YOLOv8n-based bird detection module with audio and mechanical repellents controlled by a Raspberry Pi 4 Model B. Upon bird detection, the Raspberry Pi triggers distress/predator sounds and activates a stepper motor to move reflective scare elements, conserving energy by operating only when birds are present. All components are enclosed in a weatherproof casing for outdoor use.

3.2 Bird Detection Unit

3.2.1 Model Selection

YOLOv8n, the nano version of YOLOv8, was chosen for its speed, accuracy, and low computational demand—ideal for real-time edge deployment on Raspberry Pi. It detects birds efficiently under varying environmental conditions. **Figure 29 shows** the conceptual framework of theYOLOv8n model.

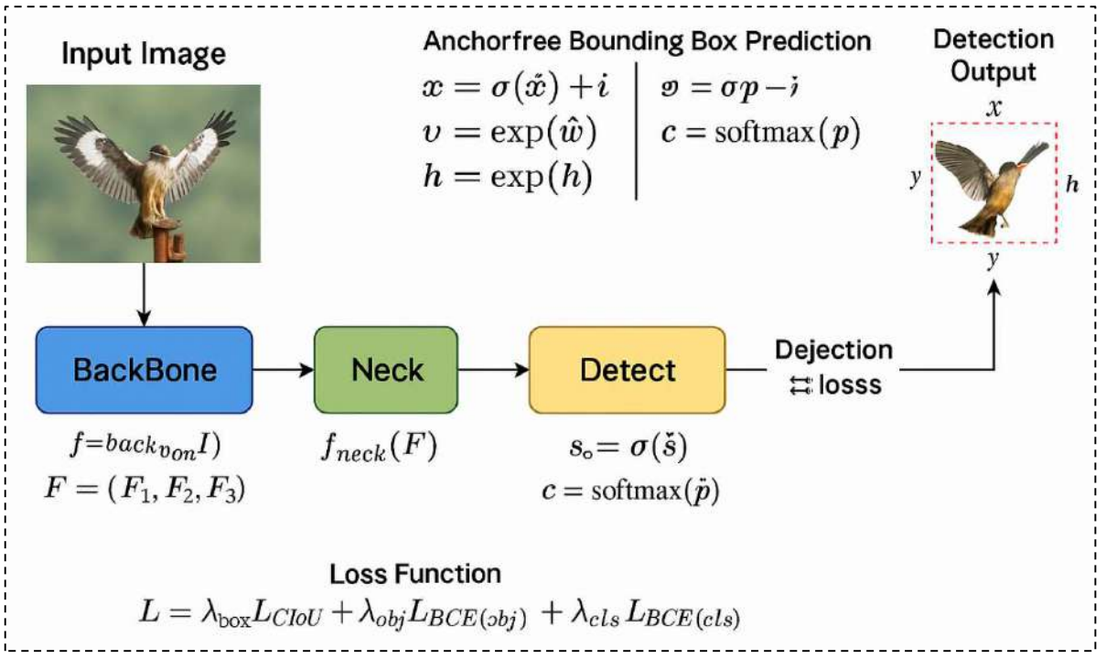

Figure 29. The conceptual framework of the YOLOv8n model

3.2.2 Dataset and Annotation

A subset of 3,000 "bird" images from the COCO 2017 dataset was used. Annotations were converted from JSON to YOLO format (class ID, normalized coordinates). After quality checks with LabelImg, ~6,500 bounding boxes were retained for training.

3.2.3 Preprocessing and Augmentation

All images were resized to 640×640 px. Augmentation using *Albumentations* (rotation, flip, brightness, blur, noise) expanded the dataset to 15,000 images, simulating diverse field conditions. Data were split as 70% training, 20% validation, and 10% testing using *Roboflow*.

3.2.4 Model Validation

Model performance was assessed using Precision, Recall, F1-score, and mAP@0.5, following standard object detection evaluation.

3.3 Bird Repelling Unit

3.3.1 Real-Time Detection

The trained YOLOv8n model (exported as ONNX) was deployed on a Raspberry Pi 4 with a USB webcam capturing 800×800 px frames. Using *OpenCV* and *Ultralytics API*, detections above a 0.32 confidence threshold triggered audio deterrents via *play_sound.py*. The system achieved 10–15 FPS.

3.3.2 Audio Amplifier

A dual-bridge stereo amplifier based on TDA2030 ICs and XL6009 DC-DC converters powered two speakers for high-quality output. Passive networks ensured low distortion and stable performance in low-voltage conditions.

3.3.3 Camera Rotation Mechanism

A 28BYJ-48 stepper motor with a ULN2003 driver controlled via GPIO enabled automated camera panning. The motor rotated 512 steps clockwise and back, enhancing field coverage.

3.4 Solar Power System Design

The solar power unit supplied energy to the Raspberry Pi, camera, and audio system for continuous field operation. The total photovoltaic power was estimated with a 30% safety margin to cover system losses. Battery capacity was designed to ensure sufficient backup based on total load, system voltage, and days of autonomy. A charge controller rated 30% above the panel's short-circuit current and an inverter 25–30% above total wattage was used to ensure safe and efficient power conversion. Below formulas were applied to design a solar power system:

$$Total\ required\ power\ (Trp) = (Tap \times Rt) \times 1.3 \text{.....(1)}$$

$$Size\ of\ the\ SP\ panel = Wp/3.4 \text{.....(2)}$$

$$Number\ of\ the\ SP\ panel = \frac{Trp}{3.4 \times Wp} \text{.....(3)}$$

$$Battery\ Capacity\ (Ah) = \frac{Total\ watt\ used\ by\ the\ system\ (watt)}{0.85\ x\ 0.6\ x\ nominal\ battery\ voltage} \times Days\ of\ autonomy \text{.....(4)}$$

$$Solar\ charge\ controller\ rating\ =\ Total\ short\ circuit\ current\ of\ PV\ array\ x\ 1.3 \text{.....(5)}$$

Where *Trp, Tap,* and *Rt* are the total required power (Wh/day), total appliances used in this system, and operational time. Wp is the total rated peak-watt (Wp/day).

3.5 System Integration and Workflow

All components were integrated into an automated control loop. YOLOv8n processed live video; detections triggered simultaneous sound and motor movement. The system continuously operated in real-time without human input, combining visual detection, audio deterrence, and mechanical motion to minimize bird-induced crop loss (**Figure 30)**.

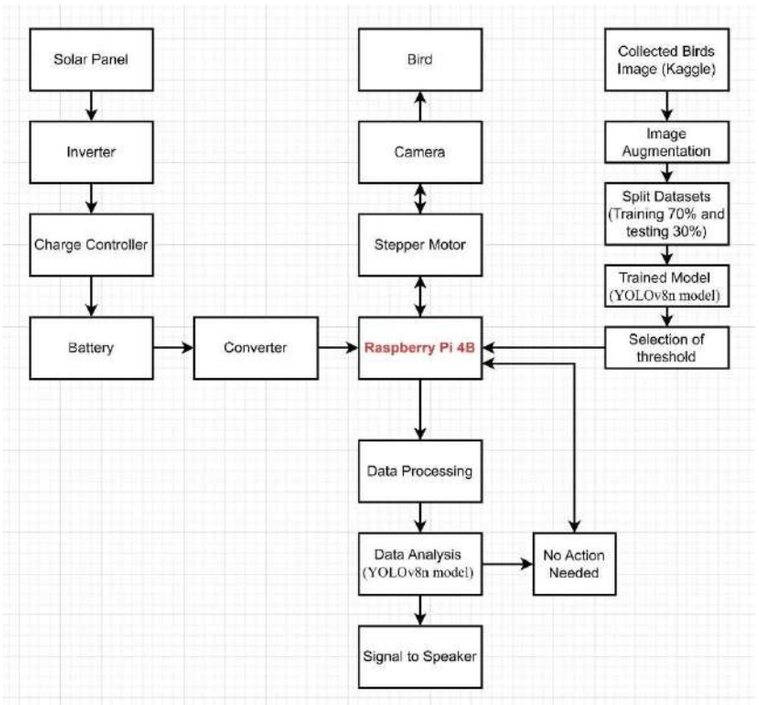

Figure 30. Flow diagram of the bird repellent

3. Results

3.1 Model Evaluation and Training Performance

The YOLOv8n model was trained using a custom bird dataset derived from native species in Bangladesh and validated with both COCO and real-world video data. The model achieved strong performance, with Precision = 0.85, Recall = 0.80, F1-score = 0.825, Specificity = 0.90, and mAP@0.5 = 0.764. These results indicate robust detection accuracy and low false alarms.

Precision–Recall and F1–Confidence curves confirmed consistent performance, with the F1-score peaking at a 0.32 confidence threshold, suggesting a balanced trade-off between sensitivity and precision. The mAP@0.5:0.95 value (0.45) indicates reliable detection consistency across varied confidence levels.

3.2 Cross-Dataset Validation with YouTube Videos

Real-world validation was conducted using annotated frames from YouTube videos featuring native birds under diverse lighting and background conditions. The model achieved superior performance with Precision = 0.923, Recall = 0.915, F1-score = 0.919, and mAP@0.5 = 0.931, confirming its adaptability to field scenarios. The average inference time was 45 ms per frame, demonstrating suitability for real-time Raspberry Pi deployment.

3.3 Loss Convergence and Training Stability

The model was trained for 20 epochs using transfer learning. Loss curves for bounding box, classification, and focal distribution showed smooth convergence, while validation losses decreased steadily. Precision and recall stabilized at 0.85 and 0.80, respectively, confirming effective learning and absence of overfitting.

3.4 Comparison with YOLO Variants

A comparative analysis (Figure 9) between YOLOv8 and its predecessors (YOLOv5–v7) showed that YOLOv8 achieved higher mAP@0.5:0.95 with fewer parameters and faster inference. The YOLOv8n variant offered the best trade-off between detection accuracy and speed, proving ideal for edge deployment in real-time bird repellent systems.

3.5 Real-Time Detection on Embedded Device

The trained model was deployed on a Raspberry Pi 4 Model B for real-time inference using a USB camera (Figure 31 and 32). The system successfully detected birds across various lighting and motion conditions, maintaining detection confidence above 0.80 in most cases. False positives were minimal due to logic filters restricting responses to bird-class detections only. These results validated reliable field performance and efficient hardware integration.

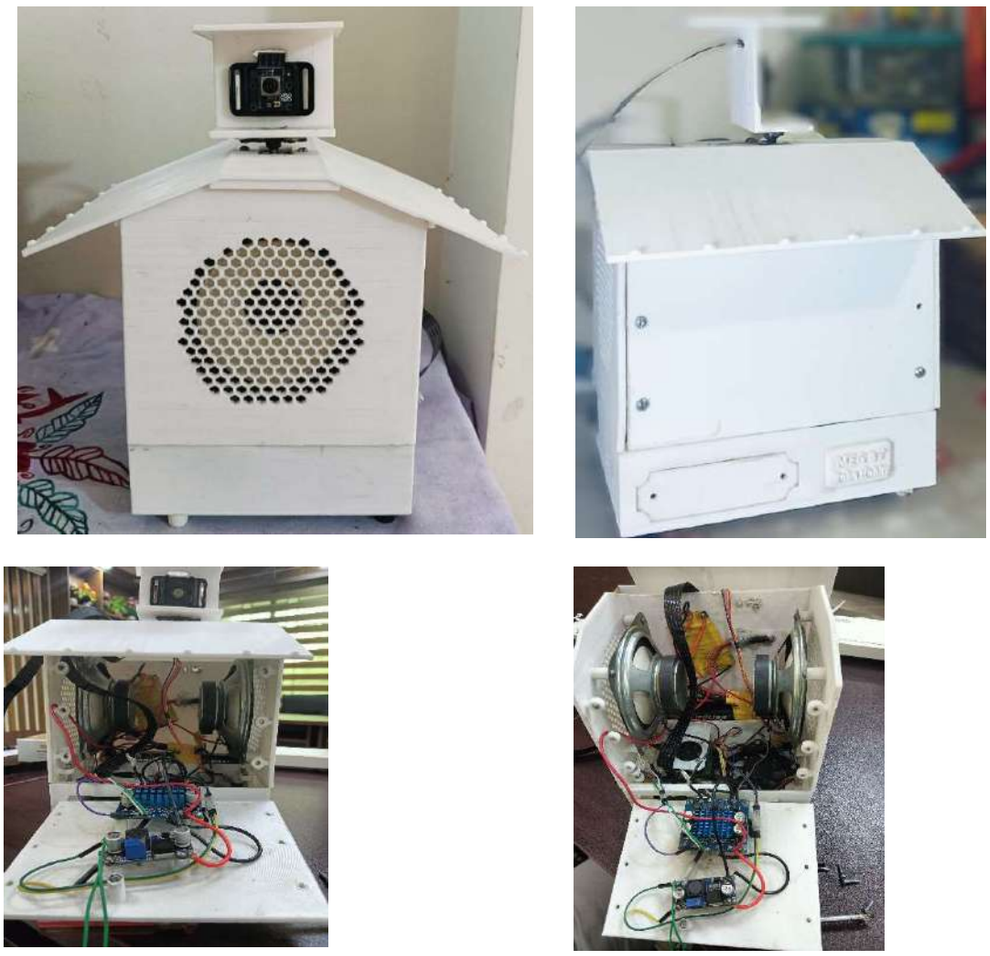

Figure 31: Proposed Bird Repellent (3D printing)

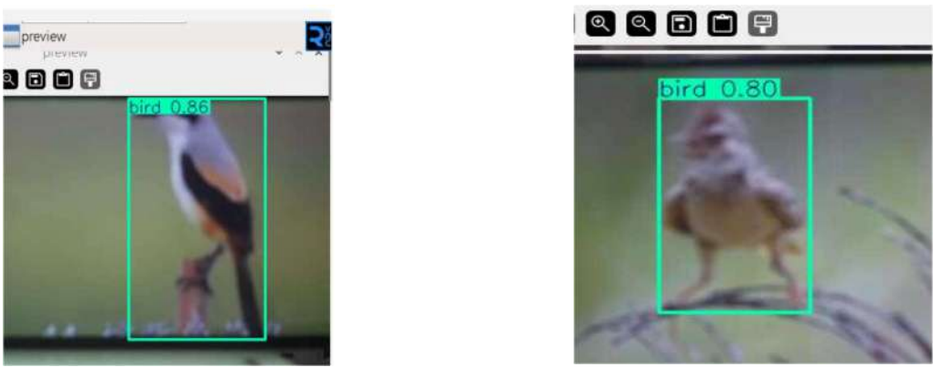

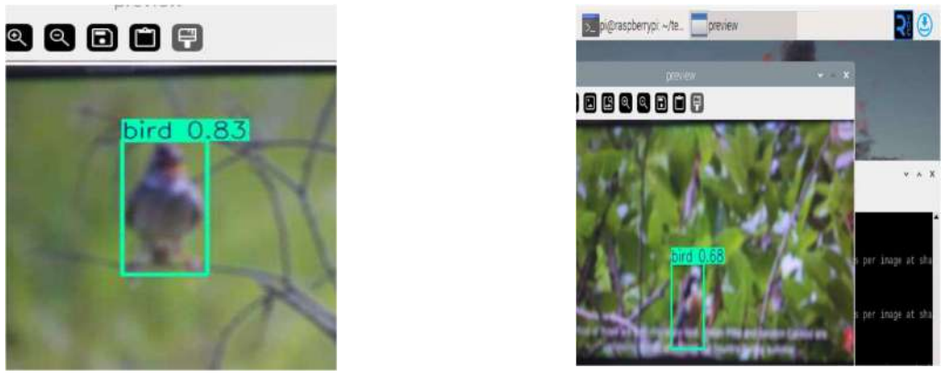

Figure 32: Detection accuracy of the proposed bird-repellent

3.6 System Assembly and Structural Validation

A CAD-based prototype demonstrated the complete system assembly, integrating the camera, solar panel, control unit, sound box, and battery on a pole-mounted structure (~1340 mm height) (**Figure 33)**. The design ensures portability, weather resistance, and solar-powered autonomy, suitable for agricultural or ecological deployment.

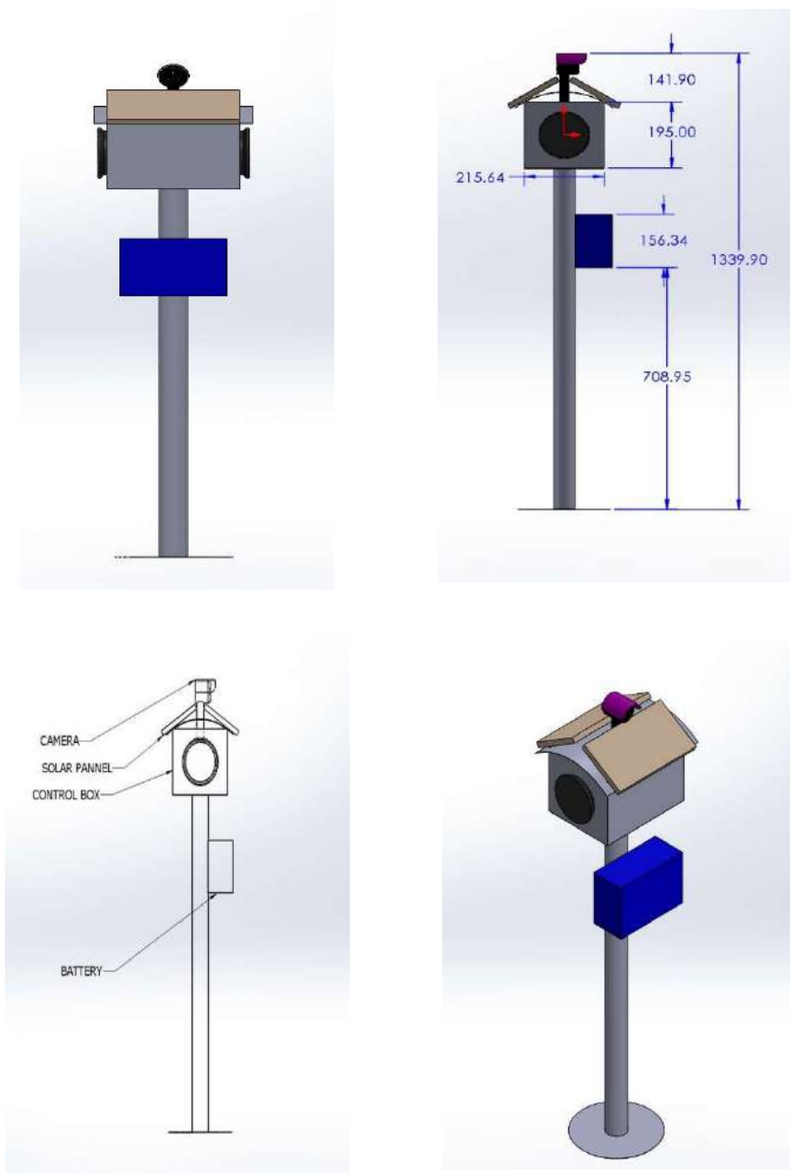

Figure 33. Assembled CAD views of the bird repellent system.

The system integrates a camera, solar panel, control unit, sound box, and battery on a stable pole-mounted structure designed for field deployment.

4. Conclusion

This study developed a real-time, solar-powered bird detection and repellent system using the YOLOv8n model on a Raspberry Pi 4. The system achieved high accuracy and efficiency, with a precision of 0.85, recall of 0.80, F1-score of 0.825, and mAP@0.5 of 0.764. YOLOv8n outperformed earlier YOLO versions in speed and parameter efficiency, making it ideal for field deployment. The system's integration of audio deterrents, motorized camera control, and solar autonomy offers a low-cost, scalable solution for reducing bird-induced crop damage. Its flexible architecture allows future upgrades for multi-class pest detection and adaptive deterrent strategies, supporting the advancement of intelligent and sustainable pest management in agriculture.

Recommendations:

Despite its effectiveness, the system has some limitations compared to high-end platforms like NVIDIA Jetson Xavier or Coral Edge TPU, which support higher processing speeds and multi-class detection but are more expensive and power-intensive. This study focuses on a low-cost, energy-efficient solution suitable for farmers, emphasizing accessibility without major performance trade-offs. Future improvements may include model quantization and pruning to reduce computational load, extending detection to multiple pest species, and integrating advanced deterrent mechanisms such as adaptive audio or light-based systems. Combining detection with reinforcement learning for smarter deterrence could further enhance system performance.

Experiment 3.2: Validation and Adaptive Field Trial of BRRI Developed Solar Light Trap

Principal Investigator: Bidhan Chandra Nath
Co-investigator(s): SP, GKB, MDH, MMA, TKR, and ABMAU

Objectives

- Evaluation of the suitability of the BRRI solar light trap for use in grain storage
- Adaptive field trial of the solar light trap in farmers' houses

Materials and Methods

The FMPHT Division of BRRI has developed and evaluated a solar light trap for use in different crops across Bangladesh. The trap has already been tested in rice fields, where it demonstrated satisfactory performance in capturing rice insects under outdoor field conditions. However, under indoor conditions, particularly with stored rice insects, the species caught have not yet been identified. Therefore, the present study was undertaken to assess the suitability of the BRRI solar light trap for protecting stored grain by capturing storage insects.

Study Location and Duration

The experiment was carried out in the BRRI storage facility at Gazipur, where both seed and non-seed rice were stored. It took place over four months, from September to December 2024, under indoor storage conditions. The investigation was undertaken within this defined timeframe to monitor and capture insect populations associated with stored grain.

Solar light trap setup

The BRRI-developed solar light trap was installed inside the grain storage facility. Figure 34 shows the main components of a typical solar-powered system. The trap was placed at an optimal height (about 1.5 m above ground) to attract storage insects effectively. It was powered by a solar panel mounted on the roof of the storage room and operated automatically from after sunset until 11:00 p.m., depending on sunlight. Notably, insect activity is usually highest within the first three hours after sunset. Two light traps were installed in separate grain storage units at BRRI, Gazipur.

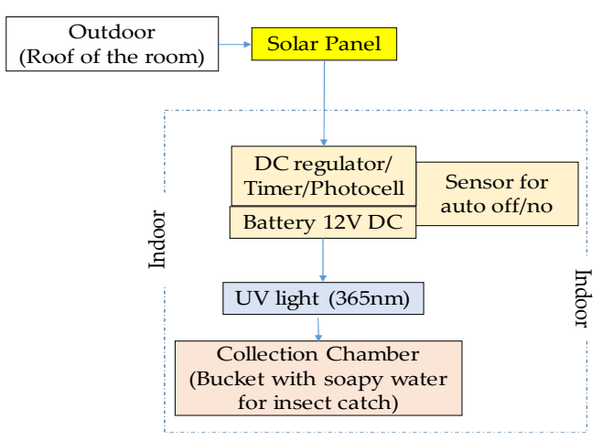

Figure 34. Flow diagram of solar light trap setup in grain storage

Insect collection and identification

During the first week of the experiment (days 1–6), insects captured in the light traps were collected hourly between 6:00 p.m. and 11:00 p.m. to assess insect abundance. At the same time, light flux was measured hourly during this period to evaluate its relationship with insect activity. After the first week, as insect captures declined, the collection frequency was reduced to once daily. Samples were collected each morning and sent to the BRRI Entomology Division for taxonomic identification, counting, and further analysis. The collected specimens were identified to the lowest possible taxonomic level using standard entomological keys and reference collections, with a focus on known grain storage pests. For further examination, a subset of insects was preserved in labeled vials filled with ethanol and stored for later identification.

Data collection and recording

For the performance assessment of the BRRI solar light trap, the following parameters were recorded: trap start and end times, number of insects captured, light intensity (Lux), and daily temperature and relative humidity. Data collection included the total number of insects trapped each day as well as the variety of species captured. Environmental conditions inside the grain store, specifically temperature and relative humidity, were monitored because these factors affect insect activity. The efficiency of the BRRI solar light trap was evaluated based on both the abundance and diversity of insect species caught.

Working principle of the solar light trap

The Farm Machinery and Postharvest Technology (FMPHT) Division of BRRI developed the solar-powered light trap used in this study, which has proven effective in rice fields. Detailed specifications are listed in Table 33. The trap stand was built using locally available materials like MS rods, MS sheets, and MS flat bars, all assembled with nuts and bolts. The solar panel, controller, battery, and bulb were obtained from the local market.

The system features a 16.8 V, 20 W monocrystalline silicon solar panel connected to a 12 V DC auto controller and a 12.8 V, 7.5 Ah lithium iron phosphate (LiFePO4) battery, providing an energy storage capacity of 54 Wh—enough to run the trap all night. A custom-made LED array combining UV (365 nm) and blue (450 nm) wavelengths was chosen for its effectiveness in attracting many stored-grain pests. The total power consumption is 3 W. The LEDs are placed above a removable collection container filled with a water–surfactant mixture (detergent or kerosene mixed with water) to prevent insects from escaping.

A photocell sensor automatically activates the system at dusk and turns it off at dawn, providing about six hours of nightly operation. The solar panel converts sunlight into DC electricity, which is regulated and stored in the battery. The bulb automatically turns on when there is no sunlight and off when sunlight is present. The estimated lifespan of the bulb and battery is around two years, while the solar panel is expected to last approximately 20 years. The design allows for easy placement on any surface, ensuring versatility for different setup conditions. The observation of light trap and insects are displayed in Plates 12 and 13.


Plate 12. Observation of captured insects and BRRI grain storage


Plate 13. Insects trapped in the Light Trap at the BRRI grain storage

Table 33: Specification of the BRRI-developed solar light trap

Particulars		Solar light trap
Solar panel	16.8V /20W	
Battery	DC 12.8V, 7.5A, Life P04 Type (Lithium Iron Phosphate), rechargeable	
Lamp	UV 12V 8W	
Weight	Approximately 12 kg	
Dimension	Main Body: Net Length 90 inches, bowl dia. 20 inches, and 2-inch dia. steel pipe	
Type of product	Eco friendly	
Type of energy	Solar energy	
No of legs	01	
Solar plate setup angle	23.5 Degree North-South	
Battery charging	8 to 10 hours	
Set up a working area	1 light trap per room	
Set up working hours	6 pm to 11 pm	
Type of moment	Flexible	
Type of colour	Bluish	

Results and discussion

The technical performance of a solar light trap depends on the number of insects captured, the intensity of the light, and the peak hours of insect capture.

Insects captured across time intervals

Figure 35 shows the number of insects collected by the solar light trap from the store paddy from the first to the sixth day of trap setting (Table 34). On the first day of observation, the highest number of insects was recorded during the early evening (6–7 pm), with Angoumois grain moths showing the most incredible abundance, reaching over 600 individuals. However, their numbers declined sharply and approached zero by 9–10 pm, indicating a short-lived peak in activity. Rice weevils were also abundant initially (~475 individuals) but exhibited a more gradual decline, maintaining moderate activity until late evening. Lesser grain borers showed relatively stable catches during the first two hours (~150 individuals), followed by a gradual decrease. In contrast, both red flour beetles and khapra beetles were consistently low in number, with slight variation across the sampling period. Overall, the results indicate that most species displayed maximum activity during the early evening, followed by a marked reduction in captures as the night progressed.

From the second to fourth days, overall captures declined gradually. However, rice weevils and Angoumois grain moths continued to dominate, with peak catches shifting between 200–300 individuals and diminishing sharply toward late evening. By the fifth and sixth days, insect numbers were markedly lower, with rice weevils and Angoumois grain moths showing reduced activity (<170 and <85 individuals, respectively), and lesser grain borers nearly disappearing from the catches. Throughout the study, red flour beetles and khapra beetles remained at very low levels (<10 individuals). Overall, the results indicate that insect activity was concentrated during the early evening hours, declined consistently as the night progressed, and showed a pronounced reduction across successive days, suggesting both diel activity rhythms and progressive depletion of active populations.

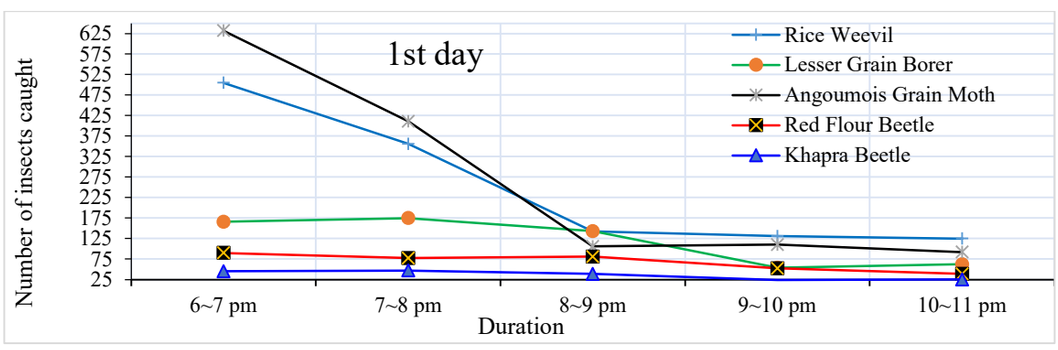

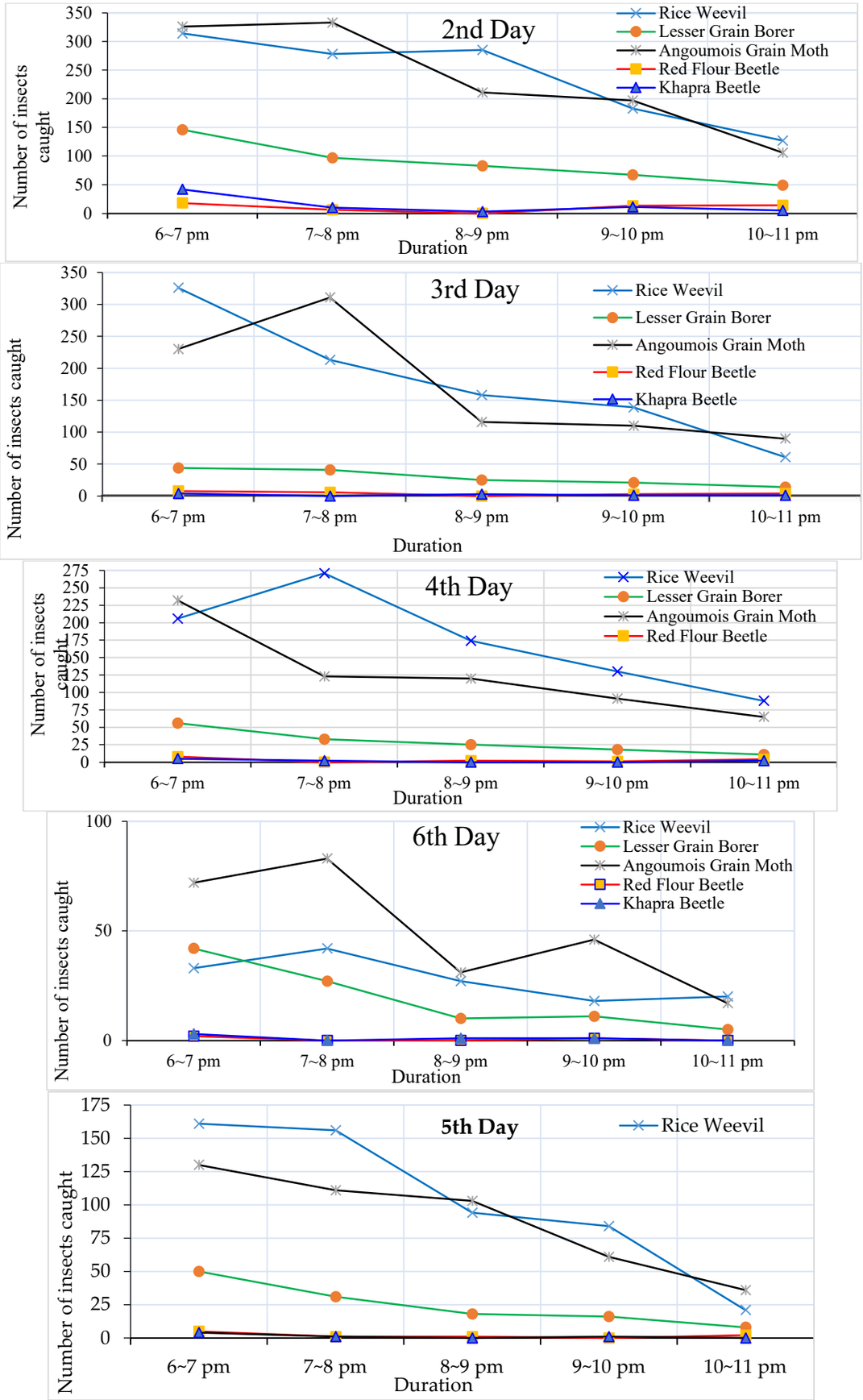

Figure 35. Number of insects captured from the first to the sixth day at hourly time intervals.

Table 34. Trap catch through the BRRI solar light trap

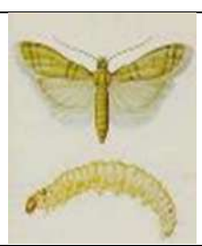	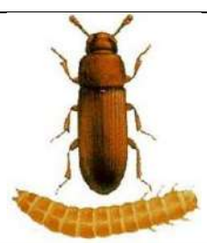			
Angoumois Grain Moth	Red Flour Beetle	Rice Weevil	Lesser Grain Borer	Khapra Beetle

Order-based total insect capture dynamics on different days

The cumulative insect catches over six days revealed apparent interspecific differences in activity and a pronounced temporal decline in overall abundance (Figure 36). Rice weevils and Angoumois grain moths were the dominant species, showing very high initial captures (>1200 individuals) but a steady reduction across successive days, suggesting either depletion of active populations or behavioral avoidance of traps. Lesser grain borers also exhibited relatively high numbers on the first two days (~600 individuals) but declined rapidly thereafter, becoming negligible by the third day onward. In contrast, red flour beetles and khapra beetles remain consistently scarce, reflecting their limited attraction to light traps or reduced flight activity under the prevailing storage conditions. The sharp decline in captures over time may be attributed to cumulative trapping pressure, changes in insect behavior, or environmental factors such as temperature and humidity influencing flight activity. These findings emphasize that while solar light traps are highly effective in monitoring dominant stored-product pests, their efficiency decreases with repeated use over consecutive days, likely due to declining population availability and species-specific behavioral traits.

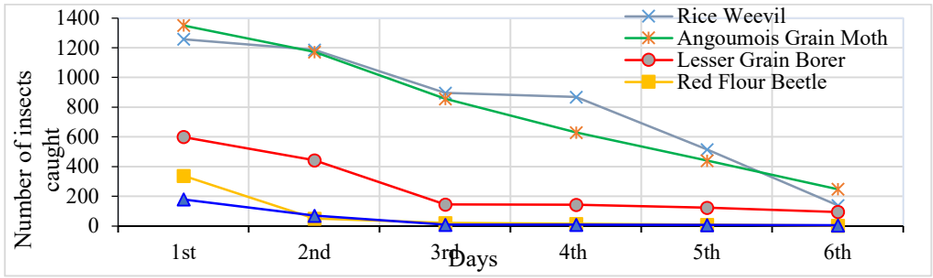

Figure 36. Order-wise total captures of insects under varying light intensities across time intervals

Light intensity with time interval

The combined analysis of the insects captured and the light intensity revealed a strong relationship between illumination and insect activity in the storage environment (Figure 37). Light intensity increased sharply from 6-7 pm (~50 lux) to a peak of around 250 lux at 7-8 pm, then gradually declined to approximately 100 lux by 10-11 pm. This trend closely matched the capture patterns of the dominant species, especially rice weevils and Angoumois grain moths, which reached maximum abundance during the period of highest light intensity and steadily declined as illumination decreased. Lesser grain borers followed a similar pattern but at lower abundance, while red flour beetles and khapra beetles remained consistently low regardless of light levels. These findings suggest that light intensity plays a key role in driving night-time insect activity, with peak captures occurring under higher illumination during early evening hours. The gradual decline in insect numbers later at night likely reflects both decreasing light levels and natural diel rhythms. Overall, the results highlight the importance of aligning solar light trap deployment with peak illumination times to optimize monitoring and management of stored-product pests.

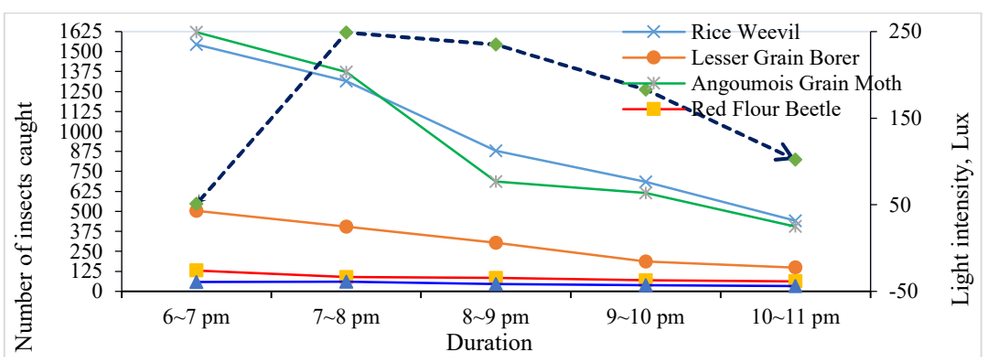

Figure 37. Relationship between light intensity and catch of stored insects in the solar light trap

Conclusion

This study confirmed the BRRI solar light trap as an effective tool for monitoring major stored-product pests, offering potential benefits for end users, manufacturers, and resource-poor farmers by reducing dependence on insecticides. Trap efficiency was strongly affected by evening light intensity, with peak captures occurring during early evening hours (7–8 pm), especially for rice weevils and Angoumois grain moths, while lesser grain borers showed moderate activity, and red

flour beetles and khapra beetles remained consistently scarce. Insect abundance decreased both within nights and across successive days, reflecting diel rhythms, cumulative trapping pressure, and possible behavioral avoidance. These findings demonstrate that solar light traps are most effective when synchronized with peak illumination periods, making them a valuable, eco-friendly monitoring tool. However, as the trial was conducted only under BRRI grain store conditions, further adaptive testing in farmer- and miller-level storage systems is needed to ensure broader applicability and adoption.

PROJECT 4: SMART AGRICULTURAL TECHNOLOGY

Experiment 4.1: Drought Hazard Variability in Bangladesh (1981–2018)

Principal Investigator: Dr. Md. Kamruzzaman Milon
Co-Investigator(s): MMR

Objective

- To generate a comprehensive national-scale drought hazard assessment for Bangladesh (1981–2018) using high-resolution rainfall data and composite indices, with the aim of supporting climate-smart agriculture (CSA) planning and policy interventions.
- Bangladesh is among the most climate-vulnerable countries in the world due to its deltaic setting, high population density, and dependence on agriculture for livelihoods and food security. While floods and cyclones receive greater attention, drought is a recurrent and less visible hazard that threatens crop yields, irrigation demand, and rural livelihoods. Historical droughts in 1979, 1982, 1989, 1994, and 1997 reduced rice production by 30–50 percent in affected districts, particularly in the northwestern Barind Tract and southwestern coastal belt. With growing reliance on groundwater for dry-season Boro rice cultivation, drought risks are intensifying under changing climatic conditions. Despite this, systematic national-scale drought hazard mapping has been limited, and most past studies have relied on single indices such as the Standardized Precipitation Index (SPI). To fill this gap, the present study applies the Effective Drought Index (EDI) and a composite Drought Hazard Index (DHI) to produce the first high-resolution hazard assessment across Bangladesh's three major rice seasons.

Data and Methods

Data Sources

Rainfall data: High-resolution (0.05°) gridded rainfall data for Bangladesh, covering 1981–2018.

Drought Index: The Effective Drought Index (EDI) was calculated every month. EDI has been widely used for drought monitoring in monsoon climates because it captures both drought intensity and persistence.

Drought Characterization

For each grid cell, drought events were identified when EDI ≤ –1.0. Three attributes were derived:
- Frequency (F): Ratio of drought months to total months.
- Duration (D): Average length of drought episodes in months.
- Severity (S): Mean cumulative deficit below the EDI threshold.

Drought Hazard Index (DHI)

The drought hazard was quantified using the following normalized composite index:

$$DHI_i = (F_i \times D_i \times S_i) / \max(F \times D \times S)$$

Where F_i, D_i, and S_i represent the frequency, duration, and severity of droughts at location i. Normalization ensures that DHI values range between 0 (no hazard) and 1 (highest hazard), allowing for spatial comparison across Bangladesh.

Results and Discussion

Rainfall Variability (1981–2018)

Annual rainfall in Bangladesh shows firm spatial heterogeneity (Figure 38). Northwestern and western districts (Rajshahi, Naogaon, Dinajpur) typically receive <1,500 mm annually, while northeastern and southeastern districts (Sylhet, Cox's Bazar) exceed 3,500–4,000 mm. Such disparities create a hydroclimatic divide between surplus and deficit regions (Shahid, 2010).

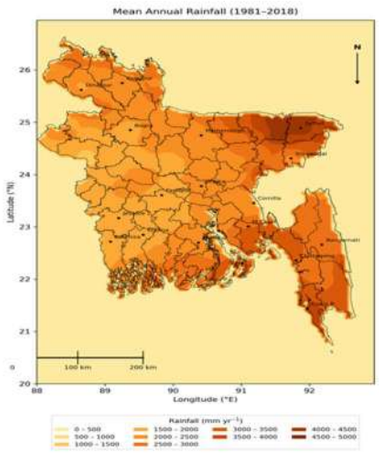

Figure 38. Mean annual rainfall distribution in Bangladesh, 1981–2018.

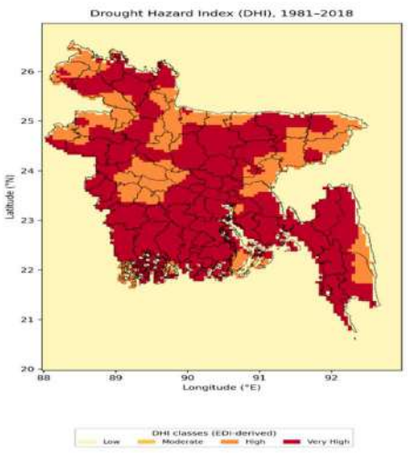

Figure 39. Spatial pattern of the Drought Hazard Index (DHI) in Bangladesh, 1981–2018.

Annual Drought Hazard

The annual DHI analysis reveals that northwestern Bangladesh (Rajshahi, Bogura, Naogaon) experiences the highest hazard (DHI = 0.62–0.78; high–very high class), with 6–8 drought events per decade lasting 3–5 months (Figure 2). In contrast, the northeast (Sylhet, Moulvibazar) records low hazard (DHI = 0.18–0.25) due to rainfall > 3,800 mm. Central districts such as Dhaka and Comilla fall in the moderate range (0.30–0.45) (Figure 39). A clear west–east gradient is evident, with the northwest facing up to threefold higher hazard than the northeast, consistent with earlier studies (Karim et al., 1990; Rahman et al., 2019).

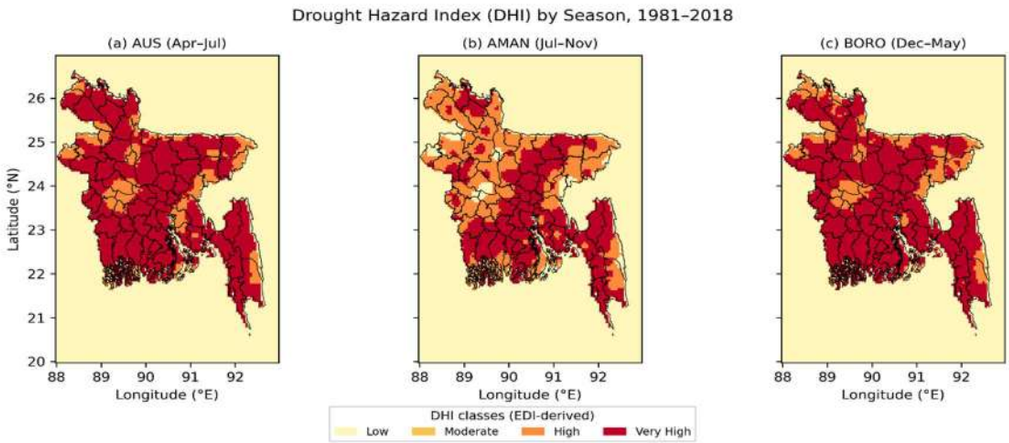

Figure 40. Seasonal Drought Hazard Index (DHI) for Bangladesh during 1981–2018: (a) Aus, (b) Aman, (c) Boro.

Seasonal Drought Hazard

The seasonal DHI (Figure 40) highlights differential vulnerability across rice seasons. During the Aus season (March–May), moderate hazard appears in western districts, coinciding with pre-monsoon rainfall deficits. The Aman season (June–November), dependent on monsoon rains, shows relatively lower hazard, though late-season droughts occasionally reduce yields. The Boro season (December–April) exhibits the highest drought hazard, particularly in Rajshahi, Rangpur, and the northwestern regions, where irrigation dependency is high. Quantitatively, more than 40% of northwestern districts fall under the “high hazard” category in Boro, compared to less than 20% during Aman. These results align with earlier findings that winter and pre-monsoon droughts are most critical for Bangladesh agriculture (Shahid, 2011; Tigkas et al., 2015). The concentration of drought hazards in the northwest suggests priority intervention zones for irrigation modernization and the deployment of drought-tolerant rice.

Conclusions

This study demonstrates that northwestern and western Bangladesh face the highest drought hazard due to rainfall scarcity and high interannual variability. The seasonal assessment highlights the Boro season as particularly vulnerable, requiring extensive irrigation support. The DHI framework, integrating drought frequency, duration, and severity, provides a robust basis for identifying drought-prone hotspots. The findings are directly relevant for climate-smart agricultural planning and water

resource management. Targeted interventions, such as drought-resistant rice varieties, groundwater management, and supplemental irrigation strategies, are essential for mitigating the impacts of drought.

Experiment 4.2: Development and Utilization of a Drone in Agriculture
Principal Investigator: S Paul
Co-Investigator: BCN, MDH, MGKB, MMR
Objectives

- To develop and assemble a drone for Agriculture
- To evaluate the performance of the developed drone
- To deploy the drone in Agriculture

Materials/Components and Method

The adoption of unmanned aerial vehicle (UAV) technology in agriculture is rapidly gaining momentum worldwide, with applications ranging from crop monitoring to precision spraying of fertilizers and pesticides. In Bangladesh, where agricultural practices are traditionally labor-intensive, the integration of drone-operated sprayers presents a transformative opportunity. This technology can address challenges such as labor shortages, uneven spraying, and high operational time, particularly in large paddy fields and other crop systems. An attempt was made to develop and utilize drones in agriculture for the Bangladesh condition. The objectives of this work were to procure all necessary components for a multi-rotor drone capable of carrying an agricultural spraying system, to assemble and integrate the propulsion, control, and spraying subsystems into a single functional unit, and to conduct an initial test under local field conditions to verify its basic flying performance and spraying capability. An agricultural drone for spraying was assembled and developed using procured materials at S Agro Drone BD in Dinajpur, under a public-private partnership (PPP) financed by the "PARTNER" project, BRRI part. The parts for the drone were procured individually to meet both performance requirements and cost considerations (Table 35).

Functional components of the drone-operated sprayer

The major components included:

Frame: The drone's frame is its main structure, holding components together and made from lightweight materials like carbon fiber. It mounts propellers, motors, batteries, and equipment, maintaining balance and stability during flight. The frame also helps control the drone's size and weight.

Motors and Propellers: The motor is essential for drone operation, powering the propellers to take off, stay stable, and control speed and direction. Its power and efficiency influence overall performance. Agricultural drones often utilize brushless motors for enhanced energy efficiency and extended operational life. The propeller generates lift and directional control by pushing air, with four propellers helping to balance the drone. Propeller size, speed, and orientation impact the drone's speed and stability.

Electronic Speed Controllers (ESCs): Electronic Speed Controllers (ESCs) regulate drone motor speed and power, converting flight signals into precise movements for stable flight, smooth acceleration, and control. In agricultural drones, reliable ESCs are crucial for handling payloads and maintaining balance during spraying.

Battery: The battery is the main power source of a drone. Agricultural drones typically use lithium polymer (LiPo) batteries, which are lightweight and provide extended power. A full charge usually supports 20 minutes of flight. It powers motors, propellers, sensors, and other electrical parts.

Flight Controller: The flight controller is the central system of a drone, coordinating sensors, GPS, cameras, and motors to ensure precise operation. It controls the drone's movement, speed, and direction, allowing agricultural drones to operate accurately and perform tasks efficiently.

Spraying System: The spray system in an agricultural drone is a crucial component, as it enables the precise application of pesticides, fertilizers, and other liquids to the field. Through this system, farmers can supply their crops with essential nutrients and effectively control harmful pests. An efficient spray system ensures that pesticides or fertilizers are applied accurately, preventing overuse or wastage, which also contributes to environmental protection.

Table 35: Different parts of the drone

		
Landing-gear	4 4-axis top plate and bottom plate	Shell Cover
		
Power distribution board and XT-60 socket	K++v2 Flight controller + GPS+ Power module +LED light +USB link cable + GPS stand	XT90T Mounting socket
		
Arm (Carbon-Tube)	Sky-droid T12 remote, receiver, and camera	Hobby-wing X8 motor and propeller
		
Herewin-6s-16000mah-lipo-battery	SKYRC-PC1080-Dual-Channel-6s-LiPo-Battery-Charger	Battery Plate
		
10-Liter-tank	5L Brushless Water Pump + Spray System with Pressure Nozzles	Amass-XT90-S-Anti-Spark-Connector
		
Tank-inlet-filter	40mm Aluminum arm pipe	Silicone Wire

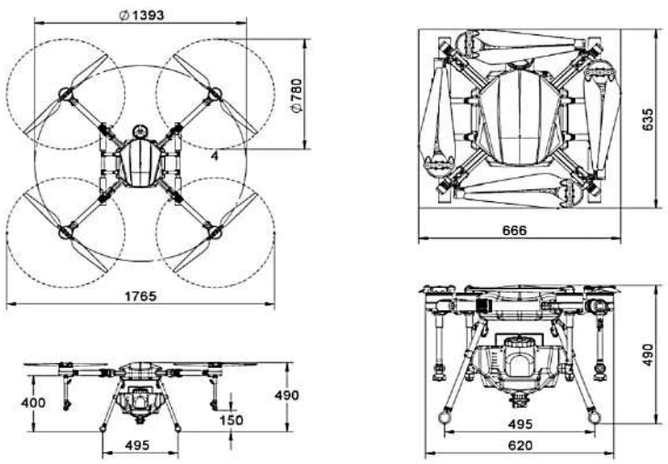

Drawing of the drone (All dimensions are in mm)

Assembly Process

The assembly was performed systematically to ensure mechanical stability and electrical safety (Plate 14):

Frame Setup: To set up the drone frame, the arms were attached to the main body, then the landing gear was fixed for stability. All parts were tightened to prevent movement during flight, and space was allocated for mounting the motors, battery, and other components. The frame was then checked for balance to ensure smooth flight.

Propulsion System Installation: The motors were securely mounted with vibration-dampening mounts to minimize shaking during flight. Propellers were attached in the correct orientation and tightened to prevent loosening. The setup was aligned to ensure balanced thrust, and the system was checked for smooth rotation and proper functioning.

Electrical Wiring: The ESCs were connected to motors and linked to the power board. The flight controller was wired to the ESCs for signals. The GPS is connected to the flight controller for navigation. All connections were then checked for proper setup.

Spraying Mechanism Mounting: For the spraying mechanism mounting, the liquid tank and pump were firmly secured to the drone's frame. Hoses were attached from the pump to multiple nozzles to ensure even distribution of the liquid. Each connection was tightened to prevent leaks during operation.

Control System Configuration: The control system was set by pairing the transmitter and receiver. The flight controller was tuned for stable take-off, smooth hovering, and accurate navigation. All control inputs were tested and then saved with these settings for future use.

Pre-Flight Inspection: All bolts were tightened to ensure the frame's stability. Connectors were examined to confirm they were securely attached and free from damage. Finally, the entire setup was reviewed to ensure it met safety standards before it was put into operation.

Plate 14. Assembly process of the drone

Results

Initial Testing

The initial testing took place under typical field conditions, characterized by calm winds, high humidity, and a cloudy sky, during the last Aman season.

Flight Performance

The assembled agricultural drone successfully performed all basic flight operations during the initial field test. The UAV achieved a smooth vertical takeoff and maintained stable hovering at various altitudes. Directional control was responsive, and no abnormal vibration or instability was observed throughout the flight. With payloads of 5, 7, and 10 liters, the drone demonstrated adequate lift capacity and movability, confirming that the propulsion system and frame structure were properly balanced and capable of supporting agricultural spraying operations.

Spraying System Performance

The spraying system functioned reliably under all tested conditions. The pump operated consistently, and the nozzles produced a uniform discharge pattern without leakage or blockages. The spray coverage appeared evenly distributed across the targeted area, with no noticeable oversaturation or untreated gaps. This result indicates that the integration of the spraying system with the UAV platform was effective and that the liquid delivery system is suitable for field applications.

Power Supply and Endurance

The Herewin-6s-16,000 mAh LiPo battery provided a stable power supply throughout the test flights. No sudden voltage drops were recorded, and the battery performance was consistent with the expected operational duration of approximately 20 minutes per full charge. However, the endurance may be affected during extended missions under full payload conditions, which requires further optimization in future trials.

System Reliability

All electronic and mechanical subsystems performed satisfactorily during the initial test. Motors, ESCs, and the pump operated within safe temperature ranges, and no overheating was detected. The transmitter–receiver maintained uninterrupted communication, ensuring complete operator control of the UAV. The overall noise level of the motors and pump remained within normal limits, suggesting smooth mechanical functioning.

Observations

Flight Stability: The drone successfully took off, maintained stable hovering, and responded well to all control inputs.

Spraying Operation: Liquid discharge was smooth and continuous from all nozzles, with no blockage or leakage detected.

System Response: No abnormal vibration, electrical malfunction, or mechanical instability was observed during the operation.
Noise Level: The motors and pump operated with a consistent sound, indicating smooth mechanical performance.
Battery Performance: The supplied battery maintained stable power throughout the test, without any sudden voltage drops.
Control Signal: The transmitter and receiver maintained a strong and uninterrupted connection during the entire trial.
Spray Pattern: The spray coverage appeared even, with no visible gaps or over-saturation in the sprayed area.
Temperature Check: Motors, ESCs, and the pump showed no signs of overheating after the short test.

Plate 15. Initial test of the drone after assembling

Key Findings

- An initial test of the developed UAV demonstrated stable flight and spraying capability with payloads up to 10 liters (Plate 15).
- Spray distribution was uniform, with no leakage or blockage detected.
- Power supply was stable, supporting 20 minutes of continuous operation.
- The system showed mechanical and electrical reliability under field conditions.
- UAV-based spraying has strong potential to reduce labor demand and increase efficiency in Bangladeshi agriculture.

Conclusion

The assembly and development of the drone-operated sprayer were completed using procured components, and it was tested under local field conditions in Bangladesh. The UAV demonstrated stable flight performance, reliable maneuverability, and effective spraying with payloads of up to 10 liters. Its spraying system functioned efficiently, ensuring uniform coverage without leakage or blockages. The power unit provided consistent performance, supporting approximately 20 minutes of continuous operation per charge. Control signals remained strong throughout the test, ensuring safe and responsive handling. These results demonstrate the feasibility of UAV-based precision spraying in reducing labor demand, saving operational time, and minimizing chemical waste in Bangladeshi agriculture. With improvements in spray calibration, GPS-guided operation, and larger-scale trials, drone technology can become a transformative tool for advancing efficiency, sustainability, and farmer-friendly practices in Bangladesh.

Recommendations

- **Systematic Field Trials:** Conduct extended trials across diverse crops, regions, and seasons to validate performance.
- **Spray Calibration:** Adjust spray rates according to local agronomic standards to ensure practical application and minimize chemical wastage.
- **Autonomous Navigation:** Integrate GPS-based autonomous spraying patterns for greater precision and reduced operator workload.
- **Battery Optimization:** Explore higher-capacity batteries or modular swappable systems to extend operational endurance.
- **Economic Assessment:** Evaluate cost-benefit and affordability for farmers to support large-scale adoption.

PROJECT 5: INDUSTRIAL AND FARM LEVEL EXTENSION OF AGRICULTURAL MACHINERY

Activity 5.1: Two-Week Residential Hands-On Training for Mechanics and Machine Operators

Course Director: Dr. Md. Durrul Huda

Course Coordinator: Subrata Paul

Co-Investigator: All Scientists of FMPHT

Objectives

- Strengthen the technical skills of mechanics and machine operators.
- Promote safe and efficient operation of BRRI-developed farm machinery.
- Enhance knowledge of machine maintenance and troubleshooting.
- Encourage the adoption of mechanized rice farming practices at the community level.

Methodology

Capacity development in agricultural mechanization is essential to increase productivity, reduce drudgery, and ensure sustainable farming practices. Skilled operators and mechanics play a crucial role in extending the service life of machinery, reducing downtime, and enhancing overall farm efficiency. With this vision, the Farm Machinery and Postharvest Technology (FMPHT) Division of the Bangladesh Rice Research Institute (BRRI) organized two residential hands-on training programs under the PARTNER Project. The training aimed to strengthen the technical knowledge and practical skills of machine operators and mechanics, focusing on the use, maintenance, and repair of BRRI-developed farm machinery.

Training Overview

- Program duration: 15 days long residential training
- Number of batches: 2
- Venue: BRRI Headquarters, Gazipur
- Organizer: FMPHT Division, BRRI
- Support: PARTNER Project (financial and technical)
- Participants: 40 (20 per batch), selected in collaboration with BRRI regional stations

Priority was given to individuals with prior experience in operating agricultural machinery to ensure that the training reached those directly engaged in mechanized farming and could create local-level impacts.

Training Curriculum

The curriculum was designed and delivered by experienced BRRI scientists. It combined classroom-based theoretical instruction with extensive hands-on sessions, ensuring maximum exposure to real-life applications.

Machines and Technologies Covered

Participants were trained on the operation, maintenance, and repair of:

- Mechanical rice transplanter
- Combine harvester
- Self-propelled reaper
- BRRI seed sower
- Prilled urea applicator
- Power and manual weeders
- Chopper machine
- Winnower machine
- Power tiller
- Maintenance and repair of diesel/petrol engines
- Implements attachment with tractor and operation

Additionally, specialized sessions were conducted on:

- Raising rice seedlings in plastic trays for mechanical transplanting
- Operation of electric motors.

Training Approach

The training program was carefully structured to ensure that participants not only learned theoretical aspects of mechanization but also gained confidence through hands-on practice under expert supervision (Plate 16). The approach followed a stepwise progression from basic familiarity with the machines to independent operation in real field conditions.

Initial Sessions: No-load Operation

The training began with introductory sessions where participants became familiar with the design, functions, and safety protocols of each machine. During this stage, they operated the equipment in

no-load conditions at the FMPHT research field and nearby roads. This method helped participants understand the basic control systems, starting and stopping mechanisms, and safe handling of the machines without the risk of field damage or crop loss.

Practical Demonstrations: Supervised Step-by-Step Operation

After the no-load sessions, detailed demonstrations were provided by BRRI scientists and technical staff. Each machine was operated step by step, with instructors explaining critical points such as adjustment of machine settings, fuel requirements, lubrication, and routine maintenance checks. Participants then repeated the demonstrated steps under close supervision, ensuring that they could replicate correct procedures independently. This stage emphasized learning by doing, allowing trainees to apply theoretical knowledge in a guided environment immediately.

Field Applications: Real Practice

To consolidate learning, participants were taken to nearby farm fields where they practiced operating the machines under actual working conditions. Activities included harvesting with the combine harvester, transplanting rice seedlings using the mechanical transplanter, applying prilled urea with the applicator, and operating reapers and weeders in standing crops. Instructors provided continuous feedback during these sessions, helping participants refine their skills and troubleshoot common problems.

Evaluation: Knowledge and Skill Assessment

At the conclusion of the training, a post-training evaluation was conducted. This assessment measured the improvement in participants' technical knowledge, operational skills, and ability to troubleshoot machinery-related issues. Feedback was also collected from participants regarding training content, delivery, and areas for improvement. In addition to certificates, participants were provided with informational leaflets and a set of essential tools to support future application of their skills in the field. The evaluation process ensured that trainees were not only competent but also confident in applying mechanization practices independently in their respective regions.

Major Activities

Key activities undertaken by participants included:

- ✓ Hands-on practice with BRRI-developed farm machinery.
- ✓ Live demonstrations of seedling raising techniques for mechanical transplanting.
- ✓ Field-level operation and maintenance of reaper, transplanter, and combine harvester.
- ✓ Practical training in the repair of diesel/petrol engines and electrical machinery.
- ✓ Skill consolidation through field-based supervised learning.

Plate 16. Pictorial view of hands-on training

Output and Achievements

- Participants trained: 40 mechanics and operators completed the program.
- Skill improvement: Participants gained confidence in operating, maintaining, and repairing key farm machines.
- Capacity building: Each participant received training materials, a certificate, and a set of essential tools to support field-level application.
- Community-level impact: The training created a pool of skilled operators capable of promoting mechanization in rice farming across different regions of Bangladesh.

Conclusion

The two-week residential hands-on training program successfully enhanced the technical capacity of mechanics and machine operators in Bangladesh. By focusing on practical skills and actual applications, the training prepared participants to operate and maintain BRRI-developed machinery efficiently. This initiative contributes to sustainable mechanization, improved productivity, and greater income-generating opportunities for farming communities.

The success of the program demonstrates the importance of continuous training and knowledge transfer in advancing agricultural mechanization.

Experiment 5.2: Training on Operation and Maintenance of Farm Machinery

Training is an effective tool to develop technical and efficient manpower for practical use, repair, and maintenance of agricultural machinery in the farmyard. Proper operation and maintenance increase the lifetime of a machine, leading to more income-generating activities (IGA) and, consequently, higher productivity. To build trained manpower on farm machinery in rural areas, the SFMRA project of the Farm Machinery and Postharvest Technology Division of Bangladesh Rice Research Institute conducted a two-day residential training programme at the BRRI headquarters in Gazipur, Chuadanga, Bottoil of Kushtia, Bogura, Cox's Bazar, and Dinajpur districts.

Two-day-long residential training

Two-day-long residential training was conducted under the financial and technical support of the SFMRA project of Farm Machinery and Postharvest Technology division in order to introduce BRRI-developed and other agricultural machines at the farmer's level; to develop skilled operators on agricultural machinery at the farm level, and to build up awareness about the use and benefit of using agricultural machines. The trainings were conducted at BRRI headquarters, Gazipur, Chuadanga, Bottoil of Kushtia, and Dinajpur district.

Twenty participants attended each training program. Participants were selected by direct consultation with BRRI regional stations and respective DAE offices, while maintaining selection criteria. Priorities were given to select the participants based on their experience in operating agricultural machinery. Lecture and practical sessions were arranged by BRRI scientists, DAE personnel (AD, DD, UAO & Aril. Engg.) and Academicians (University professors). Knowledge was shared with the participants on the operation and maintenance of the BRRI-developed machinery and technologies, and other agricultural machinery. During the practical session, participants operated machinery to gain experience with agricultural machinery operations in no-load conditions on the drying yard/road. After a successful operation in the drying yard/ road, participants were taken to the main field for practical operation of agricultural machinery.

Major activities done by the participants of the training programme

The following BRRI developed machinery, technologies, and other agricultural machinery were introduced and practically operated for the trainees during the training programme.

- Demonstration on seedling raising technique for mechanical rice transplanter
- Operation and maintenance of the mechanical rice transplanter
- Operation and maintenance of the BRRI prilled urea applicator
- Operation and maintenance of the BRRI manual and power weeder
- Operation and maintenance of the whole feed combine harvester
- Operation and maintenance of the self-propelled rice/wheat reaper
- Operation and maintenance of the BRRI open drum thresher
- Operation and maintenance of the BRRI closed drum thresher
- Operation and maintenance of the BRRI winnower
- Hands-on repair and maintenance on the diesel engine
- Practical field operation of agricultural machinery in the farm level

A total of 36 batches of the residential training programme were conducted, training a total of 740 participants, comprising 500 males and 240 females. Participants of the training programme were drawn from the BRRI R/S adjacent area and from its jurisdiction district. An inaugural session was

held on the first day of the training programme, followed by a pre-evaluation of the trainees. Lectures and mostly practical sessions were arranged in all the locations. A step-by-step procedure for raising seedlings in a tray was demonstrated to the participants. After this machine-like mechanical rice transplanter, combine harvester, a self-propelled reaper, BRRI open drum thresher, BRRI closed drum thresher, BRRI prilled urea applicator, BRRI power & manual weeder, BRRI winnower, and power tiller were operated preliminarily in no-load condition in the threshing floor/road, and after that these machines were operated by the trainees in the field one after one (Plate 17). At the end of the training, a post-evaluation and trainee's reactions regarding the training were collected. Certificates, leaflets, and a set of tools were distributed among the participants.

a) Inauguration of the training programme

b) Operation of the manual seed sower machine

c) Introduction of rice transplanter

d) Introduction of reaper and reaper binder

Plate 17. Pictorial view of hands-on training

Formal training proved to be a very effective tool, as it allowed them to be isolated from their home and concentrate fully in the classroom. The trainees requested a one-week training period instead of two days to enhance their skills in farm machinery. Trainees opined that they are now more confident about the use of the machinery, and the hand tools will be helpful in their work.

MAINTENANCE WORK

Appendix I: Support service for different divisions of BRRI rendered by FMPHT Divisional Research Workshop during 2024-2025.

Division	Type of work	N0. Of Job	Total
Farm Management	Power tiller hufs repair	02	49
	Power tiller wheel repair	14	
	Hydro tiller repair	04	
	Power thresher repair	02	
	Winnower Machine repair	03	
	Riding lawnmower Machine	01	
	Paddle Thresher repair	03	
	Air cleaner and rotary chin willing	04	
	Screw Braided	03	
	3 in GI pipe Welding	04	
	Godown gout Welding	01	
	Making net vuls key	03	
	Hand chopper	06	
Building construction	Labor Colony gate repair	01	15
	Drum cutting and adding a handle	06	
	5 in GI pipe repair	03	
	1 number gate welding	01	
	Cutting oil drums	04	
Soil Science	Paddle Thresher repair	02	04
	Making Signboard	02	
Agronomy	T.H. seven Thresher repair	01	04
	Close drum Thresher repair	01	
	Paddle Thresher repair	02	
Biotechnology	Paddle Thresher repair	01	07
	Hand Chopper	05	
	Thresher Machine repair	01	
ARD	Winnower Machine repair	01	04
	Thresher Machine repair	02	
	Paddle thresher	01	
Hybrid	Thresher machine repair	01	01
Agricultural Economies	Paddle thresher repair	02	02
GRS	Grading Machine repair	02	04
	Close drum Thresher repair	01	
	Trolley repair	01	
Plant Pathology	Paddle Thresher repair	02	92
	Cutting Plastic pots	90	
Entomology	Making hole in Mylar's seat	100	132
	Hand Trolley Bearing seating	01	
	Scanning Frame Welding	30	
	Winnower Machine repair	01	
IWM	GI pipe welding	02	10
	Setting the motor meter	01	
	Making AWD pipe	02+05	
Plant Breeding	Engine box repair	01	05
	Cutting stile drum	02	
	Thresher Machine repair	01	
	Winnower machine	01	
Physiology	Setting Power tiller Trolley	01	03
	Power Thresher Machine repair	01	
	Making Signboard	01	
Hostel	Making key ring	90	92
	Gas stone repair	02	
Agriculture Statistics	Paddle Thresher Machine	01	01
GQN	Paddle Thresher repair	01	01
Applied Research	Thresher machine	01	02
	Winnower machine	01	
Army	Loading, spinning, cutting, and welding	02	14
	Bumper Setting and welding	02	
	Seat Stand welding	03	
	Engine setting	02	
	Making Stau ring	02	
	Making low bead	01	
	Making Bumper	02	